MASKING AND ITS NEURAL SUBSTRATES IN DAY- AND NIGHT-ACTIVE MAMMALS

By

Jennifer Lou Langel

A DISSERTATION

Submitted to
Michigan State University
in partial fulfillment of the requirements
for the degree of

Neuroscience – Doctor of Philosophy

2016

ABSTRACT

MASKING AND ITS NEURAL SUBSTRATES IN DAY- AND NIGHT-ACTIVE MAMMALS

By

Jennifer Lou Langel

Light can directly and acutely alter arousal states, a process known as "masking". Masking effects of light are quite different in diurnal and nocturnal animals with light increasing arousal and activity in the former and suppressing in the latter. Few studies have examined chronotype differences in masking or the neural substrates contributing to this process. However, in nocturnal mice, masking responses are mediated through a subset of retinal ganglion cells that are intrinsically photosensitive (termed ipRGCs) due to their expression of the melanopsin protein. The goal of the studies in this dissertation was to first characterize masking responses in day- and night-active animals and then to evaluate the possibility that differences in ipRGC projections or the circuitry within their targets might contribute to species differences in masking.

First, I compared behavioral and brain responses to light *across individuals* within a species (the Nile grass rat, *Arvicanthis niloticus*). In this diurnal species some individuals become night-active when given access to a running wheel, while others do not. I found that masking responses to light and darkness in these animals were dependent upon the chronotype of the individual. Additionally, the responsiveness of neurons within two brain regions, the intergeniculate leaflet (IGL) and olivary pretectal area (OPT), was associated with the behavioral response of the animal to light.

Next, I compared behavioral responses to light and darkness *across species*, the diurnal grass rat and the nocturnal Norway rat (*Rattus norvegicus*: Long Evans (LE) strain). Overall, light suppressed general activity in LE rats, while darkness increased it, a pattern very different

from that seen previously in grass rats, in which light stimulates activity, but darkness has no effect (Shuboni et al., 2012). I also found that light induced sleep and resting behavior in LE rats and suppressed it in grass rats and that these effects lasted for at least a full hour.

To determine whether differences in the projections of ipRGCs may account for species differences in masking, I characterized the melanopsin system of the grass rat and compared it to that previously described in nocturnal rodents. I found that the grass rat retina contained the same basic subtypes of melanopsin cells and that the majority of these cells (87.7%) contained the neuropeptide, pituitary adenylate cyclase-activating polypeptide (PACAP), while 97.4% of PACAP cells contained melanopsin. Since, within the retina, PACAP is found almost exclusively in ipRGCs, I then examined the distribution of PACAP-labeled fibers originating in the retina to characterize ipRGCs projections to the brain. I found that although these were similar to those of nocturnal species, some differences existed in their density in the dorsal and ventral lateral geniculate nucleus (dLGN and vLGN) and in the rostrocaudal extent of the OPT.

Finally, to determine whether differences exist in some features of the internal circuitry of ipRGC target areas, I first examined whether there were differences in retinal input to light responsive neurons within ipRGC target areas in a diurnal and nocturnal brain. Within the IGL, the majority of light responsive neurons had close contacts with retinal fibers in both grass rats and LE rats. I then determined whether differences exist in excitatory (glutamate) and inhibitory (GABA) neuronal populations in multiple ipRGC target areas. In many areas the distributions of glutamate and GABA cells were similar in the two species, but there were differences in the vLGN (more glutamate in LE rats than grass rats) and in the lateral habenula (GABA present in grass rats but not LE rats). Overall, these studies provide insight into chronotype differences in behavioral responses to light, as well as the brain regions that may mediate those differences.

ACKNOWLEDGEMENTS

First, I would like to express my deepest gratitude to my advisor, Dr. Laura Smale, for her continued mentorship and support. She has been a wonderful role model to me as a scientist and a great friend. I enjoyed our dog walks together. I would also like to thank my guidance committee, Drs. Cheryl Sisk, Lily Yan and Weiming Li, for their valuable guidance and helpful feedback. Thank you to my collaborator, Dr. Jens Hannibal, for his valuable help and advice with the experiments in Chapter 4 and to Dr. Lily Yan in providing helpful advice for the experiments in Chapter 5.

I would also like to thank all the members of the SYNers lab (past and present). Dr. Tony Nunez, thank you for your valuable insights and feedback. Also, thank you to Dr. Andy Gall, Dr. Tomoko Ikeno, Dr. Dorela Shuboni, Dr. Carmel Martin-Fairey, Sean Deats, Joel Soler, Sam Jones, Thomas Groves, Celizbets Colon-Ortiz and Jenna Schauer. Thank you for your help and feedback. I enjoyed our time in the lab together and value your friendship. Also, thank you to all of the wonderful undergraduates and summer interns that have helped me with various projects in the lab. I am extremely grateful to the Neuroscience Program for providing helpful resources and in aiding in my development as neuroscientist and teacher. Thank you to all of my friends at MSU, you made my time here enjoyable.

Finally, I would like to thank my family and friends for their love and support. To my husband, Ross, thank you for encouraging me and for making me laugh when I needed it. Lastly, to my fur babies, Sofie, Stella and Dexter, for settling my nerves with snuggles and for helping me to take time to enjoy the outdoors.

PREFACE

Two chapters of this dissertation have been published in manuscript form.

Chapter 2

Langel J, Yan L, Nunez AA, Smale L (2014) Behavioral masking and cFos responses to light in day- and night-active grass rats. J Biol Rhythms 29:192-202.

Chapter 4

Langel JL, Smale L, Esquiva G, Hannibal J (2015) Central melanopsin projections in the diurnal rodent, Arvicanthis niloticus. Frontiers in Neuroanatomy 9.

TABLE OF CONTENTS

LIST OF TABLES

LIST OF FIGURES

KEY TO ABBREVIATIONS

ABC ..... avidin-biotin complex

ANOVA ..... analysis of variance

AR ..... antigen retrieval

BSA ..... bovine serum albumin

DA ..... day-active

DAB ..... diaminobenzidine

DD ..... constant darkness

DIG ..... digoxigenin

dLGN ..... dorsal lateral geniculate nucleus

DP ..... dark pulse

GA ..... general activity

GABA ..... gamma-aminobutyric acid

Gad ..... glutamic acid decarboxylase

GLC ..... ganglion cell layer

IF ..... immunofluorescence

IGL ..... intergeniculate leaflet

IHC ..... immunohistochemistry

INL ..... inner nuclear layer

IPL ..... inner plexiform layer

ipRGCs ..... intrinsically photosensitive retinal ganglion cells

-ir ..... -immunoreactive

IR ..... infrared

ISH ..... *in situ* hybridization

LD cycle ..... light/dark cycle

LE rat ..... Long Evans rat

LGN ..... lateral geniculate nucleus

LHb ..... lateral habenula

LP ..... light pulse

NA ..... night-active

NeuN ..... neuronal nuclear antigen

OPT ..... olivary pretectal nucleus

PACAP ..... pituitary adenylate cyclase-activating polypeptide

PBS ..... phosphate buffered saline

PER ..... period

PLi ..... posterior limitans

PLR ..... pupillary light reflex

REM sleep ..... rapid eye movement sleep

RGCs ..... retinal ganglion cells

SC ..... superior colliculus

SCN ..... suprachiasmatic nucleus

SEM ..... standard error of the mean

SSC ..... saline sodium citrate

TX Triton-X-100

Vglut ..... vesicular glutamate transport

vLGN ..... ventral lateral geniculate nucleus

VLPO ..... ventrolateral preoptic area

vSPZ ..... ventral subparaventricualr zone

WRA ..... wheel running activity

ZT ..... Zeitgeber time

CHAPTER 1: Introduction

General introduction

The earth's rotation on its axis is predictable and generates systematic, though somewhat less predictable, daily changes in ambient light and temperature. Almost all species have evolved endogenous daily timekeeping systems (circadian systems) that enable them to anticipate these changes and to coordinate their behavior and physiology accordingly. However, animals must also cope with other less predictable changes in light and temperature, like those associated with cloud cover, and behavior itself can lead to changes in exposure to light or ambient temperature (e.g. a rodent moving in and out of its burrow or a human turning on the light). These environmental variables can therefore directly lead to more acute changes in behavior, a phenomenon referred to as "masking". Both of these systems typically operate quite differently in animals with different "chronotypes", such as those that are most active during the day (diurnal animals) and those that are most active at night (nocturnal animals). The degree to which an animal is considered diurnal or nocturnal can differ between species as well as between individuals of the same species (Refinetti, 2006, 2008; Hut et al., 2012).

The environmental cue that has been best studied in the context of masking and of its influence on circadian systems is ambient light. Circadian rhythms are synchronized (entrained) to the external light/dark cycle via retinal projections to the suprachiasmatic nucleus (SCN), the primary circadian oscillator of mammals (Moore and Eichler, 1972; Moore and Lenn, 1972; Stephan and Zucker, 1972; Johnson et al., 1988). This process is very similar in diurnal and nocturnal species, as indicated by the fact that the influence of photic cues on their clocks are fundamentally the same (Smale et al., 2008). The situation is very different when we consider masking. Although some directs effects of light are very similar in diurnal and nocturnal species

(e.g. the suppression of melatonin secretion from the pineal gland) (Illnerova et al., 1979; Lewy et al., 1980; Kanematsu et al., 1994; Kalsbeek et al., 1999), its acute effects on behavior are very different. Specifically, an increase in light intensity generally increases arousal and locomotor activity in diurnal species (such as humans), and typically decreases it, and induces sleep, in nocturnal ones (Mrosovsky, 1999). Little is known about the neural pathways mediating masking effects of light on behavior, especially in diurnal species.

Light plays an essential role in the shaping of adaptive daily activity patterns, but it can have adverse effects on human health if exposure to it occurs at the wrong time of day or if its duration and intensity are insufficient. At least 15% of full time workers in the USA are engaged in shift work that exposes them to significant amounts of artificial light at night, a time when the circadian system is promoting sleep (the May 2004 Current Population Survey (Labor, 2005)). This is associated with many health problems, such as sleep disorders, reproductive failure, metabolic issues, obesity, mood disorders and breast and prostate cancer (Schroeder and Colwell, 2013; Fonken and Nelson, 2014; Bedrosian et al., 2015; Kripke et al., 2015; Stevens and Zhu, 2015). Understanding the effects of light on physiology and behavior and the mechanisms mediating these processes in diurnal species is important for the development of effective protocols for improving human health problems that are associated with inadequate and mistimed patterns of light exposure.

In this introductory chapter, I will first review what is known about the masking effects of photic cues on behavior, emphasizing differences associated with chronotype, both between and within species. I will then provide an overview of what is known about the neural pathways that mediate masking. Here, I will focus first on the retina and the role of intrinsically photosensitive retinal ganglion cells (ipRGCs), and then on an evaluation of existing data on

brain regions that receive input from these ipRGCs and their potential role in masking. Most of this literature is focused on nocturnal rodents (mainly mice), but I will also highlight what is known in diurnal species. Finally, the research questions to be addressed in each chapter of this dissertation will be summarized.

Masking: between and within species comparisons

Jürgen Aschoff (1960) was the first to use the term "masking" to describe the direct impact of any environmental stimulus (e.g. light) on behavior and saw it as something that can either attenuate or enhance the influence of the endogenous clock on that behavior (Aschoff, 1963). The focus here will be on the masking effects of light on arousal and locomotor activity, although other stimuli such as feeding cycles (Aschoff and von Goetz, 1986) and social cues (Aschoff et al., 1988) can also induce masking. Most studies of biological rhythms have focused on entrainment and employed procedures that limited masking. However, there has been a growing appreciation in recent years of the fact that interactions between masking and circadian mechanisms may be important in shaping daily patterns of activity in both diurnal and nocturnal species (Redlin, 2001). In the same animals masking may block or enhance the effects of the circadian clock on activity depending on the time of day (Aschoff and Vongoetz, 1988, 1989; Redlin and Mrosovsky, 1999b; Pendergast and Yamazaki, 2011; Shuboni et al., 2012).

As noted above, masking responses to light are generally dependent upon the temporal niche that an animal occupies (Mrosovsky, 1999; Redlin, 2001). For example, light increases locomotor activity and arousal in diurnal species such as canaries (Aschoff and Vongoetz 1989), Nile grass rats (Shuboni et al. 2012) and squirrel monkeys (Gander and Moore-ede 1983), while darkness can have the opposite effect (Gander and Moore-ede, 1983; Aschoff and Vongoetz,

1989; Shuboni et al., 2015). The reverse is true of nocturnal species such as hamsters (Aschoff and Vongoetz 1988; Redlin and Mrosovsky 1999b) mice (Butler and Sliver 2011; Mrosovsky 1994, 1999; Mrosovsky et al. 1999; Mrosovsky and Thompson 2008; Shuboni et al. 2012) and bush babies (Erkert et al. 2006); that is, light decreases locomotor activity and arousal in these species while darkness increases these variables. Additionally, light exposure at night, even as short as 5 minutes or millisecond pulses, can induce sleep in nocturnal species, such as mice and hamsters (Altimus et al., 2008; Lupi et al., 2008; Morin and Studholme, 2009; Tsai et al., 2009; Morin and Studholme, 2011; Muindi et al., 2013; Morin, 2015), while in diurnal ones, such as humans, light (even millisecond flashes) decreases subjective sleepiness and increases alertness (Cajochen, 2007; Zeitzer et al., 2011). Interestingly, under some conditions dim light can increase activity in nocturnal species, such as mice and owl monkeys (Mrosovsky, 1999; Mrosovsky et al., 2000; Mrosovsky et al., 2001; Mrosovsky and Thompson, 2008; Fernandez-Duque et al., 2010; Kronfeld-Schor et al., 2013). This phenomenon, known as "paradoxical" masking (Mrosovsky, 1999), might occur in nocturnal rodents that live underground because when they become active they leave a very dark burrow and are exposed to low levels of light in their environment (moonlight). In some other nocturnal species, such as arborial ones like owl monkeys, movements may be faster and safer under dim light conditions than in complete darkness when forms and outlines cannot be visualized (Mrosovsky et al., 2000; Fernandez-Duque et al., 2010).

While masking may play an important role in shaping species specific activity profiles, it can also be essential in providing plasticity within individuals of a species. One example is illustrated by Golden spiny mice (*Acomys rusatis*), a species in which individuals can be diurnal or nocturnal in the field, but are always nocturnal in the laboratory; their close relative, the

Common spiny mouse (*Acomys cahirinus*) is strictly nocturnal (Levy et al., 2007). As expected, Common spiny mice show nocturnal-like masking responses, such that they suppress their general activity in response to light. Golden spiny mice, however, do not display this light-induced suppression of activity in the laboratory or in semi-natural field conditions, which may enable individuals to switch from a nocturnal to diurnal pattern depending on environmental conditions (e.g. competition for resources, changes in environmental temperature) (Gutman and Dayan, 2005; Levy et al., 2007; Cohen et al., 2010; Rotics et al., 2011). Other changes in the environment, such as the introduction of a running wheel, can alter patterns of locomotor activity via masking in the Mongolian gerbil (*Meriones unguiculatus*)(Weinert et al., 2007), degu (*Octodon degus*)(Vivanco et al., 2010a; Vivanco et al., 2010b) and Nile grass rat (*Arvicanthis niloticus*)(Redlin and Mrosovsky, 2004). I will discuss issues associated with this plasticity in greater depth in Chapter 2.

Neural pathways of masking: from the retina into the brain

Discovery of intrinsically photosensitive retinal ganglion cells (ipRGCs)

For over 150 years, light was thought to be detected within the mammalian retina by only two types of photoreceptors, rods and cones (Van Gelder, 2008), but the possibility of a third type was hinted at with the discovery by Clyde Keeler in 1924 of mice that lacked rods. Keeler noted that these "rodless" mice, which were visually blind, were still able to contract their pupils in response to light stimulation (Keeler, 1927b, a; Keeler et al., 1928). Because the outer nuclear layer of the retina (where rods and cones are located) was absent in these animals, Keeler suggested that pupillary responses may be mediated by cells within the inner nuclear layer (such as bipolar cells) or ganglion cell layer of the retina (Keeler, 1928). In the 1980s and 1990s many

reports came in of retinally degenerate (*rd*) and transgenic mice that lacked rods and were visually blind but retained non-image-forming visual functions, such as the pupillary light reflex, entrainment to the light/dark cycle (Ebihara and Tsuji, 1980; Foster et al., 1991; Provencio et al., 1994) and masking (Mrosovsky, 1994). However, some cones are present in rodless mice and it remained possible that they mediate these non-image-forming visual responses, or that rods and cones play redundant roles in this process (Provencio and Foster, 1995; Freedman et al., 1999). The establishment of rodless coneless mice and the demonstration that they exhibit normal circadian and masking responses to light provided powerful evidence of the existence of a novel photoreceptor within the mammalian retina (Freedman et al., 1999; Mrosovsky et al., 2001). Furthermore, the spectral sensitivity of phase shifting and pupillary responses to light was in the range of 480 nm (blue light), outside of the range of known rod and cone opsins (i.e. photopigments) (Lucas et al., 2001; Hattar et al., 2003). Finally, Berson et al. (2002) reported that retinal ganglion cells (RGCs) projecting to the SCN are intrinsically photosensitive, indicating that there had to be a novel photoreceptor system within at least some RGCs.

The discovery of the photopigment melanopsin in photosensitive dermal cells, as well as in the brain and retina, of the African clawed frog (*Xenopus laevis*) by Ignacio Provencio in 1998 brought about the exciting possibility that mealnopsin was the missing mammalian photopigment. In fact, Provencio et al. (2000) subsequently discovered the presence of melanopsin in the human retina and it was later established that retinal cells projecting to the SCN in rats contain melanopsin (Gooley et al., 2001) and that such cells possess intrinsic photosensitivity (Hattar et al., 2002). These melanopsin-containing cells are referred to as intrinsically photosensitive retinal ganglion cells (ipRGCs) and account for 2-5% of all RGCs (Fox and Guido, 2011). Interestingly, mice lacking the gene encoding the melanopsin protein (*Opn4*$^{-/-}$) still retain non-

image-forming visual functions (masking, pupillary light reflex and phase shifting of rhythms to light), although such responses are severely attenuated (Panda et al., 2002; Ruby et al., 2002; Lucas et al., 2003; Mrosovsky and Hattar, 2003). Thus, melanopsin and rod and cone opsins may play redundant roles in the mediation of non-image-forming photic effects on physiology and behavior. In mice lacking rods, cones, and the melanopsin protein, non-image-forming responses to light are completely absent (Hattar et al., 2003; Panda et al., 2003). This finding suggests that rods and cones may either relay photic information important for non-image-forming visual functions through classical RGCs (that are not intrinsically photosensitive) or through ipRGCs themselves, since ipRGCs receive some photic information from rods and cones through bipolar and amacrine cell synapses (Belenky et al., 2003; Ostergaard et al., 2007). In fact, elimination of ipRGCs, through the use of mouse knock-in models (either using *Cre* recombinase or diphtheria toxin) or a saporin-based immunotoxin, established that ipRGCs themselves are needed for rod/cone driven non-image-forming visual functions and that other RGCs are not sufficient for relaying light information needed for these responses to the brain (Goz et al., 2008; Guler et al., 2008; Hatori et al., 2008). Since the discovery of melanopsin and its importance in non-image-forming vision, many types of ipRGCs and their projections to the brain have been documented.

ipRGCs: multiple subtypes and projection patterns

Five basic subtypes of ipRGCs (M1-M5) have been identified in the rodent retina on the basis of their morphology, projection patterns and functions (Berson et al., 2010; Fox and Guido, 2011; Reifler et al., 2015). M1 cells have dendrites in the distal ("OFF") sublamina of the inner plexiform layer (IPL) within the retina; these cells express the highest level of melanopsin, highest intrinsic photosensitivity and have the largest light-evoked currents compared to the

other non-M1 subtypes (Schmidt and Kofuji, 2009; Ecker et al., 2010; Schmidt and Kofuji, 2011; Estevez et al., 2012; Zhao et al., 2014; Reifler et al., 2015). M1 cells can be further subdivided on the basis of whether their somas reside in the ganglion cell layer (GCL) or are displaced to the inner nuclear layer (INL) (Dacey et al., 2005; Jusuf et al., 2007; Berson et al., 2010). Target brain areas of M1 cell projections are described via the use of transgenic mice with tau-LacZ inserted into the melanopsin gene locus; tau-LacZ encodes and produces a β-galactosidase enzyme (that can be visualized with X-gal staining) attached to a signaling sequence from the tau protein that enables it to be transported down the axon (Hattar et al., 2002). This approach revealed that M1 cells project to hypothalamus (ventrolateral preoptic area, SCN, ventral subparaventricular zone, peri-supraoptic nucleus), dorsal and ventral lateral geniculate nucleus (LGN), intergeniculate leaflet (IGL), pretectum (shell of the olivary pretectal nucleus (OPT), posterior limitans) and superior colliculus (SC) (Hattar et al., 2002; Hattar et al., 2006). More recently, M1 cells were further subdivided based on whether they express the transcription factor Brn3b, which is present in most M1 cells and all non-M1 cells (Chen et al., 2011). The targets of Brn3b-negative M1 cells differ from those expressing Brn3b (Chen et al., 2011); whereas, Brn3b-negative M1 cells project to the SCN and part of the IGL (photic and non-photic phase shifting) and are sufficient for photoentrainment and masking, Brn3b-positive M1 cells target the shell of the OPT (pupillary light reflex) and most of the IGL (Chen et al., 2011) and are required for the pupillary light reflex.

Recent studies have elucidated characteristics of non-M1 melanopsin-containing cells within the retina, their projection patterns and the role they may play in vision (Berson et al., 2010; Brown et al., 2010; Ecker et al., 2010; Estevez et al., 2012; Schmidt et al., 2014; Zhao et al., 2014; Reifler et al., 2015). Overall, these ipRGCs (M2-M5) contain less melanopsin than do

the M1 cells. M2, M4 and M5 cells have dendrites in the proximal ("ON") sublamina of the IPL, while M3 cells have dendrites both in the proximal and distal sublamina of the IPL. M4 cells are discerned from M2 cells by their large cell bodies (largest of all the subtypes) and M5 cells are distinguished from other subtypes due to their small receptive field size and large number of dendritic branch points. Non-M1 cells project to the SCN and IGL (similar to M1 cells), but also densely innervate the dorsal LGN, core of the OPT and SC (Baver et al., 2008; Brown et al., 2010; Ecker et al., 2010; Zhao et al., 2014) and play a role in conventional visual responses, such as contrast sensitivity and pattern discrimination (Ecker et al., 2010; Schmidt et al., 2014). Additionally, the melanopsin gene is alternatively spliced leading to the production of a long (OPN4L) or short (OPN4S) isoform of melanopsin and these isoforms are found to different degrees in different subtypes of melanopsin cells; M1 cells co-express OPN4L and OPN4S, while non-M1 cells only express OPN4L (Pires et al., 2009). The two isoforms, amazingly, contribute to different behavioral responses to light. OPN4S is essential for the pupillary light reflex, while OPN4L is essential for masking responses of wheel running and general activity to light; both OPN4S and OPN4L mediate photic phase shifting and the induction of sleep by light (Jagannath et al., 2015). Thus, different isoforms of a single gene can facilitate very different non-image-forming visual responses to the same light stimulus.

ipRGCs co-store glutamate and pituitary adenylate cyclase-activating polypeptide (PACAP)

ipRGCs use both glutamate and pituitary adenylate cyclase-activating polypeptide (PACAP) for neurotransmission and PACAP is found exclusively in the subset of RGCs that contain melanopsin (Hannibal et al., 2000; Hannibal et al., 2002; Bergstrom et al., 2003; Hannibal et al., 2004). PACAP is cleaved from preproPACAP into PACAP27 or PACAP38 with

the latter being the predominant form (Hannibal, 2006; Vaudry et al., 2009; Harmar et al., 2012). PACAP exerts its effects through three receptor proteins, PAC1, VPAC1 and VPAC2; the first of these is selective for PACAP and the latter two respond to both PACAP and vasoactive intestinal peptide (Hannibal, 2006; Vaudry et al., 2009; Harmar et al., 2012). Two studies of transgenic mice, one lacking PACAP and the other the PAC1 receptor, indicate that PACAP-PAC1 mediated signaling is needed to obtain complete masking and phase shifting responses to light (Hannibal et al., 2008; Kawaguchi et al., 2010). However, there is one report of a transgenic mouse model lacking PACAP that displayed normal masking responses to light intensities less than 50 lux (Colwell et al. 2004). The apparent discrepancies may be due to differences in the strains of mice that were used, and/or in the masking protocols employed (Hannibal, 2006). Injections of PACAP alone (either intracerebroventricular or directed at the SCN) can induce phase shifts like those elicited by light pulses (when the dose is within the nM range), while higher doses (in the μM range) induce phase shifts like those seen following exposure to non-photic stimuli (Harrington et al., 1999; Hannibal et al., 2008).

ipRGCs are the only cells within the retina that contain PACAP, which makes this peptide a useful marker of the central projections of ipRGCs in animals in which transgenic models cannot be produced. This approach has revealed that the distribution of PACAP fibers emanating from the retina is the same in hamsters, Norway rats and macaques as that of the ipRGCs described in transgenic mouse models (Bergstrom et al., 2003; Hannibal and Fahrenkrug, 2004; Hannibal et al., 2014).

Brain regions associated with masking

Most of what is known about the neural circuits involved in masking comes from several lesion studies that were focused on brain areas now known to receive input from ipRGCs, such as the SCN, LGN, IGL, OPT, and visual cortex. Two such studies examined effects of SCN lesions on masking in nocturnal hamsters and yielded very different results. One found that the lesions greatly reduced wheel running activity, but had no effect on masking in the context of an ultradian (3.5:3.5) light/dark cycle; i.e. animals still exhibited less activity during the light than the dark phase of the 7 hour cycle (Redlin and Mrosovsky, 1999a). In the second study, conducted by Li et al. (2005) using the same testing protocol, SCN lesions abolished masking responses to light; retinal projections were traced in that study to verify the completeness of the SCN lesion and they also revealed damage to the ventral subparaventricular zone (vSPZ). Li et al. (2005) suggested that either the SCN or vSPZ is necessary for masking in nocturnal hamsters (Li et al., 2005). In albino Norway rats, SCN lesions had no effect on the increase in REM sleep triggered by darkness (Sisk and Stephan, 1982) and only slightly attenuated, but did not abolish, the suppression of general activity by light (Scheer et al., 2001). Interestingly, lesions that almost completely destroyed the SCN in diurnal grass rats had little or no effect on masking (*Gall et al., unpublished observations*). It may be that the SCN/vSPZ is necessary for masking of wheel running by light in nocturnal hamsters, but that this region may not be essential for light/dark effects on general activity/sleep in nocturnal Norway rats or general activity in diurnal grass rats. Thus, more research is needed to determine whether the SCN may modulate certain aspects of masking and to determine how this may differ between diurnal and nocturnal species.

Other studies have examined the effects of lesions of the visual thalamus, pretectum and cortex on masking. In nocturnal rodents, lesions of the dorsal LGN (mice: Edelstein and

Mrosovsky 2001), IGL (hamsters: Redlin et al. 1999), SC (mice: Redlin et al. 2003) and visual cortex (mice: Redlin et al. 2003) all increase the sensitivity such that masking of activity occurs at lower light intensities than it does in control animals. Lesions of the SC/pretectum (including the OPT) abolish the masking response of dark-induced REM sleep in albino rats (Miller et al., 1998). In diurnal Nile grass rats, lesions of the IGL increase nighttime activity overall and masking responses are reversed, such that light decreases activity at night (Gall et al., 2013); a reversal in masking effects of light is also seen in Nile grass rats with OPT lesions (*Gall et al., unpublished observations*). Thus, the IGL and OPT may contribute to the differences in how diurnal and nocturnal species respond to light, but these structures are not necessary for the suppression of activity by light. These lesion studies suggest that the neural pathways mediating masking may be redundant and multiple brain regions may play a role in producing the species-specific masking response (Redlin, 2001). Therefore, pathways that produce negative masking are likely to be quite different from those mediating positive masking, and one may be more important in nocturnal species and the other in diurnal ones.

Overview of chapters

The purpose of this dissertation work was to elucidate the neural pathways mediating the acute effects of light on behavior and how they may differ in a diurnal versus nocturnal brain. The research described below approaches this issue via: (1) examination of direct effects of light on behavior and the brains of day- and night-active animals (Chapters 2 and 3), (2) characterization of non-image-forming visual pathways that originate in ipRGCs in a diurnal rodent (Chapter 4), and (3) examination of the hypothesis that anatomical/functional differences

associated with chronotype exist within brain regions that have been implicated in masking and that receive input from these ipRGCs (Chapter 5).

CHAPTER 2: Behavioral Masking and cFOS Responses to Light in Day and Night Active Grass Rats

INTRODUCTION

Light shapes an organism's daily activity profile in two general ways. First, it entrains endogenously generated circadian rhythms to the environmental light-dark cycle, which it does in mammals through a projection from the retina to the suprachiasmatic nucleus (SCN) (Moore and Eichler, 1972; Moore and Lenn, 1972; Stephan and Zucker, 1972). Light can also have more acute effects on arousal, a process known as masking. Whereas bright light increases arousal in diurnal species ("positive masking"), it decreases arousal and induces sleep in nocturnal ones ("negative masking") with the reverse pattern of responsiveness often being true of darkness (Mrosovsky, 1999). However, masking can vary among individuals within a species and can sometimes be modified in striking ways by changes in the environment. For example, in some diurnal rodents masking effects of light can be reversed with the introduction of a running wheel (Redlin and Mrosovsky, 2004; Weinert et al., 2007; Vivanco et al., 2009).

Here we used the Nile grass rat to examine intraspecific variation in masking responses to light and darkness. One advantage of studying variation in masking *within* a species is that any differences in response to light can be attributed to the chronotype and not merely to a difference between the species. The Nile grass rat is native to sub-Saharan Africa and is strongly diurnal in the field and under standard laboratory conditions (Katona and Smale, 1997; McElhinny et al., 1997; Blanchong and Smale, 2000). This species is adapted to a diurnal way of life as indicated by body temperature rhythms, sleep, and reproductive behavior (McElhinny et al., 1997; Schwartz and Smale, 2005); the visual system is also equipped for a diurnal life with a ratio of cones to rods that is 10x higher than that seen in typical nocturnal rodents (Gaillard et al., 2008;

Hut et al., 2012) and a superior colliculus that is the same size as that of a nocturnal laboratory rat four times its size (Gaillard et al., 2008; Gaillard et al., 2013). When given access to running wheels, however, some grass rats run during the day, while others restrict their wheel running to the night (Blanchong et al., 1999). These night active (NA) grass rats retain some diurnal characteristics, such as the timing of the body temperature nadir (Blanchong et al., 1999) and longer nighttime sleep bout lengths (Schwartz and Smale, 2005), while displaying some nocturnal characteristics, such as having PER1/2 rhythms in many extra-SCN oscillators that are 180° out of phase with those of day active (DA) grass rats (Ramanathan et al., 2010). The NA profile of wheel running persists in constant darkness (Mahoney et al., 2001), suggestive of a change in the circadian regulation of activity in these animals.

In the current study, we tested the hypothesis that mechanisms controlling masking and the circadian drive for activity are associated. A circadian drive for daytime activity together with an arousal response to light may help consolidate locomotor activity and confine it to the daytime in diurnal species, with the reverse processes occurring in nocturnal ones. If the above coupling hypothesis is correct, then masking responses to bright light and darkness should depend upon the prevailing chronotype of the individual. To determine whether this is the case, we exposed DA and NA grass rats to pulses of light and darkness across the night and day, respectively.

The second part of this study focused on potential brain regions mediating masking and whether the responsiveness of cells in these areas to light is dependent upon the behavioral response of the animal. Currently, very little is known about how the neural pathways contributing to this process may differ in diurnal and nocturnal animals. Lesion studies suggest that two brain areas that receive direct retinal input, the intergenticulate leaflet (IGL) of the

thalamus (Redlin et al., 1999; Gall et al., 2013) and the olivary pretectal area (OPT) of the pretectum, may play a role (Miller et al., 1998). Both the IGL and OPT receive input from melanopsin-containing retinal ganglion cells, which are essential for normal circadian entrainment, the pupillary light reflex, and masking responses to light in nocturnal mice (Hattar et al., 2006; Goz et al., 2008; Guler et al., 2008; Hatori et al., 2008). Melanopsin-containing retinal ganglion cells are also present in the retina of diurnal mammals, including two species of *Arvicanthis* (*A. niloticus*, Langel et al., 2015; *A. ansorgei*, Karnas et al. 2013) and humans (Provencio et al., 2000; Hannibal et al., 2004), but their specific role in irradiance detection in diurnal species is yet to be determined. Here we measured the light-induced expression of the immediate early gene cFOS in the IGL and OPT in grass rats to determine if these structures respond differently in the diurnal and nocturnal chronotypes.

METHODS

Animals

Adult female grass rats from a breeding colony maintained at Michigan State University were used in this study. Animals were singly housed in plexiglass cages (34 x 28 x 17 cm^3) with access to food (PMI Nutrition, Prolab RMH 2000, Brentwood, MO, USA) and water *ad libitum*. To identify day active (DA) and night active (NA) wheel runners, each cage was equipped with a running wheel (17cm diameter, 8cm width). Each wheel revolution was picked up by a monitoring system (VitalView, MiniMitter, Bend, OR, USA) and measured as a single count. General activity (GA) was monitored via an infrared (IR) detection system (VitalView, MiniMitter, Bend, OR, USA) with sensors located on the lid of each cage. For both wheel running activity (WRA) and GA, all counts were binned into 5-minute periods. Actograms were

created using ClockLab (Actimetrics, Inc.). All experiments we performed in accordance with guidelines established by the National Institutes of Health Guide for the Care and Use of Laboratory Animals and the Michigan State University Institutional Animal Care and Use Committee. All efforts were made to minimize the number of animals used in these experiments.

Chronotype Determination

Animals were housed with a running wheel for at least 2 weeks in a 12:12 LD cycle (40-175 lux at side of cage; variation in light intensity had no effect on present results). White fluorescent bulbs provided illumination during the light period and a red light (<1 lux) was kept on throughout the night. The proportion of wheel running that occurred during the light period divided by the total wheel running across the 24-h day was used in categorization of animals as DA or NA. Animals were considered to be DA when that ratio was >50% and wheel running activity occurred across the light phase, and as NA when that ratio was <50% and at least 100 wheel revolutions occurred between Zeitgeber Time (ZT, where ZT0 = lights-on) 18-20. Animals that fit neither of the above criteria were excluded from the analyses. After 3 weeks, DA and NA animals were randomly reorganized in the housing room to ensure that equal numbers of DA and NA animals would have access to IR sensors, which were limited.

Behavioral Response of Masking to 2-h Pulses in LD Conditions

Administration of each 2-h pulse of darkness or light (during the light and dark phases of the 12:12 LD cycle, respectively) involved a 3 day protocol that was repeated in succession; this design was similar to those used by Redlin and Mrosovsky (2004) and Shuboni et al. (2012) (see Figure 2.1). The first day (maintenance day) was used for weekly cage changes and upkeep of

the housing room. The second day (baseline day) was used for comparison to the next day's activity during the light or dark pulse. On the third day (experimental day) all animals received a single dark (room lights turn off) or light (room lights turn on) pulse. Dark pulses (DPs) were administered at ZTs 0, 2, 4, 6, and 8, and light pulses (LPs) at ZTs 12, 14, 16, 20, and 22. All light pulses were administered before any of the dark pulses. The light pulses were given in the order of ZT16, 14, 22, 20, and 12, followed by the dark pulses in the order of ZT8, 2, 6, 4, and 0. It took a total of 30 days to complete the protocol (10 dark/light pulses given during a 3-day protocol). Some animals switched their wheel running patterns after the start of the experiment and were excluded from the analyses. Two cohorts of animals were used for the dark pulse portion of the experiment because the number of DA animals remaining at the conclusion of the series of light pulses was low. Thus, a total of 46 animals were used (n = 30 from cohort 1 exposed to both light and dark pulses and n = 16 from cohort 2 exposed to only dark pulses). Of those 46 animals, 22 did not meet the criteria for inclusion as either DA or NA subjects and were excluded from analysis (n = 15 from cohort 1 and n = 7 from cohort 2). The data below, therefore, come from 15 of 30 animals exposed to the series of light pulses (n = 4 DA, 11 NA), and 24 of 46 animals exposed to the dark pulses (n = 9 DA, 15 NA).

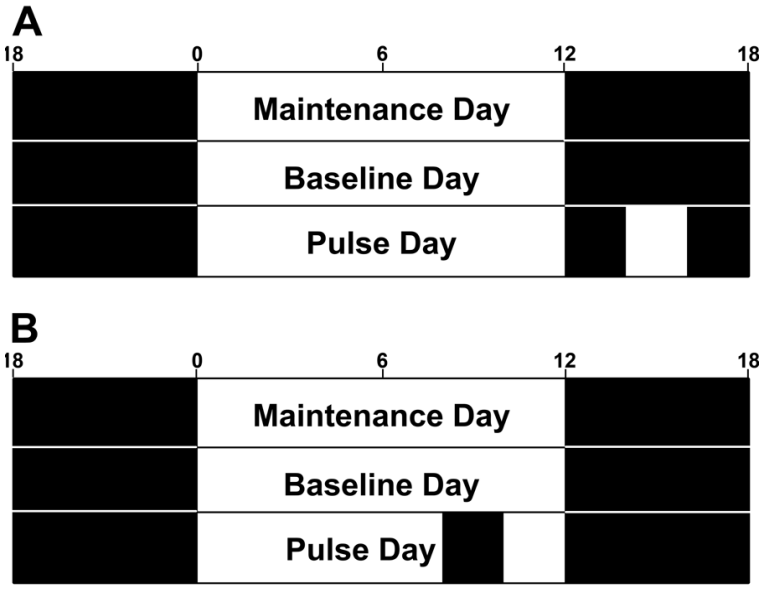

Figure 2.1. Basic protocol illustrated with two examples. White bars indicate periods of lights on; dark bars indicate periods of lights off. Day 1 and 2 (Maintenance Day and Baseline Day, respectively) consisted of a 12:12 light/dark cycle. Cage cleaning occurred on the Maintenance Day, while the animals were left undisturbed on the Baseline Day. A single 2hr light pulse (ZT14 pulse represented in A) or dark pulse (ZT8 pulse represented in B) was administered on Day 3. This 3-day protocol was then repeated for the next dark or light pulse. Dark pulses were given at ZTs 0, 2, 4, 6, and 8, while light pulses were given at ZTs 12, 14, 16, 20, and 22. The entire experimental design took 30 days to complete.

Brain Responses to Light Pulses

A total of 35 grass rats were used to measure light-induced cFOS expression in response to a 1-h LP at ZT14. In this experiment some DA grass rats did not show a behavioral response at all to the LP and they were evaluated as a separate group. Overall this study included 8 DA controls unexposed to light, DA animals with (n = 7) and without (n = 5) a light-induced increase in activity, 7 NA controls and 8 NA animals exposed to light (all of which decrease their activity

in response to the light).

Tissue collection

Animals were sacrificed immediately following the 1-h LP at ZT14, or at the same time on a control night with sodium pentorbital (Nembutal; Ovation Pharmaceutical, Deerfield, IL, USA; 0.5 cc/animal) and perfused transcardially with 0.01M phosphate-buffered saline (PBS, pH = 7.4) followed by 4% paraformaldehyde (Sigma-Aldrich, St. Louis, MO, USA) with 75 mM lysine (Sigma-Aldrich) and 10 mM sodium periodate (PLP; Sigma-Aldrich) in 0.1M phosphate buffer (PB). Brains were harvested and post-fixed in PLP for 4-h followed by at least 24-h in 20% sucrose solution in 0.1M PB at 4°C. Coronal sections (30μm) were cut on a cryostat and collected in 3 alternating series. Tissue was stored in cryoprotectant (Watson et al., 1986) at -20°C until further processing.

Immunohistochemistry (IHC)

One series of sections from each animal was processed for staining of cFOS using methods described in detail in Castillo-Ruiz et al. (2010). The rabbit anti-c-Fos primary antibody (Santa Cruz Biotechnology, Dallas, TX) was used at a concentration of 1:25,000 and the secondary biotinylated donkey anti-rabbit antibody (Jackson ImmunoReseach Laboratories, West Grove, PA) was used at a concentration of 1:200; normal donkey serum used as a blocking agent. Following the reaction, sections were mounted on gelatin-coated slides, dehydrated, and coverslipped using dibutyl phthalate xylene (DPX; Sigma-Aldrich).

Cell-Counting Procedure

cFOS-immunoreactive cells were counted using a camera lucida drawing tube mounted on a Zeiss light microscope (Axioskop 2 Plus; Zeiss, Göttingen, Germany) by an investigator unaware of the experimental group to which each animal belonged. Bilateral counts across two sections were averaged for each brain area. Cells were counted using a 10x (IGL) or 25x (OPT) objective and manual traces of the borders of the caudal IGL and rostral OPT were made corresponding to atlas plate 71 of the rat brain atlas by Paxinos and Watson (5^{th} edition)(Paxinos and Watson, 2005).

Statistical Analysis

Wheel running and general activity were each subject to four different two-factor repeated measures analyses of variance (ANOVA). Specifically, for each of these dependent variables separate analyses were done on data from DA and NA animals, and the analyses of effects of dark pulses during the light period and of light pulses during the dark period were done separately. In each of these ANOVAs one factor was time (ZTs 0, 2, 4, 6, 8 for the analyses of effects off dark pulses during the light period and ZTs 12, 14, 16, 20, and 22 for analyses of effects of light pulses during the dark period), and the second factor was light treatment (light pulse vs. baseline in one analysis and dark pulse vs. baseline in the other analysis). Each of the two factors was treated as repeated measures (i.e. there were no between subject factors in any of the analyses). Significant interactions between time and light treatment were followed by analyses of each light treatment at each time point via the use of paired sample t-tests (2-tailed test). Significant main effects of time were followed up with post-hoc analyses using pairwise comparisons with a Bonferroni adjustment.

In the cFOS experiment, a two-factor ANOVA was used to determine whether cFOS expression in each brain area was affected by chronotype (factor 1; DA vs. NA) and pulse (factor 2; control vs. light pulse); cFOS counts were square root transformed to equalize the variance amongst the groups. Significant interactions were broken down by analyses of simple main effects of pulse for each chronotype. Two distinct groups arose within the DA grass rats (those that responded with an increase in WRA to the ZT14 light pulse vs. those that did not change their WRA at all), so a multivariate one-factor ANOVA was used to test whether cFOS expression in each brain area was affected by group (control vs. light pulsed with masking response vs. light pulsed with no masking response). A post-hoc Tukey test was conducted to identify significant pairwise mean differences between the DA groups. Two distinct DA groups did not arise during the 2-h pulse at ZT14 in the first experiment, so the DA animals were analyzed as a single group in that study. SPSS version 19 was used for all statistical tests and tests were considered significant if $p < .05$. Data are presented as the mean ± standard error of the mean (SEM) in all figures.

RESULTS

Wheel running and general activity of day and night active grass rats

DA grass rats (n = 10) displayed bouts of WRA across the light phase of the light-dark cycle, whereas NA (n = 14) grass rats restricted their WRA to the dark phase. Representative actograms of a single DA and NA grass rat are displayed in Figure 2.2. Records of GA revealed that DA grass rats were active in their cages primarily during the day (Figure 2.2A). Interestingly, though they did not run in their wheels during the day, NA grass rats were very active in their cages at this time (Figure 2.2B).

DA grass rats ran more in their running wheels during the day, exhibited a gradual decrease in activity after lights off, and an anticipatory increase in activity before lights on (Figure 2.2C). NA grass rats ran in their wheels very little during the day, had an abrupt and rapid increase in WRA at lights off, which was sustained until around ZT20 to ZT21 at which point WRA decreased substantially; NA grass rats underwent an increase in WRA before lights on that was very similar to that seen in DA grass rats, but they stopped running abruptly when the lights came on. Our measures of GA of DA and NA grass rats were influenced by the revolutions of the running wheel, so the representation of the average GA looks similar to that of the average WRA (Figure 2.2D). However, NA grass rats displayed higher bouts of general activity across the daytime (Figure 2.2D).

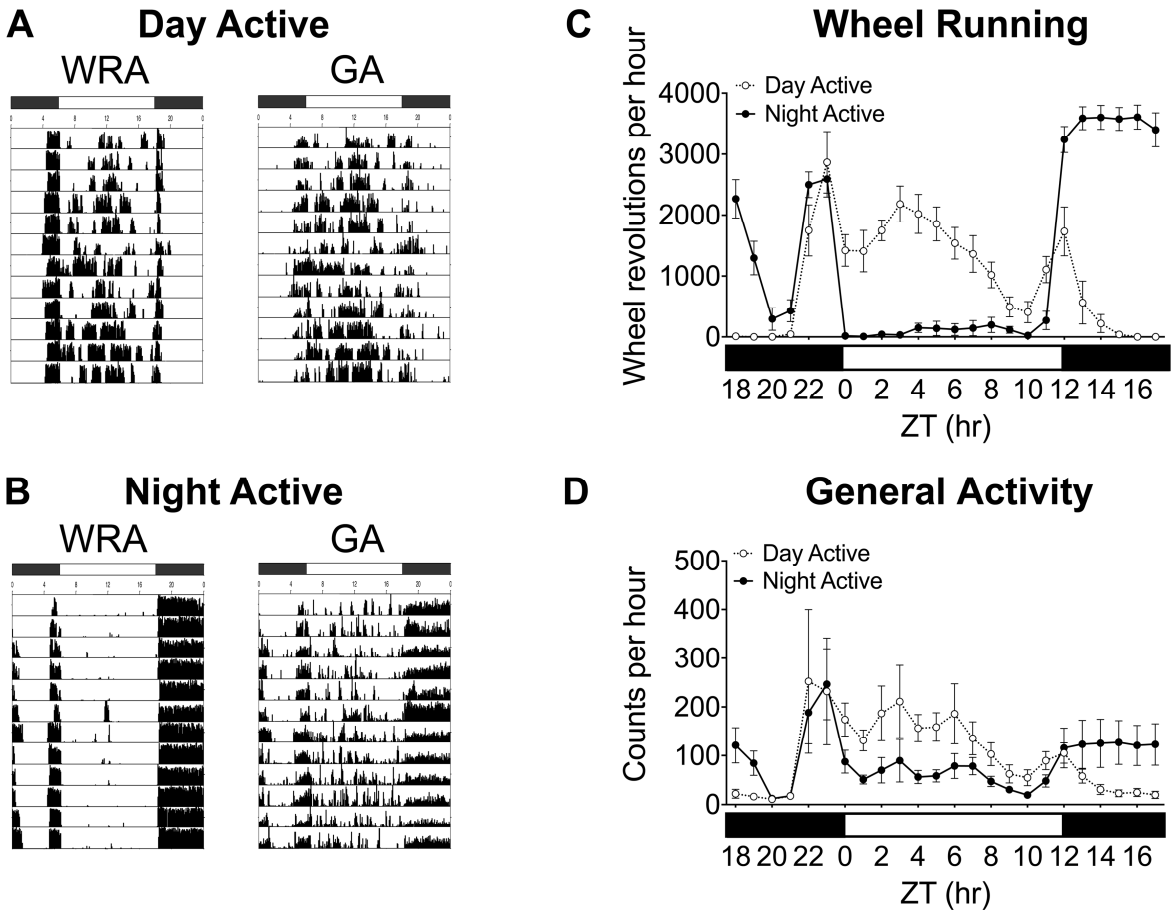

Figure 2.2. Actograms of wheel running activity (WRA) and general activity (GA) of a single DA (A) and NA (B) grass rat, as well as average wheel revolutions (±SEM; C) and general activity counts (±SEM; D) over a 4 day monitoring period in 12:12 LD for all of the DA (open circles) and NA (closed circles) grass rats used in this study. White bars indicate lights on, and dark bars indicate lights off.

Effect of 2-h light pulses on WRA and GA

WRA among DA animals was not affected by time (p = .25) nor by an interaction between time and light (p = .32) and, although light pulses at night appeared to increase WRA, the effect did not reach significance (main effect of lighting condition: $F_{1,3}$ = 6.90, p = .08) (Figure 2.3A). Among NA grass rats, the time x pulse interaction was significant ($F_{4,40}$ = 11.92, p < .01) (Figure 2.3B) such that WRA decreased in response to light at all time points (p < .01) except ZT20 (p = .33).

GA among DA grass rats was significantly increased by light pulses at night ($F_{1,3}$ = 12.36, p = .04) but there was no main effect of time (p = .18) nor an interaction between time and lighting condition (p = .19) (Figure 2.3C). Among NA grass rats, GA was not affected by the light pulses (p = .20), time (p = .20), nor by an interaction between these two variables (p = .19) (Figure 2.3D).

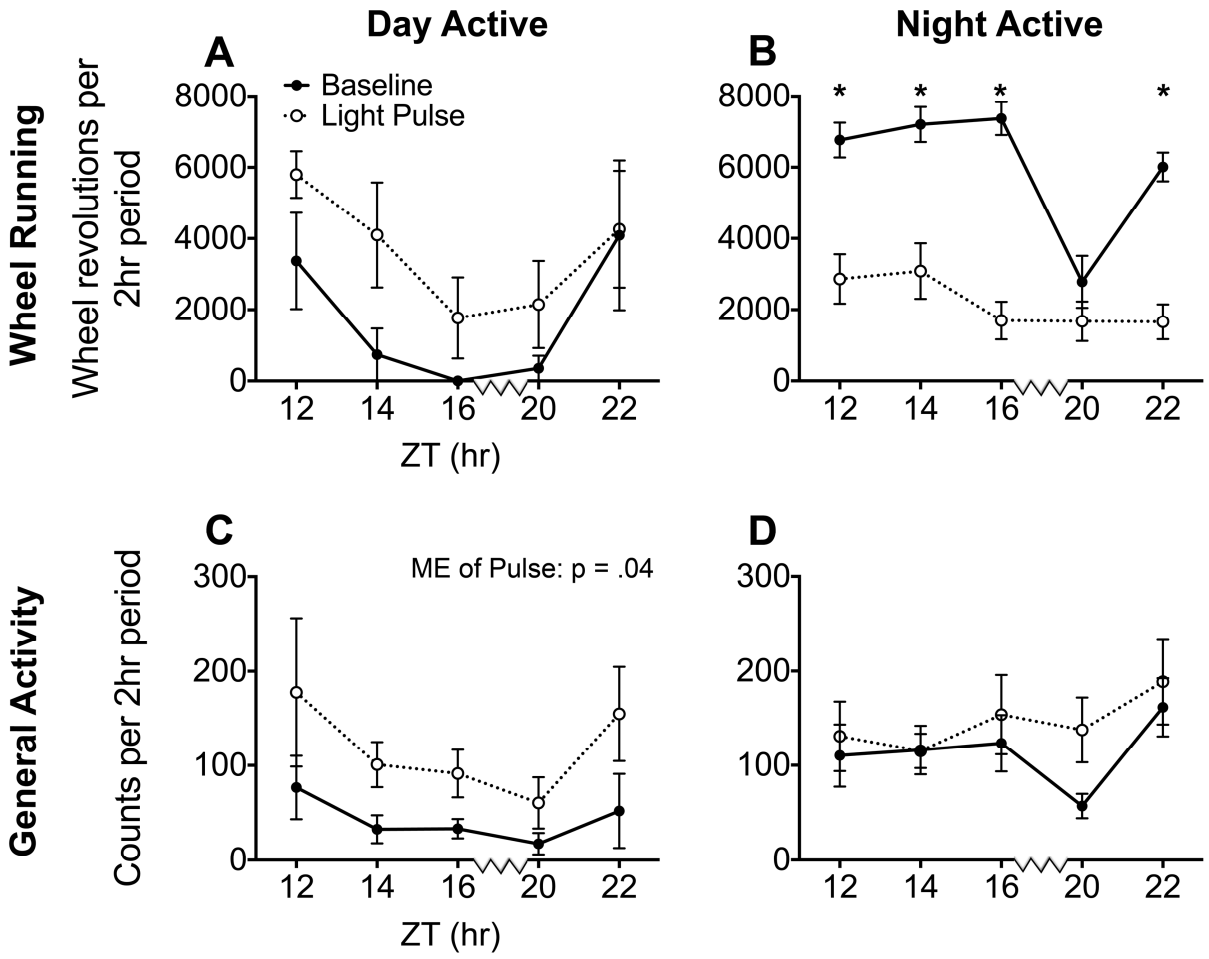

Figure 2.3. Average wheel running (A, B) and general activity (C, D) of DA and NA grass rats during each 2-h light pulse and the same 2-h on the previous day. Overall, DA grass rats tended to increase their wheel running in response to the light pulses (A), while NA grass rats decreased their wheel running at all time points except ZT20 (B). The general activity of DA grass rats was significantly increased overall in response to the light pulses (C), while the general activity of NA grass rats did not change. *Asterisks indicate a significant difference between the baseline night and the corresponding light pulse night. Light pulses were delivered at 2-h intervals with the exception of the 4-h interval indicated by the jagged line on the x-axes between ZT16 and ZT20.

Effect of 2-h dark pulses on WRA and GA

Dark pulses during the day appeared to decrease WRA in DA grass rats though the effect was not significant (main effect of lighting condition: $F_{1,8} = 4.06$, $p = .08$); this ANOVA also revealed no effect of time ($p = .50$) and no interaction between time and lighting condition ($p = .28$) (Figure 2.4A). In the NA grass rats, dark pulses significantly increased WRA ($F_{1,14} = 8.08$, $p = .01$), while the interaction between time and lighting condition ($F_{4,56} = 3.63$, $p = .06$) and the main effect of time ($F_{4,56} = 3.37$, $p = .06$) both approached significance such that the main effect of lighting condition appeared to be driven primarily by the dark pulse given during the early part of the day (ZT0) (Figure 2.4B).

Dark pulses decreased GA in DA grass rats (main effect of lighting condition: $F_{1,8} = 18.74$, $p < .01$), but there was no main effect of time ($p = .20$) and no interaction between time and lighting condition ($p = .54$) (Figure 2.4C). Among NA grass rats there were no main effects of lighting condition ($p = .76$) or time ($p = .10$), and there was no interaction between these variables ($p = .20$) (Figure 2.4D).

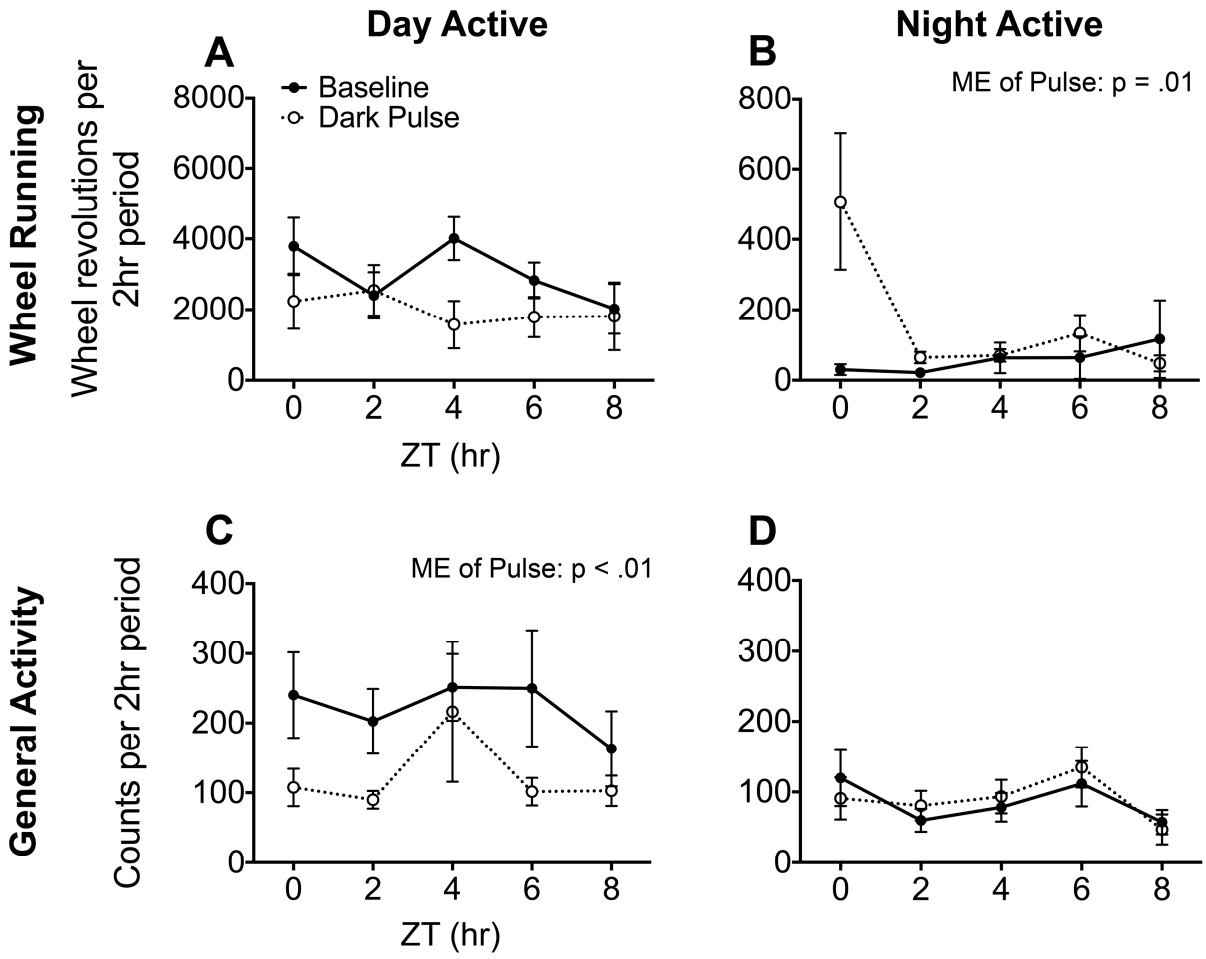

Figure 2.4. Average wheel running (A, B) and general activity (C, D) of DA and NA grass rats during each 2-h dark pulse and the same 2-h on the previous day. Overall, DA grass rats tended to decrease their wheel running in response to the dark pulses (A), while NA grass rats significantly increased it (B). The general activity of DA grass rats was significantly decreased overall in response to the dark pulses (C), while the general activity of NA grass rats did not change in response to the dark pulses (D).

cFOS expression in response to 1-h LP starting at ZT14

WRA of all groups included in this experiment is illustrated in Figure 2.5. In the IGL, there was a significant interaction between chronotype and pulse ($F_{1,25}$ = 7.90, p < .01), such that a 1-h LP at night induced an increase in cFOS in the IGL of DA grass rats ($F_{1,13}$ = 27.48, p < .01), but not NA grass rats (p = .63)(Figure 2.6A-B).The same pattern was seen in the OPT, where the interaction between chronotype and pulse was significant ($F_{1,25}$ = 4.13, p = .05), such that the 1-h LP increased cFOS in DA ($F_{1,13}$ = 13.03, p < .01) but not NA (p = .63) (Figure 2.7A-B) grass rats. cFOS was high in the IGL and OPT of both control and light-exposed NA animals.

As noted above, in one subset of DA animals WRA did not change in response to the LP, which enabled us to examine relationships between effects of light on activity and on cFOS more precisely. Within the IGL, cFOS expression differed between the DA groups ($F_{2,17}$ = 10.01, p < .01), such that it was only induced by the LP in those DA animals whose behavior was also increased (p < .01); DA grass rats that did not respond behaviorally to the LP did not differ from DA controls (p = .67) (Figure 2.6C). The same pattern was seen in the OPT, where cFOS expression differed between the groups ($F_{2,17}$ = 7.98, p < .01), such that it was only elevated by light in DA animals whose activity was also stimulated by that light (p < .01); cFOS did not differ between DA controls and those whose behavior was unresponsive to the light (p = .93) (Figure 2.7C).

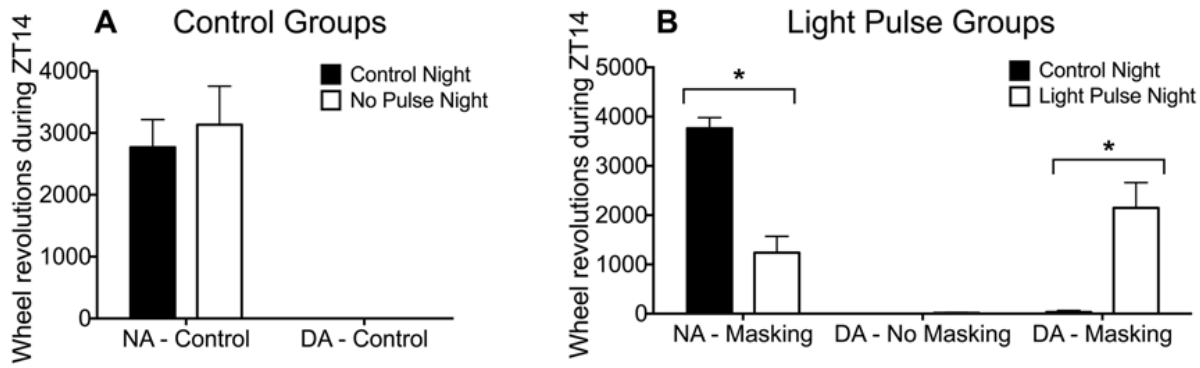

Figure 2.5. Wheel revolutions at ZT14-ZT15 of animals used in the cFOS experiment. Animals in the control groups (A) did not receive a 1hr light pulse prior to sacrifice and wheel-running activity before sacrifice (ZT14-ZT15) is depicted by the white bars (labeled "No Pulse Night"). Paired t-tests indicate that there was no difference in wheel running on the night of sacrifice (No Pulse Night) compared to the same hour the night before (Control Night; dark bars) for neither the night active (NA) control group ($p = .15$) nor the day active (DA) control group ($p = .62$). The animals in the light pulse groups (B) received a 1hr light pulse from ZT14-ZT15 on the "Light Pulse Night" (white bars). Paired t-tests indicate that there was a significant difference in wheel running during the 1hr light pulse compared to the same 1hr the night before (Control Night; dark bars) in the NA group ($p < .01$), such that the 1hr light pulse significantly reduced wheel running in these animals. The DA group that displayed a masking response to light (DA – Masking) significantly increased their wheel running in response to the 1hr light pulse ($p = .01$), while the DA group that did not show a masking response (DA – No Masking) displayed virtually no wheel running during the 1hr light pulse or during the same hour on a control night ($p = .19$).

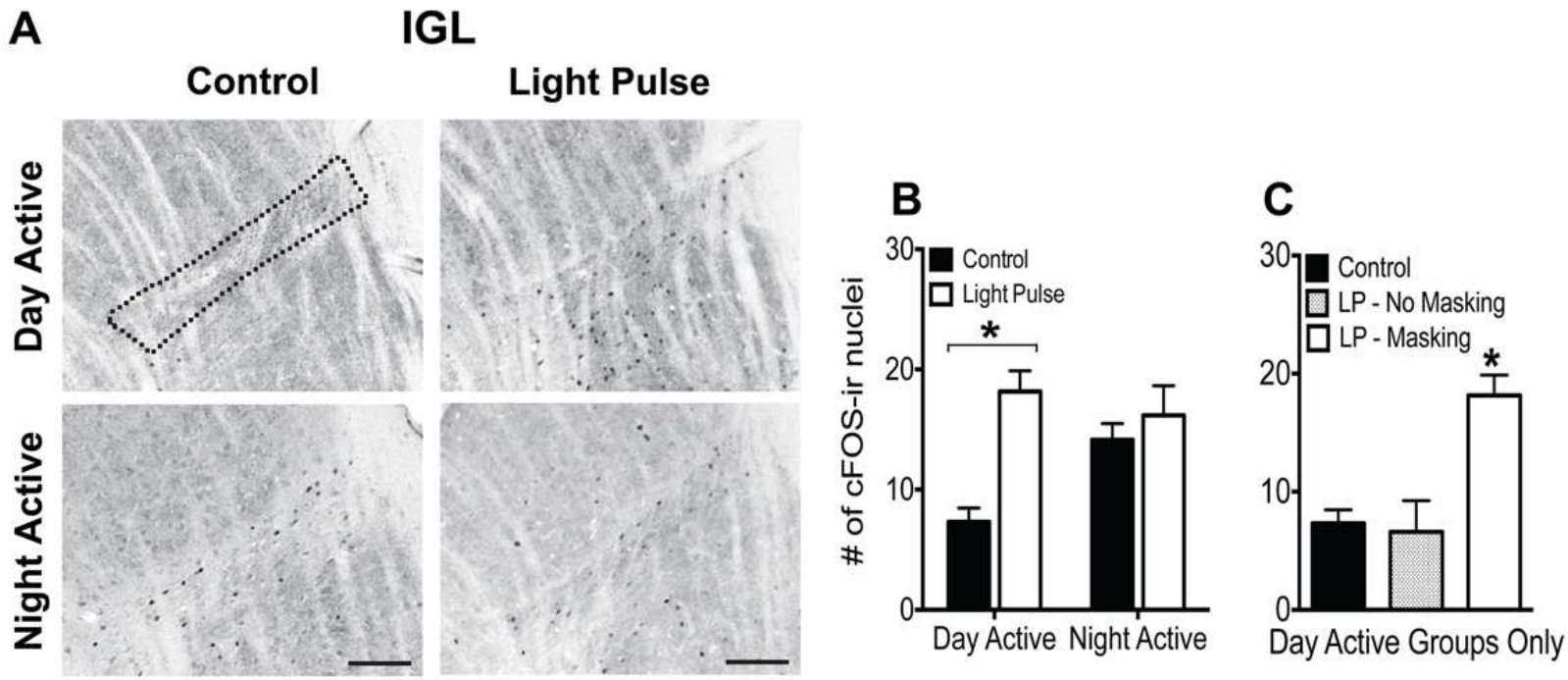

Figure 2.6. cFOS expression in the IGL of DA and NA grass rats on a control night or after a 1-h light pulse at ZT14. (A) Representative photomicrographs of cFOS expression in the IGL of day and night active grass rats on a control night or after a 1-h light pulse at ZT14. Scale bars represent 100μm. (B) Numbers of cells expressing cFOS in the IGL of DA and NA grass rats perfused on a control night (DA: n = 8; NA: n = 7) or after a 1-h light pulse at ZT14 (DA: n = 7; NA: n = 8). (C) A third group of DA grass rats received a light pulse at night but did not display a behavioral response to it (LP – No Masking; n = 5) and the cFOS expression within this group is plotted with the other two DA groups (Control; LP – Masking). Asterisks indicate a significant elevation of cFOS expression in the IGL of the DA (B) or a significant elevation relative to all DA groups (C).

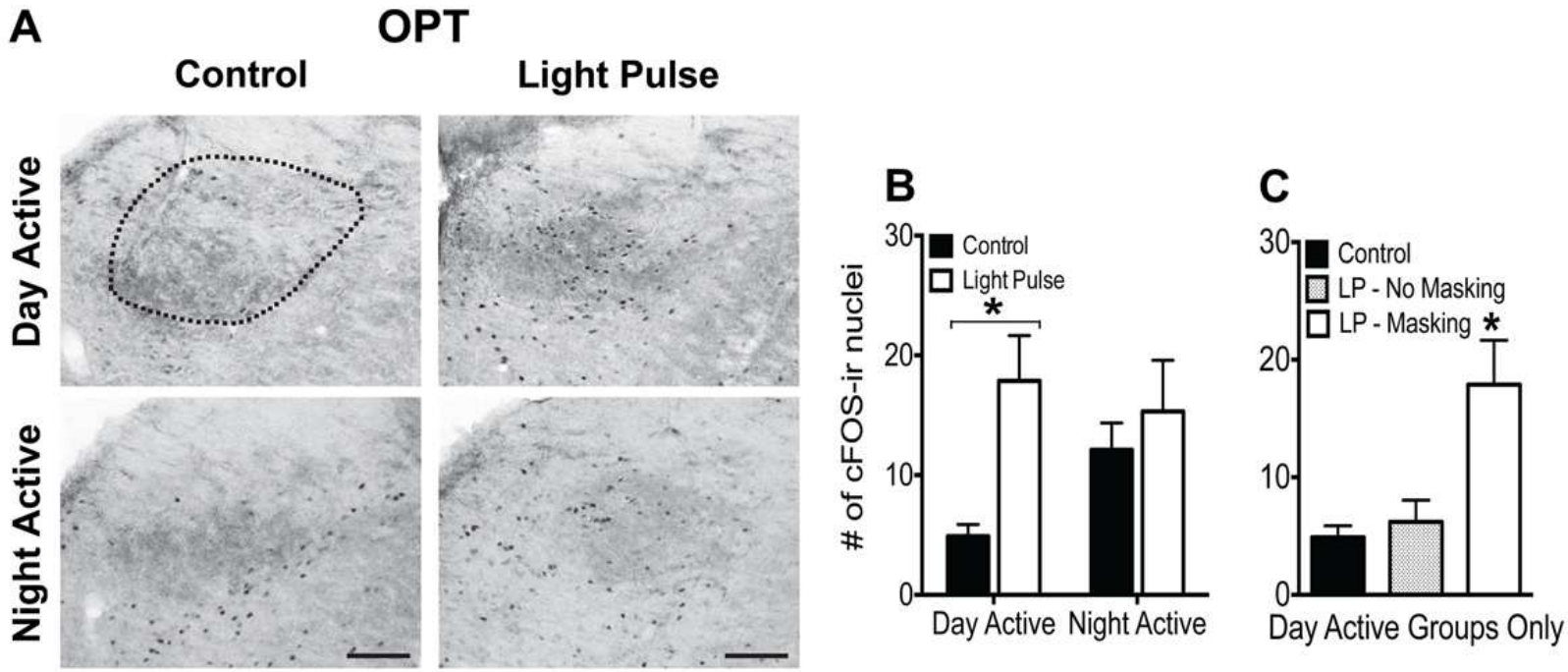

Figure 2.7. cFOS expression in the OPT of DA and NA grass rats on a control night or after a 1-h light pulse at ZT14. (A) Representative photomicrographs of cFOS expression in the OPT of DA and NA grass rats on a control night or after a 1-h light pulse at ZT14. Scale bars represent 100μm. (B) Group averages of the number of cells expressing cFOS in the OPT of DA and NA grass rats perfused on a control night (DA: n = 8; NA: n = 7) or after a 1-h light pulse at ZT14 (DA: n = 7; NA: n = 8). (C) A third group of day active grass rats received a light pulse at night but did not display a behavioral response to it (LP – No Masking; n = 5) and the cFOS expression within this group is plotted with the other two day active groups (Control; LP – Masking). Asterisks indicate a significant elevation of cFOS expression in the OPT of the DA group (B) or a significant elevation relative to all DA groups (C).

DISCUSSION

The effects of light on resetting the phase of circadian rhythms are the same in the DA and NA grass rats, as their phase response curves are virtually indistinguishable (Mahoney et al., 2001), but here we found that mechanisms mediating the direct effects of light on WRA are clearly somewhat different. This basic distinction has been well established when nocturnal and diurnal species are compared (Smale et al., 2003), but not when individual differences within a species are considered. Individual differences are particularly interesting because they reveal the presence of a high degree of plasticity. That is, the NA pattern is induced in some animals by the presence of a running wheel, but these animals are diurnal with respect to both masking and circadian influences on general activity when there is no wheel. This suggests that two key drivers of an animals' adaptation to its temporal niche, the circadian influence on activity and masking, may be linked in some way at a mechanistic level in these animals.

A previous study from Redlin and Mrosovsky (2004) examined masking responses to changes in lighting intensity in grass rats that were maintained with and without running wheels. All of their animals were diurnal with respect to GA but when the wheel was introduced a range of patterns emerged. While the absolute level of WRA during the day was quite variable, the ratio of dark vs. light phase WRA was significantly higher than the dark vs. light ratio of GA (in the absence of a wheel). Redlin and Mrosovsky (2004) also found that exposure to the same photic stimuli could have opposite effects on general activity (which was more diurnal), and wheel running (which was more nocturnal). In the current study we were able to show that photic stimuli presented under identical experimental conditions have very different acute effects on the same behavior (i.e., WRA) as a function of whether the animals are NA or DA, again illustrating

that the differences in the overall patterns of wheel running are associated with differences in masking behavior.

Another difference between the study of Redlin and Mrosovsky (2004) and ours is in the lighting conditions used to assess masking behavior. Redlin and Mrosovsky (2004) exposed animals to one-hour LD cycles across the light phase of a 12:12 LD cycle; during this time, 30min of bright light (1,000 lux, for entrainment purposes) was followed by 30min of light of varying intensities (0 lux to 2,200 lux) and activity was averaged across 30min periods for comparisons. A second approach used by Redlin and Mrosovsky (2004) was to measure overall changes in GA and WRA activity in a skeleton photoperiod. These protocols revealed direct effects of light on wheel running, but did not permit assessment of time of day effects. Our approach revealed that the acute effects of light and darkness were in fact both time-dependent in the NA grass rats (Figure 2.3 and 2.4).

The design of the current study also enabled us to measure WRA and GA concurrently, which revealed interesting differences. Although the NA grass rats reduced their WRA in response to light pulses at night, their GA did not change at that time. Interpretation of this result is complicated by the fact that the IR detectors used for GA picked up some movement of the wheels as well. However, the fact that NA grass rats did significantly reduce WRA, but not GA suggests that either (1) these animals were just as active outside of the wheel with the light pulses as without them or (2) these animals actually increased their activity outside of the wheel when WRA decreased. Either way, inhibitory effects of light in NA grass rats were restricted to wheel running. Furthermore, although NA grass rats restricted their WRA to the night, they were active outside of the wheel during the daytime (refer to Figure 2.2B and D). Both findings highlight the fact that one should be cautious about making general conclusions regarding

masking on the basis of WRA. Wheel running and general activity represent distinct behavioral states and some features of their regulation, such as activation of circuits associated with reward and addiction, are quite different (Sherwin, 1998; Novak et al., 2012).

Several recent studies of rodents that are diurnal in nature have revealed interesting and paradoxical patterns of masking in the lab. Some of these diurnal rodents have nocturnal patterns of GA in the lab (spiny mice, Levy et al. 2007; fat sand rats, Barak and Kronfeld-Schor 2013; tuco tucos, Tomotani et al. 2012) and in others GA is diurnal but the introduction of a wheel can lead to running at night rather than during the day (*Octodon degus*, Kas and Edgar 1999; Nile grass rats, Blanchong et al. 1999; Mongolian gerbils, Weinert et al. 2007). In most of these species light can produce negative masking when the animals are night active. In degus, the NA pattern is produced in some individuals by negative masking and in others by circadian mechanisms (Otalora et al., 2013), whereas the two processes appear to operate together to drive the NA pattern in grass rats. This can be inferred from the facts that (1) wheel running in all NA grass rats was directly inhibited by light (Figure 2.3), and (2) in an earlier study the NA pattern persisted when animals were released into DD from LD (Mahoney et al., 2001). This species difference suggests that the neural mechanisms determining the contribution of masking and circadian processes to chronotype are more tightly linked in grass rats than in degus.

Very little is known about how the neural mechanisms mediating the masking responses to light may differ in diurnal and nocturnal species. Two brain areas that receive dense input from melanopsin-containing retinal ganglion cells and may be important are the IGL and OPT (Hattar et al., 2006). The role of the IGL, which projects to the SCN, has been studied primarily in the context of how it modulates effects of light on the circadian clock, but there is some evidence that it also contributes to the direct effects of light on behavior (Redlin et al., 1999; Gall

et al., 2013). In diurnal grass rats maintained without access to a wheel, IGL lesions lead to night active profiles of general activity both in an LD cycle and in constant conditions, and they lead to a reversal in masking such that animals reduce their activity in response to light (Gall et al., 2013). The OPT, which plays an important role in regulation of pupillary constriction, may also contribute to masking, as lesions of the pretectum that include the OPT attenuate masking of REM sleep by darkness in albino rats (Miller et al., 1998).

The responsiveness of cells within the IGL and OPT to photic stimulation has been examined in multiple studies. Results have been varied, as in some cases there is an induction of cFOS by light, in others there is no change, and in some there is a light induced decrease in cFOS. Differences in the time of day, the duration of exposure to the light, the species, and strains of animals used may have contributed to the discrepancies (Park et al., 1993; Krajnak et al., 1997; Lupi et al., 1999; Prichard et al., 2002; Juhl et al., 2007; Lupi et al., 2012; Shuboni, 2013). Most studies, however, find that light increases cFOS in the IGL and OPT, whether animals are diurnal or nocturnal (Krajnak et al., 1997; Prichard et al., 2002; Juhl et al., 2007; Lupi et al., 2012; Shuboni, 2013).

In the current study, light induced an increase in cFOS in the IGL and OPT of DA grass rats, but in NA grass rats cFOS was high on a control night and was not changed by the 1-h light pulse (Figure 2.6 and 2.7). Furthermore, this induction of cFOS in DA grass rats only occurred in those animals that displayed an increase in WRA in response to the light. This association raises the possibility that increased neuronal activity in the IGL and OPT contributes to the behavioral response to light, and/or that neuronal activity in these brain regions is induced by increased levels of WRA in the DA grass rats (Janik et al., 1995; Smale et al., 2001). The absence of a cFOS response to light in the IGL and OPT of NA grass rats could mean several things: (1)

cFOS may not be an adequate indicator of light responsiveness in these regions, (2) light-induced changes in neuronal activity in these regions may not be necessary for masking, (3) a light-induced decrease in cFOS may take longer than 1 h, or (4) some populations of cells within these regions may be stimulated by light while others are activated by wheel running such that there are no changes in overall levels of cFOS. In fact, in the IGL of rats, neurons that contain enkephalin can respond to photic stimulation with an increase in cFOS, whereas those containing neuropeptide-y do not (Juhl et al., 2007); the latter population expresses higher levels of cFOS in association with heightened WRA in both hamsters and grass rats (Janik et al., 1995; Smale et al., 2001). The phenotype of light responsive cells in these areas needs to be determined in grass rats as it may provide insight into the relationships between their activity and the direction of the behavioral response to light.

Conclusion

In summary, the present study illustrates how masking responses to light and darkness are dependent upon the chronotype of the individual. Our findings suggest a linkage between masking and circadian mechanisms in grass rats such that if the circadian system drives WRA up at night, that activity can be directly suppressed by light, and vice versa. The mechanisms responsible for the association between masking and circadian regulation may help individuals occupy different temporal niches when environmental conditions change. It is tempting to speculate that neural processes accounting for the plasticity of masking responses to light exist within brain areas that receive input from melanopsin-containing retinal ganglion cells. This is suggested by the current evidence that cells within two such structures, the IGL and OPT, respond to light in different ways in DA and NA chronotypes.

CHAPTER 3: Masking responses to light and darkness in diurnal grass rats (*Arvicanthis niloticus*) and nocturnal Long Evans rats (*Rattus norvegicus*)

INTRODUCTION

Light both entrains endogenous daily (circadian) rhythms central to a mammal's internal clock and it more directly and acutely affects locomotor behavior, a process known as masking. While light stimulates an increase in activity in day-active species, it decreases it in nocturnal ones (reviewed in Redlin 2001). This could reflect a simple reversal of the valence of signals along the same neural circuits through which the light information is transmitted and processed, or perhaps separate parallel pathways are activated to a greater or lesser extent in nocturnal and diurnal species. Existing data shed little light on these issues and the ranges of behaviors and time points that have been examined have been limited. Some studies of masking in diurnal and nocturnal rodents have looked at effects of light on general activity of animals housed without running wheels (Cohen et al., 2010; Shuboni et al., 2012; Barak and Kronfeld-Schor, 2013), but most have used wheel running as the behavioral measure (Mrosovsky, 1994; Redlin and Mrosovsky, 1999b; Redlin, 2001). This can be problematic because the presence of a wheel can lead to major changes in activity patterns of some diurnal rodents, even causing them to become effectively nocturnal (Redlin and Mrosovsky, 2004; Refinetti, 2006; Weinert et al., 2007; Hagenauer and Lee, 2008; Vivanco et al., 2010a; Langel et al., 2014). Additionally, the motivation to run in a wheel, which is powerful (Meijer and Robbers, 2014), is mediated by reward pathways that are associated with addiction (Novak et al., 2012). Masking effects of light on wheel running may therefore reflect, at some level, different mechanisms from those mediating its effects on general activity, sleep, or other behaviors (e.g. Altimus et al., 2008).

The current studies examined questions of how diurnal and nocturnal species may differ with respect to the direct effects of light on behavior in the absence of running wheels. We used the Nile grass rat (*Arvicanthis niloticus*) as our diurnal model and the Norway rat (*Rattus norvegicus*) as our nocturnal one. In the first study we assessed masking effects of photic stimuli at different times of day on general activity of Norway rats to determine whether and how it differs from that seen previously in diurnal grass rats (Shuboni et al., 2012). In the second study we addressed the question of what types of behaviors are induced or suppressed in response to light, and how this differs in grass rats and Norway rats. Here, we used video analyses to determine how time spent engaging in different types of behaviors (e.g. resting, sleeping, exploring, feeding, drinking and grooming) changed in response to a 1-hour pulse of light at night in both species.

METHODS

Animals

Adult male Nile grass rats (weight: 72-115 g) from a breeding colony maintained at Michigan State University and male Norway rats (Long Evans strain, LE; initial weight: 175-199 g) purchased from Harlan laboratories (Indianapolis, IN, USA) were used in this study. Animals were individually housed in plexiglass cages (Nile grass rat: 31.2 x 23.5 x 15.2 cm; LE rat: 47.6 x 25.9 x 20.9 cm) and maintained in a 12:12 light/dark (LD) cycle (lights on at 06:00 h). Cool white fluorescent bulbs provided illumination during the daytime (~300 lux), while a dim red light (< 2 lux) was kept on throughout the night. Food (Nile grass rats: PMI Nutrition, Prolab RMH 2000, Brentwood, MO, USA; LE rats: Teklad Rodent diet 8640; Harlan, Madison, WI) and water were provided *ad libitum*. General activity was detected with infrared sensors located

on the lid of each cage and then recorded and analyzed with the VitalView system (MiniMitter, Bend, OR, USA). All experiments were performed in accordance with the guidelines established by the National Institutes of Health Guide for the Care and Use of Laboratory Animals and the Michigan State University Institutional Animal Care and Use Committee. All efforts were made to minimize the number of animals used in these experiments.

Locomotor responses to 1-hour light or dark pulses in LD conditions

LE rats (n = 10) were exposed to one-hour pulses of darkness or light during the light and dark phases of a 12:12 LD cycle, respectively, as part of a 3-day protocol (Langel et al., 2014) that was repeated in succession. Briefly, the first day was used for upkeep of the housing room, the second day (baseline day) was used for comparison to the next day's activity during the light or dark pulse and the third day (experimental day) animals received a single light pulse (room lights turn on) or dark pulse (room lights turn off). The light pulses were delivered in the following sequence: Zeitgeber times (ZT, where ZT0 = lights-on and ZT12 = lights-off) 22, 14, 18; this was followed by the following sequence of dark pulses: ZT10, 2, and 6. One IR sensor malfunctioned during one of the light pulse nights so recordings from only 9 rats were used in the analyses. To facilitate comparisons between the nocturnal LE rats and diurnal grass rats, values from male grass rats (n = 10) reported in Shuboni et al. (2012) are plotted in Figure 3.1 adjacent to figures from the current data from LE rats.

Behavioral responses to a 1-hour light pulse at ZT16

Video recordings using infrared cameras were obtained from both LE rats (n = 6) and grass rats (n = 6) on a control night and a night in which animals were exposed to a 1-hour light

pulse beginning at ZT16. Due to technical difficulties with the recordings of 2 LE rats, only videos from the remaining 4 LE rats were analyzed. Videos were scored for active (exploring, eating, drinking, grooming) and non-active (resting, sleep) behaviors using EthoLog software (Ottoni, 2000; http://www.ip.usp.br/docentes/ebottoni/EthoLog/ethohome.html). We scored "sleep" when the animal was in a hunched or curled position and the head was not resisting gravity (as in Morin and Studholme, 2009), and "rest" when the animal was immobile, in a sitting posture in which the eyes could be either open or closed. The total duration of each behavior was calculated across the 1-hour light pulse or the same time interval on a control night and the percentage of each behavior across that 1-hour was determined

Statistical analysis

A two-factor, repeated measures analysis of variance (ANOVA) with a Geisser-Greenhouse correction was used to analyze general activity in the first experiment. The analyses for the effects of dark pulses during the light period and light pulses during the dark period were done separately. Lighting condition (dark pulse vs. baseline in one analysis and light pulse vs. baseline in another) and time (ZTs 2, 6 and 10 for the dark pulse data and ZTs 14, 18 and 22 for the light pulse data) were the two within-subjects factors (there was no between-subjects factor). Significant interactions between lighting condition and time were followed by analyses of each light treatment at each time point via the use of paired samples *t*-tests (2-tailed test). Significant main effects of time were followed with post hoc analyses using pairwise comparisons with a Bonferroni adjustment.

For the video scoring data, paired *t*-tests (2-tailed) were used to compare the percentage of each behavior during the 1-hour light pulse at ZT16 versus the same 1 hour on a control night.

Separate analyses were done on the grass rat and LE rat data. The video scoring data were also examined in 15-minute periods across the 1-hour light pulse and the same 1-hour on the baseline night. To analyze these, a two-factor, repeated measures ANOVA with a Geisser-Greenhouse correction was used with lighting condition (light pulse vs. baseline) and time (15, 30, 45 and 60 minutes) being the within-subjects factors. All the percentage data were subject to an arcsine transformation prior to the analyses to equalize the variance among the groups. SPSS version 21 (SPSS, Inc., IBM Company, Chicago, IL) was used for all statistical tests and results were considered significant if $p \leq .05$. Data are presented as the mean ± standard error of the mean (SEM) in all figures.

RESULTS

Locomotor responses to 1-hour pulses in LD conditions

One-hour pulses of light at night significantly decreased general activity in nocturnal LE rats (main effect of lighting condition: $F_{1, 8} = 238.78$, $p < .01$; Figure 3.1A). There was also a main effect of time ($F_{2, 16} = 4.29$, $p = .047$), such that LE rats were more active at the end of the night (ZT22), regardless of lighting condition, than during the middle of the night (ZT18; $p = 0.03$), but there was no difference when comparing the other time points ($ps > .34$). There was no interaction between time and lighting condition ($p = .70$) in the data from the LE rats. Interestingly, at ZT18 the suppression of activity continued for an hour after the light pulse ended (i.e. when the room returned to darkness; data not shown); this was not the case for the 1 h period after presentation of the light at ZT14 and 22. The direction of the masking responses in LE rats were opposite to that of grass rats in which light significantly increased general activity across the night (main effect of lighting condition: $F_{1, 9} = 14.58$, $p < .01$; male grass rat data from

Shuboni et al., 2012) (Figure 3.1B); there was no main effect of time (p = .16) and no interaction between time and lighting condition (p = .27) in the data from grass rats (Shuboni et al., 2012). Darkness, however, significantly increased general activity in LE rats (main effect of lighting condition: $F_{1, 8}$ = 8.84, p = .02). Although this effect appeared to be driven by the dark pulses given during the early and mid-day (Figure 3.1C), there was no effect of time (p = .32) and no interaction between time and lighting condition (p = .99). The effect of the dark pulses on general activity did not extend beyond their duration (data not shown). In grass rats, dark pulses had no effect on general activity levels at any time during the day (ps > .13; Figure 3.1D) (Shuboni et al., 2012).

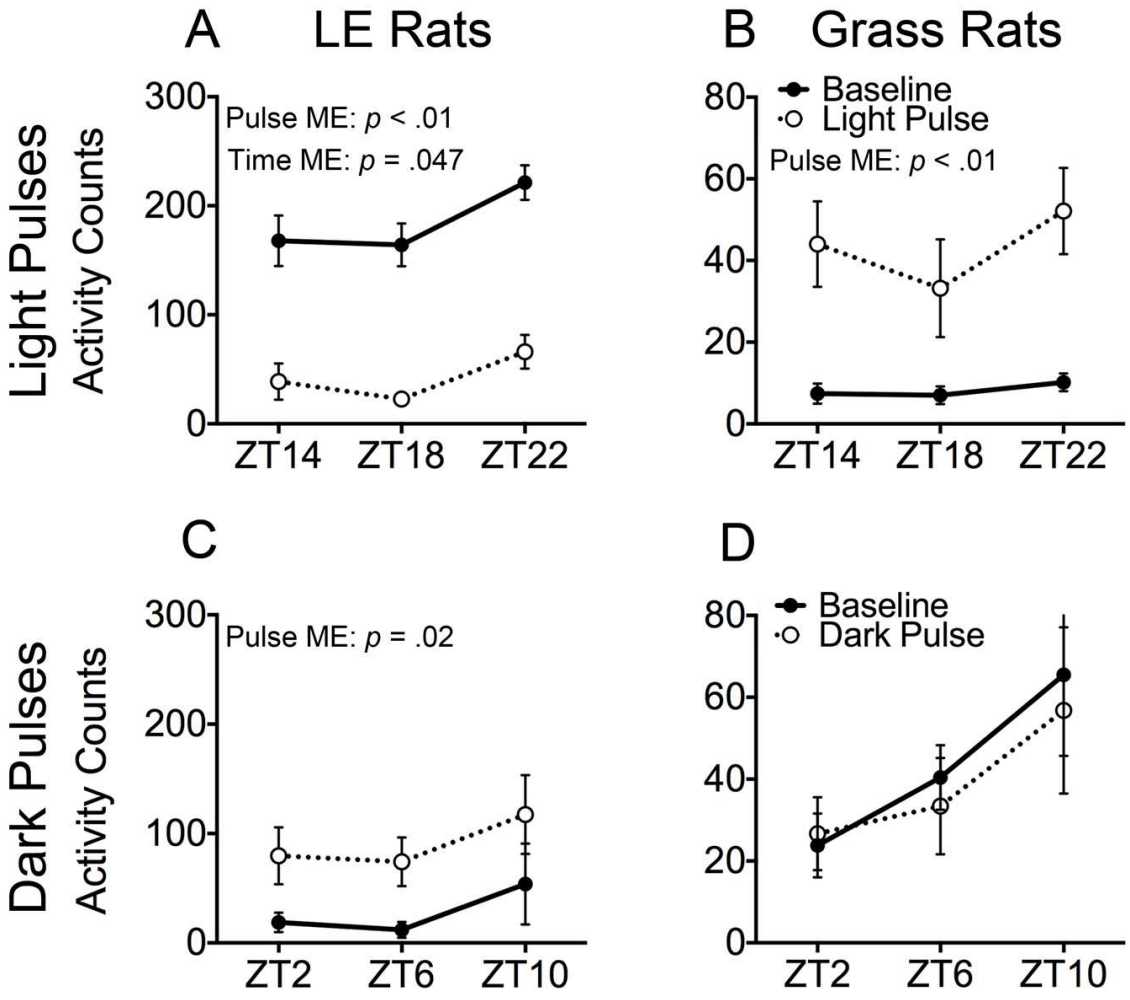

Figure 3.1. Average general activity counts in nocturnal Long Evans (LE) rats (A, C) and diurnal grass rats (B, D) during each 1-hour light or dark pulse (dashed lines) and during the same 1 h interval on the previous day (baseline; solid lines). LE rats decreased their general activity overall in response to the light pulses compared to their baseline night activity (A), while grass rats increased their general activity during the light pulses compared to the baseline night (B). Dark pulses increased general activity overall compared to the baseline day in the LE rats (C), but had no effect on activity in the grass rats (D). Grass rat data are plotted from values reported for males in Shuboni et al. (2012).

Behavioral responses to a 1-hour light pulse at ZT16

Nocturnal LE rats displayed high amounts of active behaviors (exploring, grooming, feeding and drinking) on the control night between ZT16-17 (Figure 3.2A), while the opposite was true of the diurnal grass rats (Figure 3.2B). In LE rats, exposure to a 1-hour light pulse significantly decreased grooming ($t(3) = 5.96$, $p < .01$), but did not significantly affect the other scored behaviors (eating: $p = .06$, exploring: $p = .08$, drinking: $p = .08$, sleeping: $p = .10$, resting: $p = .29$; Figure 3.2C). However, there was a significant increase in the inactive behaviors (sleep and rest combined) in response to the 1-hour light pulse at night among the LE rats ($t(3) = 17.10$, $p < .01$). Grass rats exposed to a 1-hour light pulse slept less ($t(5) = 2.64$, $p = .046$) and also increased their exploratory behavior ($t(5) = 2.57$, $p = .050$), while other measures did not differ significantly between the control night and the light pulse night (all $ps > .29$; Figure 3.2D). No difference was observed in grass rats when the inactive behaviors were combined (sleep and rest) ($p = .21$)(Figure 3.2B and D). However, 2 of the 6 grass rats engaged in far more inactive behaviors, particularly sleep (sleep and rest: $M = 74\%$; sleep only: $M = 28\%$), during the 1-hour light pulse than the other 4 grass rats (sleep and rest: $M = 30\%$; sleep only: $M = 1\%$; individual data from grass rats and LE rats are presented in Table 3.1). When these two outliers were excluded from the analysis there was a significant reduction in inactive behaviors among the grass rats (sleep and rest combined: $t(3) = 5.03$, $p = .02$).

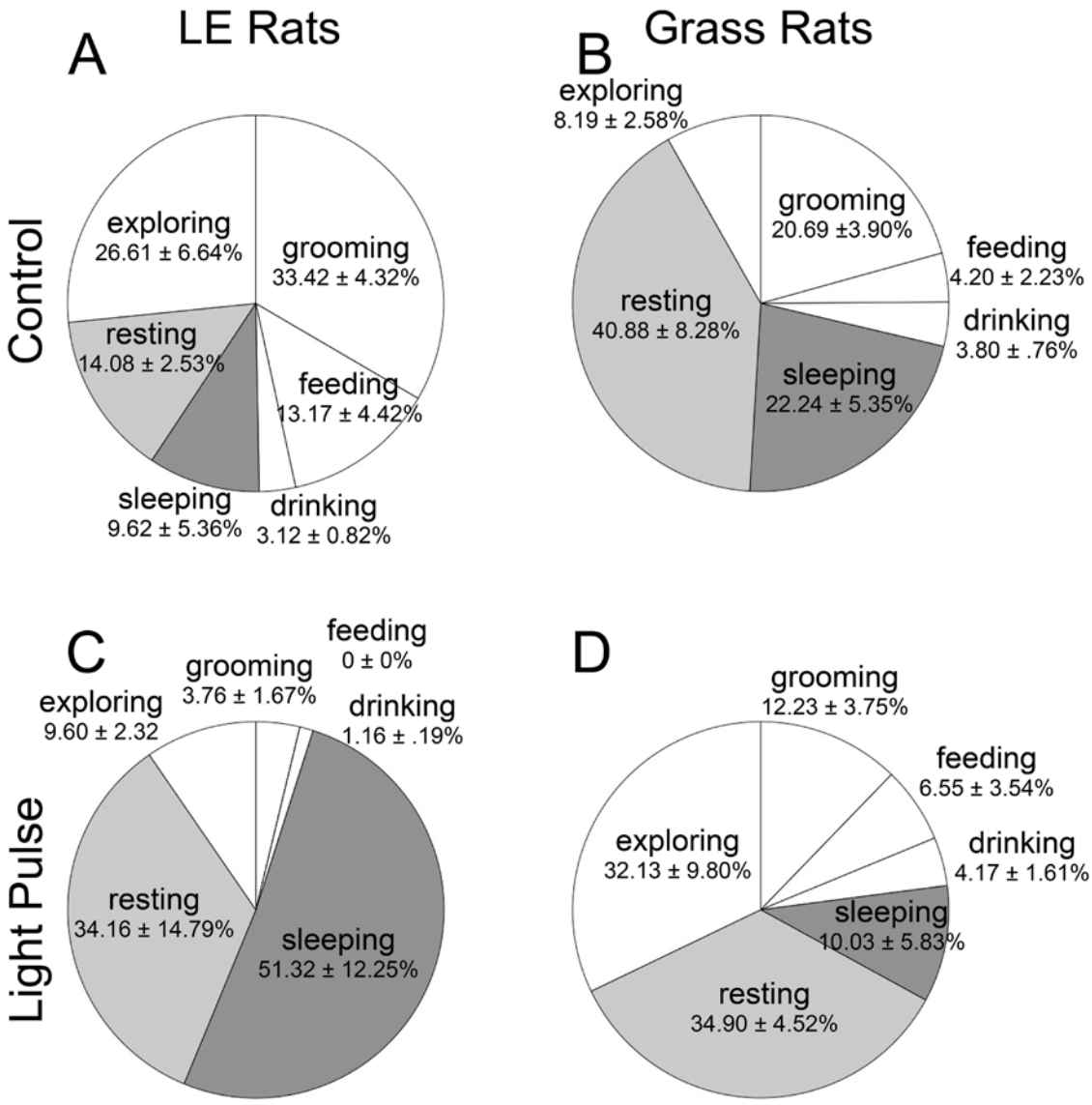

Figure 3.2. Light has opposing effects on various behaviors of nocturnal Long Evans (LE) rats and diurnal grass rats. Pie charts represent the average percentage of active (unfilled slices) and non-active (gray slices) behaviors across a 1-hour light pulse at ZT16 and the same 1 hour on a control night in both the LE rats (A, C) and grass rats (B, D). LE rats displayed higher levels of active behaviors on the control night (A), while grass rats had higher levels of sleep and resting on the control night (B). Light increased sleep/resting in LE rats (C), while light decreased sleep and increased exploring in grass rats (D).

Table 3.1. Percentage of time spent sleeping, resting, and in these behavioral states combined during a 1-hour light pulse at ZT16 in the individual grass rats and Long Evans (LE) rats. The two outlier grass rats with highest levels of sleep and rest are highlighted in bold font.

	Grass Rats						LE Rats			
Animal ID	1	2	3	4	**5**	**6**	1	2	3	4
Sleeping (%)	4.1	0	0	0	**24.0**	**32.1**	65.7	61.4	63.5	14.7
Resting (%)	22.3	22.8	39.3	32.8	**50.2**	**42.1**	16.3	20.5	21.5	78.4
Sleeping and Resting (%)	26.4	22.8	39.3	32.8	**74.2**	**74.2**	82.1	81.8	85.0	93.1

Analyses of the sleep and rest behavior scores broken down into the 4 successive 15-minute intervals enabled us to determine whether animals adapted to the light or whether its effects persisted for a full hour. These analyses revealed that the sleep/rest behavior induced by light in the LE rats persisted across the 1-hour period of the light pulse (main effect of lighting condition: $F_{1, 3} = 186.53$, $p < .01$); there was no main effect of time ($p = .10$) and no interaction between time and lighting condition ($p = .14$). Interestingly, by the last 15-minute period of the 1-hour light pulse almost 100% of the behaviors scored were either sleep or rest (Figure 3.3A). Among grass rats the amounts of sleep and rest did not change overall in response to the 1-hour light pulse (no main effect of lighting condition: $p = .23$) and also did not vary across that 1-hour period (no main effect of time $p = .44$), and there was no interaction between these two variables ($p = .42$). However, when the two outliers, described above, that displayed high amounts of sleep during the light pulse were excluded (animal ID 5 and 6 on Table 3.1), there was a significant main effect of time ($F_{1, 3} = 26.82$, $p = .01$), such that sleep/rest behavior was suppressed in the remaining 4 grass rats (Figure 3.3B); there was no effect of time ($p = .40$) and no interaction between time and lighting condition ($p = .40$).

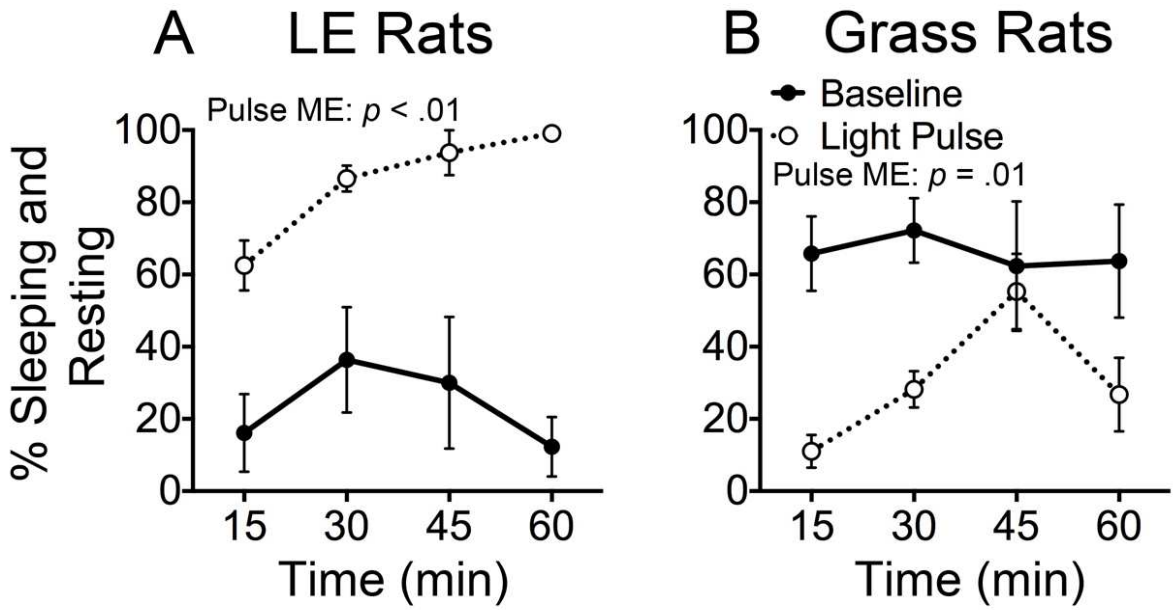

Figure 3.3. Average percentage of time spent sleeping and resting for each 15-minute period across a 1-hour light pulse that began at ZT16 (dashed lines) or during the same 1 hour on a baseline night (solid lines) in nocturnal Long Evans (LE) rats (n=4; A) and diurnal grass rats (n=4; B). Light significantly increased sleep and resting behavior in the LE rats and by the last 15-minute period of the 1-hour light pulse almost 100% of the behaviors scored were either sleep or rest (A). Although sleep and resting did not change in the analysis of all six grass rats, when the two outliers were excluded (animal ID 5 and 6 in Table 3.1), a significantly suppressive effect of light on sleep and resting was observed (B).

DISCUSSION

In our first experiment we characterized masking effects of light and darkness on general activity across the day and night (3 time points each) in LE rats, enabling us to identify similarities and differences between these animals and diurnal grass rats described in Shuboni et al. (2012) (Figure 3.1). Most studies of masking focus on one time point during the day (a single dark pulse) or night (a single light pulse) or when animals are maintained in an ultradian cycle (3.5 hours of light followed by 3.5 hours of darkness) (for example: Altimus et al., 2008; Lupi el al. 2008; Tsai et al. 2009). These protocols do not allow for analysis of time of day effects on masking so relatively little is known about whether and how direct effects of photic stimuli might interact with circadian influences. Here, we found that light pulses greatly suppressed general activity across the night in nocturnal LE rats, whereas the same protocol enhanced such activity across the night in diurnal grass rats (Shuboni et al., 2012)(Figure 3.1). The suppression of activity by light pulses at night could theoretically be due to phase shifting effects (Redlin and Mrosovsky, 1999b) since pulses of light induce phase delays in the circadian clock in the early subjective night and advances in the late subjective night, both of which could shift the clock to a time when the LE rat is normally inactive (late and early day, respectively). However, this is unlikely to account for the patterns that we saw, as these shifts would have had to be at least 2 hours. This is even less likely to explain the response to light at ZT18, as in this case a phase shift induced by the light would have had to be 6 hours to produce the pattern we observed. Interestingly, at this time point the suppressive effect of the 1-hour pulse of light continued for one hour following the return to darkness. The sustained suppression of activity to pulses of light at night also occurs in hamsters (Redlin and Mrosovsky, 1999b) and even mice exposed to brief millisecond pulses of light over a 5 minute period (Studholme et al., 2013).

Although we did not find a time of day effect on the magnitude of masking responses to light pulses at night in the LE rats, they have been described in other species. Suppressive effects of light are greatest during the early portion of the night in both nocturnal hamsters (Redlin and Mrosovsky, 1999b) and mice (Pendergast and Yamazaki, 2011; Shuboni et al., 2012), and light enhances activity the most during the later part of the night in diurnal canaries (Aschoff and Vongoetz, 1989). Time of day effects on masking may vary between species and may depend upon the type of activity measured, but they may also be evident in some masking protocol but not others. We therefore cannot rule out the possibility that a rhythm in sensitivity, or responsiveness, to light at night might be evident in LE rats under other conditions (e.g. different light intensities).

Interestingly, whereas dark pulses increased general activity across the light phase in LE rats, they had no effect at all in grass rats (Shuboni et al., 2012) (Figure 3.1). Thus, the mechanisms mediating masking responses to darkness during the day are not simply operating in a reverse fashion in the two species. Darkness during the day also enhances wheel running in nocturnal hamsters (Aschoff and Vongoetz, 1988) and general activity in nocturnal common spiny mice (*Acomys cahirinus*) (Cohen et al., 2010), but has little effect on wheel running in mice (Doyle et al., 2008). Although darkness during the day did not suppress activity in grass rats it can in some diurnal species, such as canaries (Aschoff and Vongoetz, 1989), and it can induce somnolence in humans (Vandewalle et al., 2006). The absence of masking to darkness in grass rats could have ecological relevance because in the wild these animals live in dark underground burrows that they enter and exit throughout their daytime active period.

In our second experiment we used video analyses to look more deeply into the behavioral changes that are triggered by exposure to light at night in diurnal grass rats and nocturnal LE rats.

Again, the patterns of response differed in the two species, as the light induced sleep/resting in LE rats, while in grass rats it suppressed sleep and increased exploratory behavior (Figure 3.2). The induction of sleep and resting in LE rats persisted across the 1-hour light pulse and all rats spent close to 100% of their time either sleeping or resting during the last 15 minutes of the pulse (Figure 3.3). In mice, light pulses at night induce both slow-wave sleep (SWS) and rapid eye movement (REM) sleep and the effects seem to be mediated through the melanopsin protein, since mice lacking it do not have sustained increases in SWS or REM sleep for the entire duration of the light pulse (Altimus et al., 2008; Lupi et al., 2008; Tsai et al., 2009; Morin and Studholme, 2011; Muindi et al., 2013). Melanopsin deficient mice do, however, show an increase in sleep only during the first 30 minutes of the light pulse, suggesting that rods and cones play a role in the initial induction of sleep by light (Altimus et al., 2008; Muindi et al., 2013). Interestingly, light suppresses wheel running in melanopsin deficient mice for longer periods of time (100 minutes of a 3-hour light pulse), though the response is reduced and does not persist as it does in wild type mice (Mrosovsky and Hattar, 2003). Together, these data suggest that melanopsin is essential for maintenance of masking responses to light over long periods of time (Mrosovsky and Hattar, 2003; Lupi et al., 2008; Morin and Studholme, 2011; Muindi et al., 2013).

In the overall group of grass rats, light had no effect on resting, or on the combination of sleep and resting. However, inter-individual variation in the responsiveness of these behaviors to the light was striking and dichotomous. In two of the six individuals, 74% of the time during the light pulse was spent in sleep/rest behavior whereas the remaining four animals spent only 23-39% of their time in that state. Most strikingly, while these 2 outliers spent 24% and 32% of their time in the sleep state, the others spent either 4% (n=1) or no time at all (n=3) in this state (Table

3.1). When the two outliers were excluded from the overall analyses, a significant light-induced suppression of rest/sleep emerged (Figure 3.3). The dichotomous nature in the responses to light in our sample of grass rats provides a striking example of natural variability in masking responses of these animals. Another context in which we see tremendous variability is when these animals are provided wheels to run in, as some individuals adopt a nocturnal preference and others a diurnal one (Blanchong et al., 1999). It is tempting to speculate that the two grass rats that were less responsive to light (i.e. continued to sleep) in the current study represent those that are predisposed to be active at night when given access to a running wheel.

Conclusion

The present results illustrate the nature of the differences in the patterns of behavioral responses to light and darkness in two murid species kept under similar experimental conditions. One-hour pulses of light across the night stimulate increases in activity in the diurnal grass rats (Shuboni et al., 2012) but had the opposite effect in nocturnal LE rats. A more detailed analysis revealed that four hours into the dark phase (ZT16) a 1-hour light pulse suppressed general activity and induced a significant increase sleep/rest behavior in nocturnal LE rats while the opposite pattern was observed in diurnal grass rats (an increase in general activity and suppression of sleep). Dark pulses during the day were quite different in that they induced a significant change in the behavior of the LE rats, an increase in activity, but had no effect at all in the diurnal grass rat (Shuboni et al., 2012). The neural pathways mediating these behavioral differences have not yet been identified, but they may reside within brain structures receiving direct input from the retina, or they might emerge from differences within in circuits downstream from them.

CHAPTER 4: Central melanopsin projections in the diurnal rodent, *Arvicanthis niloticus*

INTRODUCTION

In mammals, light has a strong impact on daily activity rhythms by synchronizing an organism's internal clock with rhythms in the external environment (i.e. light entrainment) and through more acute effects on general activity (a phenomenon known as masking). While entraining effects of light on the internal clock are very similar in diurnal and nocturnal species (reviewed in Smale et al., 2003), masking effects are quite different, with light increasing locomotor activity in diurnal species and decreasing activity and inducing sleep in nocturnal ones (Aschoff and Vongoetz, 1989; Redlin and Mrosovsky, 1999b; Shuboni et al., 2012). The neural pathways contributing to these differences are not well understood but they are likely to involve circuits that receive signals, directly or indirectly, from a subset of retinal ganglion cells that are intrinsically photosensitive (ipRGCs). These cells, which contain the photopigment melanopsin, are important for non-image-forming visual functions, such as entrainment, masking, melatonin suppression and regulation of the pupillary light reflex. Within the last decade it has been shown that these light regulated functions are driven from signals generated not only from melanopsin activation, but also from the classical photoreceptors, rods and cones. When genetically removing rods, cones or melanopsin, masking still occurs (Mrosovsky et al., 2001; Panda et al., 2002), but removal of all three types of photoreceptors or ipRGCs eliminates masking and entrainment (Hattar et al., 2003; Panda et al., 2003; Goz et al., 2008; Guler et al., 2008; Hatori et al., 2008). It is clear, therefore, that ipRGCs play an essential role in transmission of photic signals that lead to a masking response in nocturnal mice. The question of whether this is also the case in diurnal species is an open one, and differences along circuits that process signals from

ipRGCs could theoretically contribute the differences in the acute effects of light on activity in day- and night-active animals.

Many brain areas such as the suprachiasmatic nucleus (SCN), lateral geniculate nucleus (LGN), pretectum, and superior colliculus are innervated by ipRGCs in nocturnal mice, as indicated by studies of transgenic models (Hattar et al., 2006; Brown et al., 2010; Ecker et al., 2010). Another approach to determine central projections of ipRGCs in other animals has been to use a combination of a classical anterograde tracer (cholera toxin subunit β; CT-β) injected into the eye and co-staining for one marker of ipRGC fibers, the neuropeptide, pituitary adenylate cyclase-activating polypeptide (PACAP), in retinal target areas of the brain (Bergstrom et al., 2003; Hannibal and Fahrenkrug, 2004; Hannibal et al., 2014). In the retina of mammals examined so far, PACAP is exclusively expressed within RGCs that contain melanopsin both in diurnal and nocturnal species (Hannibal et al., 2000; Hannibal et al., 2002; Bergstrom et al., 2003; Hannibal et al., 2004; Hannibal et al., 2014).

One diurnal model available for investigation of neural pathways involved in masking is the Nile grass rat (*Arvicanthis niloticus*). These animals are native to sub-Saharan Africa and are diurnal both in the field and in the laboratory (Katona and Smale, 1997; McElhinny et al., 1997; Blanchong and Smale, 2000). They have a cone-rich retina, as do most other diurnal species; specifically, the ratio of cones to rods is 10 times higher in the Nile grass rat than in typical nocturnal rodents (Gaillard et al., 2008; Hut et al., 2012). In Nile grass rats, as in other diurnal animals, masking responses to light are the reverse of those seen in nocturnal species, such that light serves to increase, rather than decrease, general activity (Shuboni et al., 2012). Additionally, many retinorecipient areas of the brain that may receive input from ipRGCs exhibit an increase in the immediate early gene product, FOS, in response to light in this species, whereas under the

same conditions the response varies across regions in nocturnal mice (Shuboni et al., 2015). ipRGCs have not yet been described in the Nile grass rat but they have in a related day-active species, the Sudanese grass rat (*Arvicanthis ansorgei*). Although several characteristics of these cells are similar to those reported in nocturnal rodents, some differences exist in the firing patterns of a select subtype of ipRGCs (Karnas et al., 2013a). The questions of whether ipRGCs co-store PACAP and whether the central projections of these cells are different in diurnal grass rats (either Nile or Sudanese) from those seen in nocturnal rodents have, however, not been addressed.

In the work described here we sought to determine whether retinal circuits and projections known to play a central role in masking in nocturnal rodents are present in the Nile grass rat. First, we described the melanopsin cells in the retina of the Nile grass rat and asked whether PACAP is expressed within these cells, as is the case in other species. We then characterized the distribution of central projections of PACAP-containing RGCs. To do this, we labeled PACAP within the brains of sham and enucleated Nile grass rats, and we examined overlap between PACAP fibers and retinal inputs in animals that had received intraocular injections of the anterograde tracer cholera toxin subunit β (CT-β). Results are discussed in the context of patterns previously described in nocturnal rodents (Hannibal and Fahrenkrug, 2004; Hattar et al., 2006; Engelund et al., 2010; Engelund et al., 2012) to determine the nature of the similarities and potential differences between the ipRGC systems of day- and night-active species.

METHODS

Animals

Adult male Nile grass rats from a breeding colony maintained at Michigan State University were used in this study. Animals were housed in plexiglass cages (34 x 28 x 17 cm^3) with access to food (PMI Nutrition, Prolab RMH 2000, Brentwood, MO, USA) and water *ad libitum*, and were maintained on a 12:12 light/dark cycle (lights on at 0600 h) unless otherwise indicated. All experiments were performed in accordance with guidelines established by the National Institutes of Health Guide for the Care and Use of Laboratory Animals and the Michigan State University Institutional Animal Care and Use Committee. All efforts were made to minimize the number of animals used in these experiments.

Enucleations

Nine Nile grass rats were anesthetized with isoflurane and were either bilaterally (n = 3) or unilaterally (n = 3; right eye removed only) enucleated or they underwent sham surgery (n=3). For enucleations, the eye was held with forceps, the optic nerve and blood vessels were severed and the eye was removed. Absorbable gelatin was inserted into the orbit and the eyelid was sealed with Vetbond (3M, St. Paul, MN). Control grass rats were anesthetized but neither eye was removed. All animals were perfusion fixed 14 days after surgery and brains were collected and processed for visualization of PACAP (see below).

Anterograde tracing

Five intact Nile grass rats were anesthetized with isoflurane and then received 5 µl intravitreal injections through a Hamilton syringe (Reno, NV) of cholera toxin subunit β (CT-β)

conjugated to Alexa Fluor 488 (7 μg/μl; C-22841) in the right eye and Alexa Fluor 594 (5 μg/μl; C-22842) in the left; both were purchased from Molecular Probes (Eugene, OR) and were dissolved in 2% dimethylsulfoxide (DMSO) in 0.9% saline vehicle. Seven days following surgery, grass rats were perfusion fixed (see below).

Tissue collection

We collected brains from the animals described above and both retinas from 3 other animals maintained in a 12:12 light/dark cycle (LD) and 4 animals that were kept in constant darkness (DD) for 5 days prior to sacrifice. All of these animals were anesthetized with an intraperitoneal injection of either sodium pentorbital (Nembutal; Ovation Pharmaceutical, Deerfield, IL; 0.5 cc/animal) or urethane (Sigma-Aldrich, St. Louis, MO; 1,500 mg/kg) and transcardially perfused with 0.01 M phosphate buffered saline (PBS; pH 7.4; 150-200 mL/animal) followed by Stefanini's fixative (2% paraformaldehyde and 0.2% picric acid in 0.1 M PBS; Sigma-Aldrich, St. Louis, MO; pH 7.2; 150-200 mL/animal; brain tissue) or 4% paraformaldehyde (in 0.1 M PBS; Sigma-Aldrich, St. Louis, MO; 150-200 mL/animal; retinal tissue). Brains and eyes were extracted, postfixed in Stefanini's fixative or 4% paraformaldehyde for 12-18 hours, then immersed for at least 48 h in 20% sucrose solution in 0.1 M phosphate buffer (PB) and kept at 4 °C. Brains were cut into coronal sections (30 μm) using a microtome (for single-label PACAP immunohistochemistry) or a cryostat (for brains labeled with fluorescent agents). Three alternating series of sections were collected from each brain and were stored in cryoprotectant at -20 °C until further processing. Retinas were orientated and dissection was performed by first removing the cornea, followed by removal of the lens. Hereafter, four cuts were made to mark the superior, nasal, inferior and temporal quadrant and for orientation a

small cut was made in the superior quadrant. The eye was then held in place by needles and the vitreous was gently removed with forceps and filter paper. After gentle dissection along the ora serrata and cut of the optic nerve, the retina was removed and kept in cryoprotectant solution (30 % sucrose, 1% polyvinyl-pyrrolidone (PVP-40), 30 % ethylene glycol, 0.05 M sodium phosphate buffer, pH 7.2) for better conservation, and thereafter stored at – 20 °C until immunohistochemically processed.

Antibodies

A mouse monoclonal anti-PACAP antibody (MabJHH1; diluted 1:5) recognizing the epitope between amino acids 6-16 was used for both the brain and retinal tissue; this antibody has equal affinity for PACAP-27 and PACAP-38 (Hannibal et al., 1995) and shows no staining in brain sections from PACAP deficient mice (our own unpublished observations). Preabsorbtion of the PACAP antibody with PACAP (Hannibal et al., 1995) and omission of the primary/secondary antibody from the immunohistochemistry procedure abolished staining. A rabbit anti-melanopsin antibody (41K7; diluted 1:5,000; (Hannibal et al., 2002)) directed against the C-terminal of melanopsin was used together with a N-terminal rabbit anti-melanopsin antibody (PAI-780, Fisher Scientific Inc., Barrington, IL; 1:5,000) to stain melanopsin cells in the retina. No staining is observed with either of these antibodies in melanopsin deficient mice (own unpublished observation).

Immunohistochemical procedures

Retinas: PACAP + melanopsin immunofluorescence (IF)

To label both PACAP and melanopsin in the retina, double label IF was used. Tissue was rinsed with 0.25 % Triton-X-100 (TX) in 0.01M PBS between all steps of the procedure, and all incubations included 0.25% TX and 0.25% bovine serum albumin (BSA). All rinses and incubations occurred at room temperature, unless otherwise noted. Retinas were first treated with antigen retrieval (AR) solution in citrate buffer (pH 6.0, Sigma-Aldrich, St. Louis, MO) at 80 °C for 1.5 h. Next, tissue was pre-incubated with 1% H_20_2 in 0.01 M PBS for 10 min, blocked with 5% normal donkey serum for 20 min, and then incubated with the PACAP antibody for 72 h at 4 °C. Retinas were then incubated in the secondary antibody, biotinylated donkey anti-mouse (1:800 for PACAP; Jackson, 715-065-151) over night at 4 °C. Next, tissue was incubated in avidin-biotin complex (ABC) solution (0.9% each of avidin and biotin solutions) for 30 min, biotinylated tyramide (1:50; PerkinElmer, SAT700001EA) for 1 h, and finally Alexa Fluor 488-conjugated streptavidin (1:500 for PACAP; Jackson, 016-540-084). Hereafter, tissue was placed in 1% H_20_2 in 0.01 M PBS for 15 min, washed in PBS and incubated in the mixture of N- and C-terminal melanopsin antibodies for another 72 h at 4 °C. After a rinse, the retinas were then incubated in Envision reagent (1:2; Dako, K4002) overnight and visualized by tyramide conjugated Alexa Fluor 594 (Molecular Probes, Eugene, OR).

Brain: PACAP

The immunohistochemistry (IHC) procedure used for single labeling of PACAP in the brain was like that used for PACAP in the retina with the following exceptions: the AR step was not included, incubation with the PACAP antibody was for 48 h, the concentration of the

biotinylated tyramide in which sections were incubated was 1:100, and after the 30 minute incubation in ABC solution, sections were rinsed two times in 0.25% TX in 0.01M PBS, then placed in Tris buffer (pH 7.6) for 10 min, preincubated in 0.06% diaminobenzidine (DAB, Sigma-Aldrich) in Tris buffer for 30 s and reacted with 0.01% hydrogen peroxidase for 2.5 min.

Immunofluorescence (IF) was used to label PACAP in one series of brain sections from each of the CT-β injected animals. The procedure was similar to that used for PACAP + melanopsin IF, except that incubation of the antibodies were somewhat shorter (48 h in the PACAP antibody and 1 h in the secondary), and Cy5-conjugated streptavidin (Jackson, 016-170-084) was used instead of Alexa Fluor 488-conjugated streptavidin.

Photomicrographs

Images of DAB stained tissue were taken with a digital camera (MBF Bioscience Inc., 2007) attached to a Zeiss light microscope (Axioskop 2 Plus, Carl Zeiss, Göttingen, Germany), while fluorescent images were obtained using an iMIC confocal microscope (Till Photonics, FEI, Germany) equipped with appropriate filter settings for detecting DAPI, Cy2/Alexa Fluor 488, Texas Red/Alexa Fluor 561/594 and Cy5. Determination of whether PACAP and melanopsin were present in a single cell was done with a co-localization plug-in module in ImageJ/Fiji software (version. 1.47q, NIH, USA) in which the points of two 8-bit images with both antigens appeared white (we used default value = 255). Pixels were considered to reflect co-localization of the antigens if their intensities were higher than the threshold of their respective channels (we used a threshold set at 50-100 depending on the background noise) and if the ratio of their intensity was higher than the ratio setting value (we used the default set at 50%). Melanopsin/PACAP cell counts were performed on areas from six pieces of the same retina in

which cells were stained well for both PACAP and melanopsin; areas in which one or both immunoreactions were insufficient were excluded. The sizes of the pieces ranged from 0.65 to 8.7 mm^2 and represented both the central and peripheral retina. The retina was photographed with an iMIC confocal microscope (Till Photonics, FEI, Germany) using the wide field camera and 10X objective. Photographs were taken of each part of retina and stitched together using the LA Stitch plug-in in Fiji software (version 1.47q, NIH, USA) to create an image of the entire retina. Each of these was then analyzed using the cell counter plug-in Fiji to mark and count which cells contained only PACAP, only melanopsin, or both. Counts of melanopsin-stained cells were performed on retinas from animals either maintained in LD or kept in DD for 5 days, since a previous report in Brown Norwegian rats indicated that melanospin expression is highest in animals maintained in constant darkness (Hannibal et al., 2013). The entire retina was photomicrographed with the iMIC confocal microscope with five stacks separated by 8 μm (Z-axis = 40 μm) of the entire retina covering the ganglion cell layer until the inner nuclear cell layer (see Figure 4.2). After stitching all Z-stacks together using the LA Stitch plug-in in Fiji software (version 1.47q, NIH, USA), melanopsin cell subtypes, as defined previously in mouse retina (reviewed in Cui et al. 2015, Fox and Guido 2011, and Schmidt et al. 2011), were counted using the 3D cell counting module in Fiji. Retinal projection (fluorescent CT-β and PACAP staining) images were obtained by the iMIC confocal microscope using filter settings for Alexa Fluor 488, 595 and 647 and images were stitched together by using Fiji with the plates being combined in Illustrator CS4 after adjusting in Photoshop CS4 (Adobe, San Jose, CA). All images were adjusted for brightness and contrast, as well as for size.

RESULTS

Melanopsin in the grass rat retina

Melanopsin expression was examined in flat mount retinas from animal housed in a 12:12 light/dark cycle and from animals housed in constant darkness due to previous reports in rats showing a slight increase in melanopsin protein expression during prolonged periods in constant darkness (Hannibal et al., 2013). Melanopsin positive cells were found in the ganglion cell layer (GCL) and displaced in the inner nuclear layer (INL) in the superior half of the retina (Figure 4.1). Melanopsin was located mainly in the cell membrane of the soma and dendritic processes but in animals kept in constant darkness melanopsin was also found in the membrane of axons projecting to the optic nerve (Figure 4.1). As previously reported in mice (reviewed in Cui et al. 2015, Fox and Guido 2011, and Schmidt et al., 2011), melanopsin-containing cells could be identified as being either as subtype M1 (cell soma in the GCL or in the INL and dendrites in the distal ("OFF") sublamina of the inner plexiform layer (IPL), known as S5), M2 (weak melanopsin expression, cell soma in the GCL and dendrites in the proximal ("ON") sublamina of the IPL, known as S1) or M3 (cell soma in the GCL and dendritic processes in both S1 and S5) (Figure 4.2). We were unable to identify melanopsin cell types as M4 or M5 in the grass rat retina. Whereas M1 and M3 cells (~74% of all ipRGCs), as well as M2 cells (~6% of all ipRGCs) were scattered relatively evenly across the entire retina, displaced M1 cells (i.e. with cell bodies in INL; ~20% of all ipRGCs) were located primarily in superior regions of the retina (Figure 4.1). Interestingly, a large number of melanopsin-expressing cells were found in of the superior, nasal, and temporal periphery of the grass rat retina (Figure 4.1A-B) as recently described in the rat (Vugler et al., 2008) and mouse (Semo et al., 2014; Valiente-Soriano et al., 2014). These cells all co-stored PACAP (see also below). Cell counts revealed that in animals

housed in a 12:12 light/dark cycle, 1,138 ± 89 melanopsin cells (27.6±1.3 cell/mm^2) were present whereas in animals housed in constant darkness, 1,402 ± 52 melanopsin cells (32.7±1.3 cell/mm^2) were counted; this difference was not statistically significant ($t(3) = 2.165$, $p = 0.12$). However, the dendritic network appeared to be denser and axonal staining of melanopsin was present in animals housed in constant darkness.

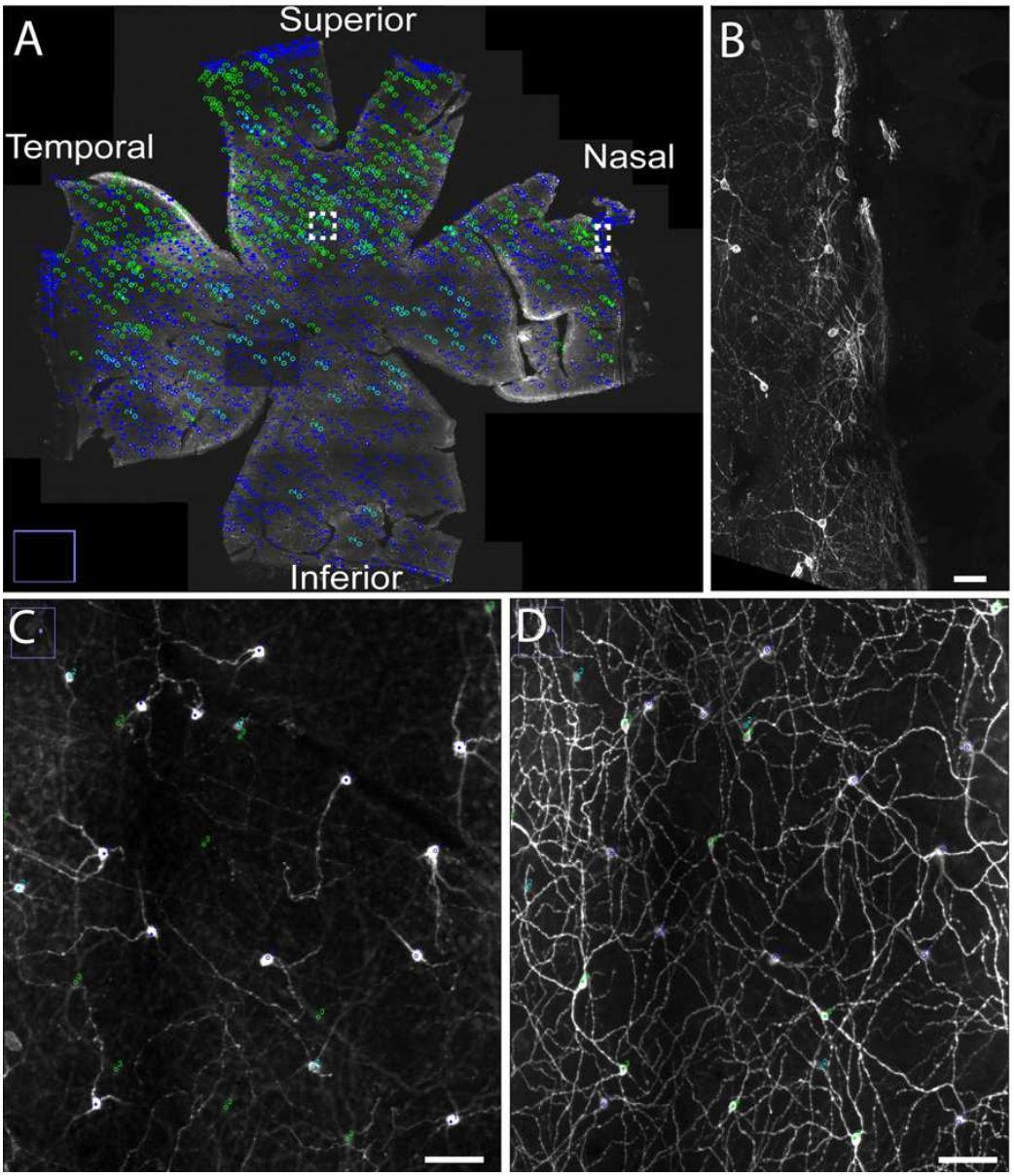

Figure 4.1. The distribution of different subtypes of ipRGCs across the Nile grass rat retina. M1 and M3 ipRGCs (dark blue) and M2 (light blue) cells are evenly distributed across the retina, whereas displaced M1 cells (green) are located primarily in its superior region (A). A higher power image of M1 cells is shown in B, which represents the boxed area in the nasal region of panel A. Melanopsin cells in the superior aspect of the retina (boxed region in A) are seen in the ganglion cell layer (GCL) (C) and in the inner plexiform layer (IPL) (D), where a dense plexus of melanopsin-containing fibers can also be seen. Scale bars: B-D = 50 μm.

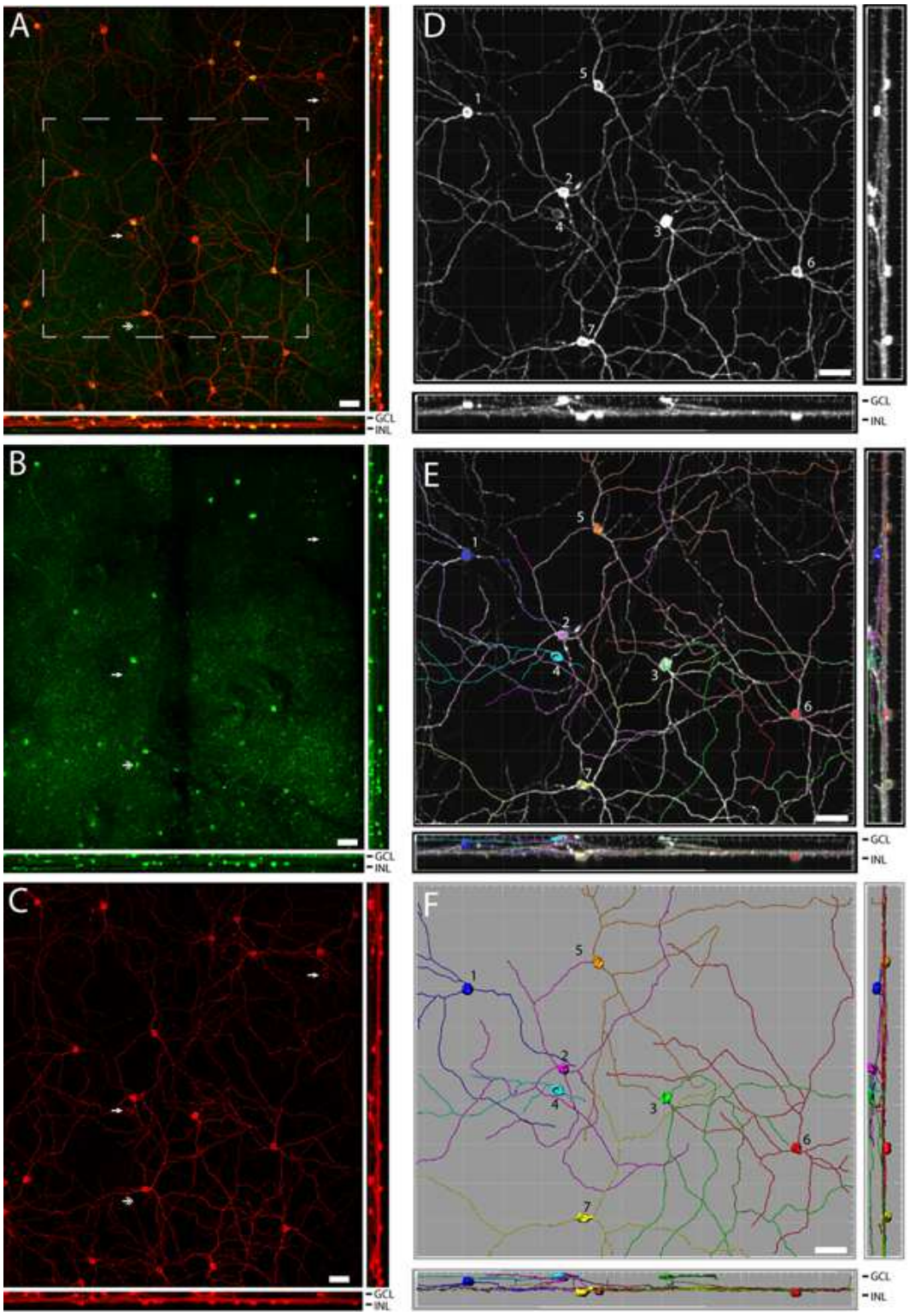

Figure 4.2. PACAP is found in several subtypes of melanopsin cells in the Nile grass rat retina. An extended view across the Z-stack of melanopsin (red) and PACAP (green; overlay in

Figure 4.2. (cont'd)

yellow) in the retina is depicted in A, while single labels for PACAP and melanopsin are depicted in B and C, respectively. In A-C, the two single arrowheads indicate two melanopsin-expressing cells that do not express PACAP, while the double arrowhead indicates a PACAP-expressing cell that does not express melanopsin. Extended views of the melanopsin cells are shown before (D) and after (E and F) analysis of the dendritic processes. In panels D-F the various subtypes of melanopsin-expressing cells are marked 1-6. 1 = M1, 2 and 3 = M3, 4 = M2, and 5-7 = displaced M1 cells. GCL = ganglion cell layer, IPL = inner plexiform layer and INL = inner nuclear layer. Scale bars: 45 μm.

Melanopsin and PACAP in the grass rat retina

A total of 633 cells containing melanopsin were counted in six pieces of the same retina. Of these, 555 (87.7%) co-stored PACAP (Figure 4.2 and 4.3); this percentage ranged from 84-94 across the different pieces of retina. PACAP was seen in all subtypes of melanopsin cells. A very small number of cells (only 15 out of 570, 2.6%) containing only PACAP (i.e. no melanopsin) were counted. None of the six pieces of the retina had a melanopsin cell density that was below the average density found when counting the total number of melanopsin cells. This finding in the grass rat retina was similar to that of the monkey retina (Hannibal et al., 2014), in which a very small number of cells containing melanopsin, but not PACAP, or PACAP, but not melanopsin, were found (Figure 4.2). Since we found some variation between the numbers of melanopsin/PACAP containing cells in the different pieces of retina we cannot exclude the possibility that some melanopsin cells don't express PACAP (and vice versa) but more likely this finding is due to low levels of expression of PACAP or melanopsin in some cell types.

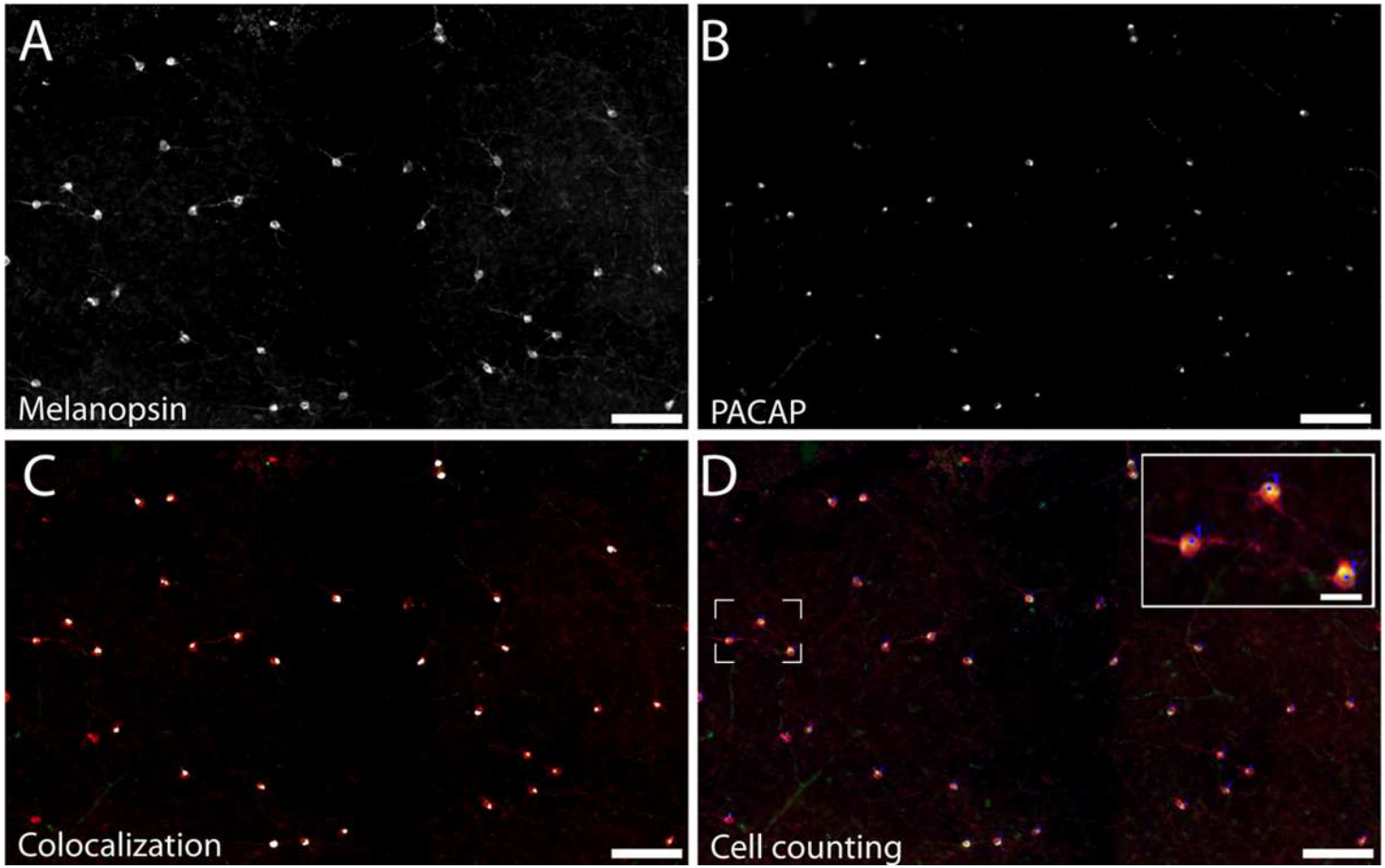

Figure 4.3. Staining for melanopsin and PACAP reveals that they are expressed in the same cells in the Nile grass rat retina. Photomicrographs depict melanopsin-immunoreactive (ir) cells (A), PACAP-ir cells (B) and the overlay of staining for PACAP and melanopsin (C; melanopsin-ir in red and the pixel overlap of melanopsin-ir and PACAP-ir in white). Manual counts of cells expressing melanopsin and PACAP were done in Fiji (D). Scale bars: A-D = 100 µm and insert in D = 30 µm.

PACAP fibers in retinorecipient regions of the grass rat brain

PACAP-immunoreactivity in the grass rat brain was observed in many regions known to receive input from ipRGCs in rats (Hannibal and Fahrenkrug, 2004) and in mice (Hattar et al., 2006). The structures described below are ones that had noticeable reductions in PACAP-immunoreactive (ir) fibers following removal of the eyes and a high degree of overlap between the distributions of PACAP and CT-β-labeled fibers. These areas included the suprachiasmatic nucleus (SCN), lateral geniculate nucleus (LGN), pretectum, and superior colliculus (SC). Other hypothalamic structures, such as the ventrolateral preoptic area, subparaventricular zone and lateral hypothalamus, are known to receive input from ipRGCs in nocturnal rats (Hannibal and Fahrenkrug, 2004) and mice (Hattar et al., 2006). However, it was difficult to determine if this was the case in grass rats, as retinal input to these areas is minimal (Todd et al., 2012; Gaillard et al., 2013) and many non-retinal PACAP-ir fibers are present throughout the hypothalamus (data not shown).

Suprachiasmatic nucleus (SCN)

In the rostral SCN of sham grass rats, PACAP-ir fibers were more ventrally located (Figure 4.4A), while in the mid-caudal portions of the SCN, PACAP labeling was present across the nucleus (Figure 4.4B and 4.5). PACAP-ir fibers were greatly reduced in bilaterally enucleated grass rats compared to shams throughout the rostrocaudal extent of the SCN (Figure 4.4C-D). In unilaterally enucleated grass rats PACAP fiber labeling was reduced but still present (Figure 4.4E-F); the reduction was similar in the SCN ipsilateral and contralateral to the eye that had been removed, indicating that PACAP fibers from the retina have bilateral projections to the

SCN. This was confirmed by the bilateral tracing experiments, which also show that the majority of PACAP-immunoreactive nerve fibers in the SCN originate from the retina (Figure 4.5).

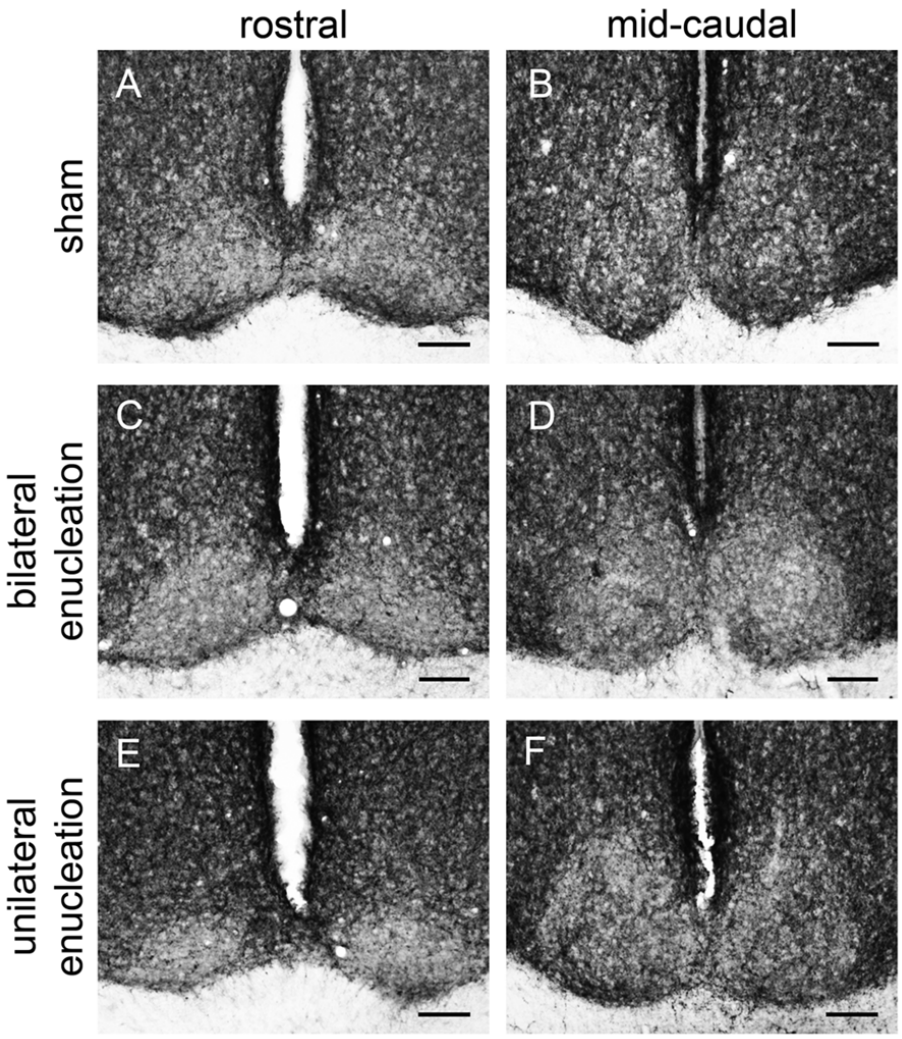

Figure 4.4. PACAP-immunoreactive (ir) fibers in the rostral and mid-caudal suprachiasmatic nucleus (SCN) of sham, bilaterally and unilaterally enucleated Nile grass rats. Sham Nile grass rats had PACAP-ir fibers in the ventral portion of the rostral SCN (A) and in both the dorsal and ventral part of the mid-caudal SCN (B). Bilateral enucleation reduced PACAP-ir fibers across the rostrocaudal extent of the SCN (C & D). Unilateral enucleation reduced PACAP-ir fibers in the SCN, but some were still present, particularly in its mid-caudal region (E & F). Scale bars: 100 μm.

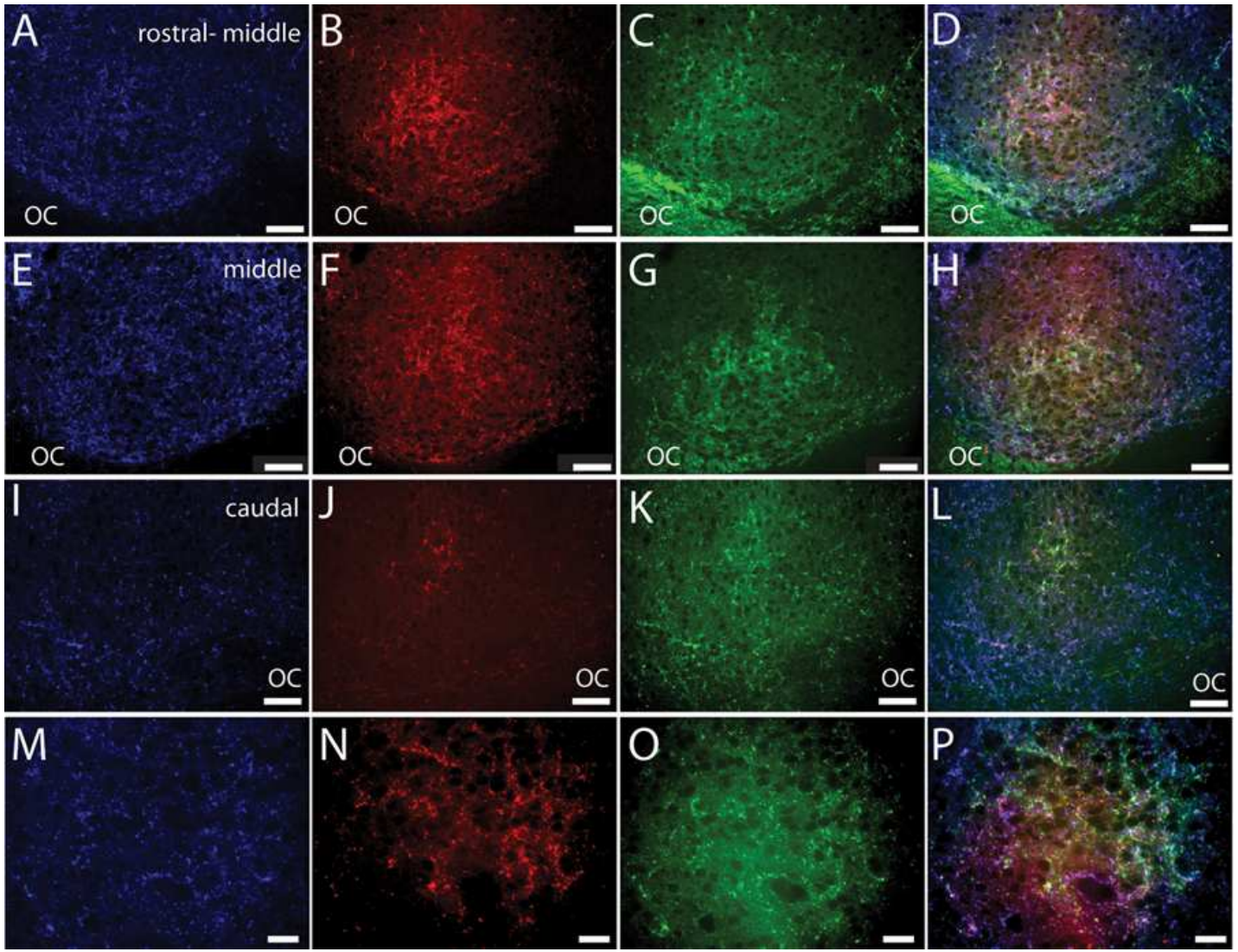

Figure 4.5. PACAP-immunoreactive (ir; blue; A, E, I, M) fibers and CT-β-labeled retinal fibers from the ipsilateral (red; B, F, J, N) and contralateral (green; C, G, K, O) eye in the rostral-middle (A-D), middle (E-H), and caudal (I-L) left

Figure 4.5. (cont'd)

suprachiasmatic nucleus (SCN). An overlay of the PACAP staining and the tracers is pictured in D, H, L and P. Magenta and cyan colors in D, H, L, and P represent the overlap of the PACAP-ir labeling and CT-β-labeled retinal fibers, each of which can be seen at all levels of the SCN. Low magnification images of various levels of the SCN are presented in A-L and higher magnification images of areas shown in E-H are illustrated in M-P. OC = optic chiasm. Scale bars: A-L = 50 μm and M-P = 20 μm.

Lateral geniculate nucleus (LGN)

The bilateral retinal tracing demonstrates a distinct pattern of projections from the eye to this part of the grass rat brain (Figure 4.6). Most of these fibers come from the contralateral eye (Figure 4.6), as previously shown in these animals (Gaillard et al., 2013). Fibers labeled by CT-β injections into the ipsilateral eye were mostly concentrated in a distinct region of the central part of the dorsal LGN (dLGN) and of the ventral LGN (vLGN) and because of this, such ipsilateral fibers clearly demarcate the intergeniculate leaflet (IGL). Most of the dLGN was devoid of PACAP, but some thick PACAP-ir fibers were found in its most rostral region (Figure 4.7 and 4.8A); this pattern was similar to that of melanopsin cell projections to this area in mice (Hattar et al., 2006; Ecker et al., 2010). These PACAP-ir fibers were eliminated with bilateral removal of the eyes (Figure 4.8B) and were only present in the dLGN contralateral to the remaining eye in unilaterally enucleated animals (Figure 4.8C, D) indicating that melanopsin/PACAP projections from the retina to this region are completely crossed. Very few PACAP-ir fibers were observed in mid-caudal dLGN (Figure 4.6 and 4.7); however, those seen were overlaid with CT-β-labeled retinal fibers from the contralateral eye (Figure 4.6C-F).

Relatively few PACAP-ir fibers were found in the ventral portion of the vLGN (Figure 4.6, 4.7 and 4.8). Their distribution in this region overlapped to some extent with that of CT-β-labeled retinal fibers emanating from the ipsilateral eye (Figure 4.6G-J). A few PACAP-ir cells were present in the vLGN. These cells were in the outer boundaries (most medial and lateral portion) of the vLGN and were relatively sparse in the central region.

Intergeniculate leaflet (IGL)

PACAP-ir fibers densely innervated the IGL and spanned across its full rostrocaudal extent (Figure 4.7). Although PACAP-ir labeling was not reduced in bilaterally enucleated grass rats in the most rostral portion of the IGL (Figure 4.8A-B) PACAP-ir in the mid-caudal region of the IGL was substantially reduced after removal of both of the eyes (Figure 4.8E-F). In unilaterally enucleated animals PACAP-ir was diminished slightly more on the side of the brain contralateral to the eye that had been removed (Figure 4.8G-H), indicating that many of these fibers are crossed; however, many fibers were still present on both sides of the IGL, indicating that PACAP-ir projections from the retina to the IGL are bilateral. This was supported using bilateral tracing, which demonstrated a high degree of overlap between the retinal tracers from the two eyes with PACAP fibers in the IGL (Figure 4.6K-N). Similar to the vLGN, a few PACAP-ir cells were found within the IGL (Figure 4.8E-H).

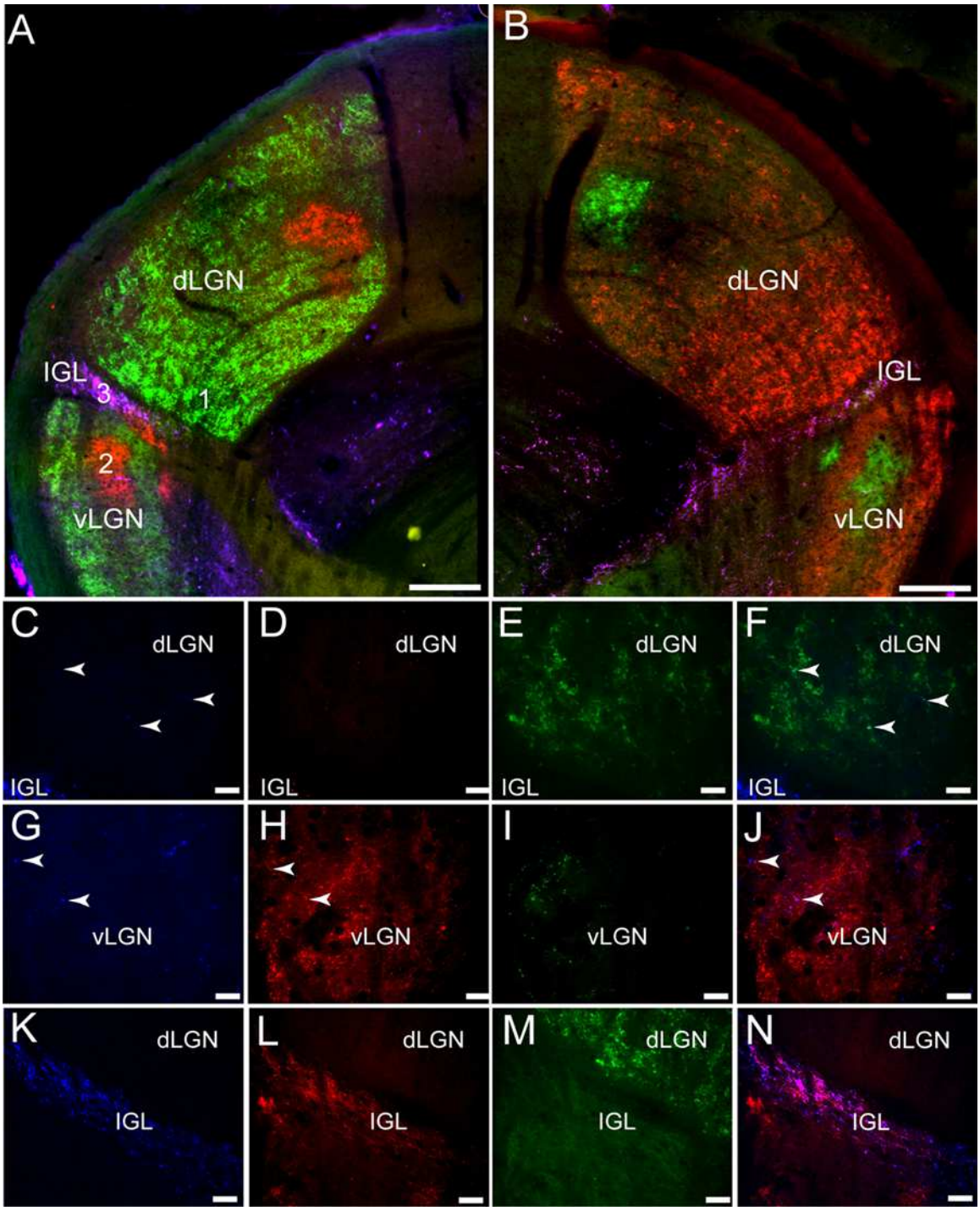

Figure 4.6. PACAP-immunoreactive (ir; blue) fibers and CT-β-labeled retinal fibers from the left (red) and right (green) eye in the lateral geniculate complex (LGN) of the Nile grass rat. Low magnification images of the left LGN are shown in A and of the right in B. Higher magnification images in C-N depict the numbered regions in B (1 = C-F, 2 = G-J, 3 = K-N). Few

Figure 4.6. (cont'd)

PACAP-ir fibers were seen in the dorsal LGN (dLGN; C) where inputs from the contralateral eye were present (E and F); some PACAP-ir fibers were present in the ventral LGN (vLGN; G) where retinal fibers from the ipsilateral eye were concentrated (vLGN, H and J). A dense plexus of PACAP-ir fibers could be seen in the intergeniculate leaflet (IGL; K); there was a high degree of overlap between them and CT-β-labeled retinal fibers (L-M). Scale bars: A and B = 200 μm, C-J = 20 μm and K-N = 40 μm.

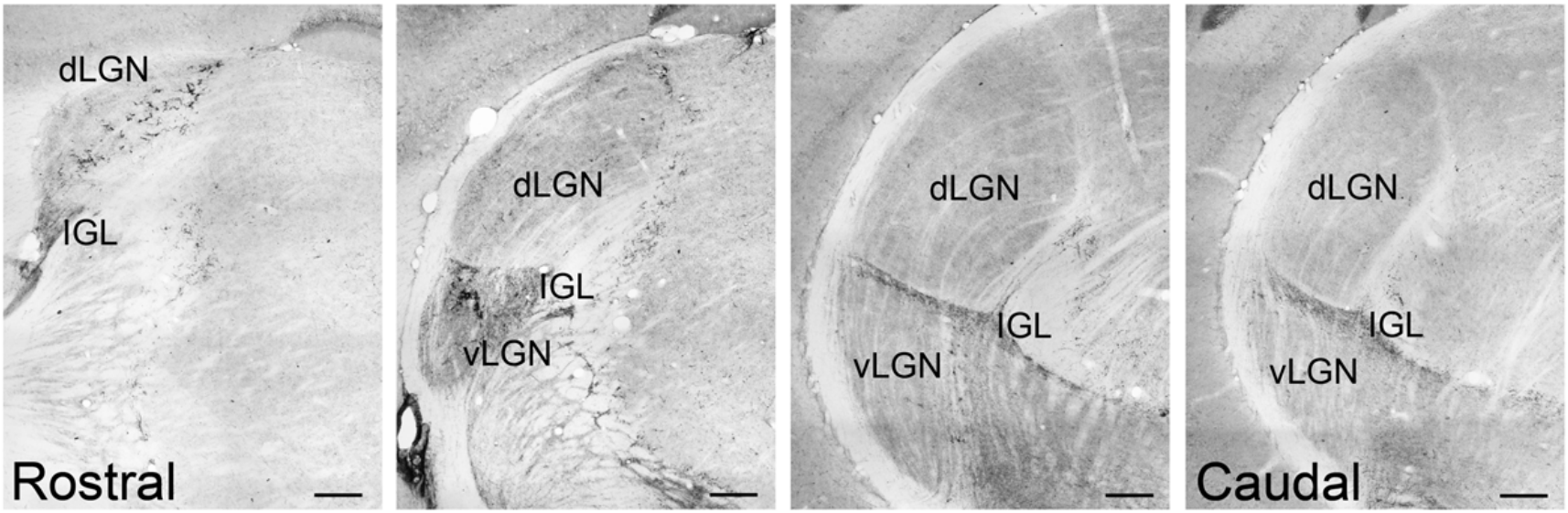

Figure 4.7. PACAP-immunoreactive (ir) fibers across the rostrocaudal extent of the lateral geniculate nucleus (LGN) of the Nile grass rat. PACAP-ir fibers were present in the dorsal aspect of the LGN (dLGN) only in its most rostral region, whereas they were observed in the full rostrocaudal extent of the intergeniculate leaflet (IGL); very few fibers were seen in ventral LGN (vLGN). Scale bars: 200 μm.

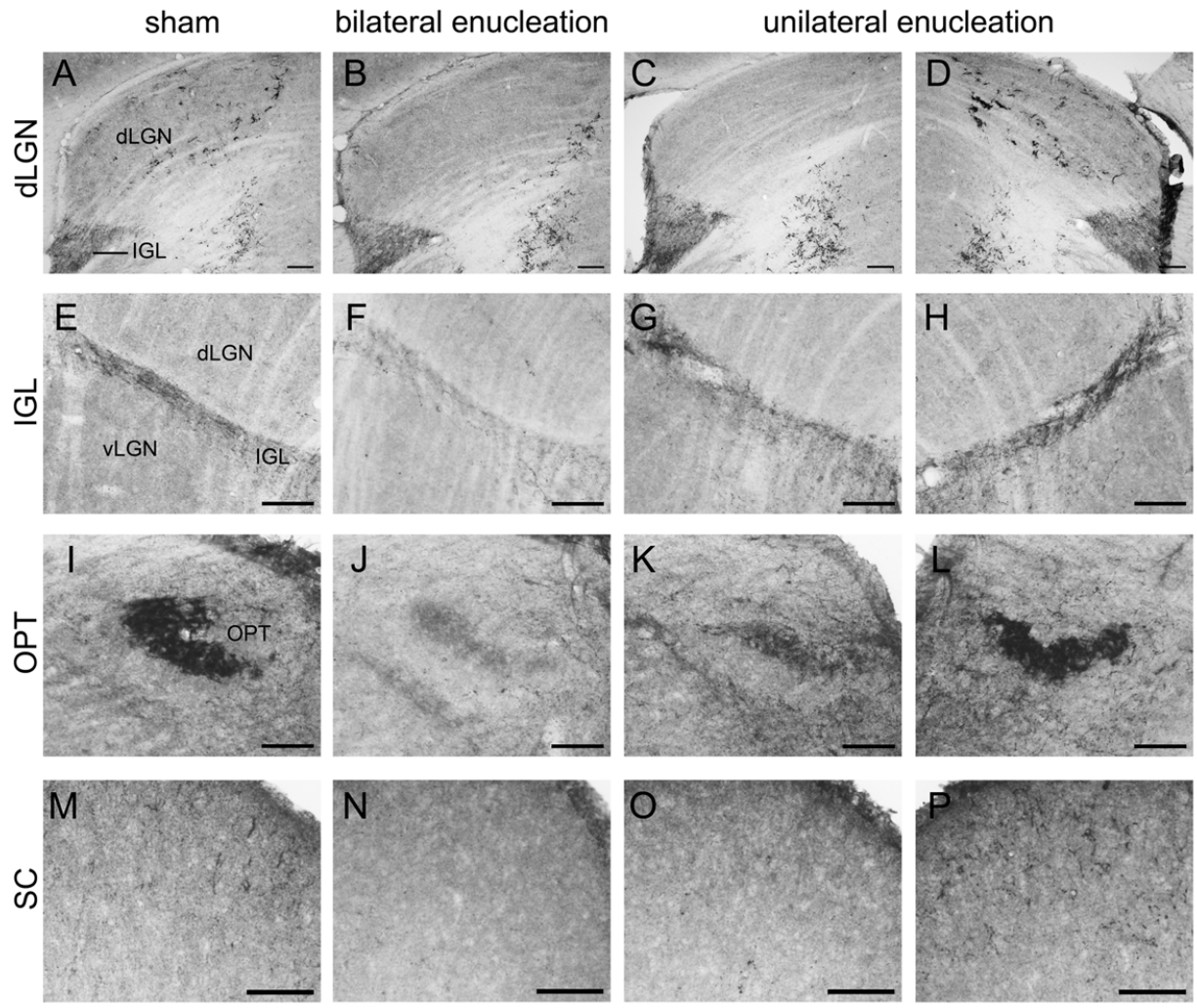

Figure 4.8. PACAP-immunoreactive (ir) fibers in the dorsal lateral geniculate (dLGN), intergeniculate leaflet (IGL), olivary pretectal nucleus (OPT), and superior colliculus (SC) of sham, bilaterally and unilaterally enucleated Nile grass rats. PACAP-ir fibers were observed in the dLGN (A), IGL (E), OPT (I) and SC (M) of sham Nile grass rats; PACAP-ir labeling was greatly reduced in all of these regions in bilaterally enucleated Nile grass rats (B, F, J, N) indicating that most of these fibers come from the retina. Unilateral enucleation reduced PACAP-ir fibers more in the regions contralateral to the eye that was removed (C, G, K, and O) than ipsilateral to it (D, H, L and P), indicating that many (though not all) of these fibers are crossed. Scale bars: 100 μm.

Pretectum

PACAP-ir fibers within the pretectum were concentrated in the olivary pretectal nucleus (OPT; Figure 4.8I and 4.9). Although the rostrocaudal extent of the grass rat OPT, as defined by retinal projections, is extensive (~1,080 μm) (Gaillard et al., 2013), PACAP was only observed in its most rostral region (Figure 4.9). Most PACAP-ir fibers in the OPT originated from the retina, as bilateral enucleation greatly reduced their density (Figure 4.8J). PACAP-ir fibers were observed in both the left and right OPT in unilaterally enucleated grass rats, but more were present in the OPT ipsilateral to the eye that had been removed, indicating that most fibers are crossed (Figure 4.8K-L). This observation was supported by the high degree of overlap between CT-β positive retinal fibers and PACAP-ir fibers within the OPT (Figure 4.10), especially at its most rostral pole (Figure 4.10A-B, E-G). A distinct distribution of ipsilateral and contralateral innervation was revealed by the bilateral tracer injections which demonstrated that contralateral projections target the central and ventral OPT, while input from the ipsilateral eye is concentrated in the peripheral part of the dorsal region of the OPT (Figure 4.10C-D). Most prominent co-localization between PACAP and Ct-β was found in the central and ventral part of the OPT.

Another pretectal structure that contained PACAP-ir fibers was the posterior limitans (PLi). Although PACAP-ir did not seem to be reduced in enucleated grass rats, overlap between PACAP-ir and the retinal tracer from the contralateral eye indicate that a few of these fibers originate from the retina (Figure 4.11A-B). However, many PACAP-ir fibers in the PLi did not overlap with the retinal tracers, indicating that many of the PACAP fiber within this area do not originate in the retina.

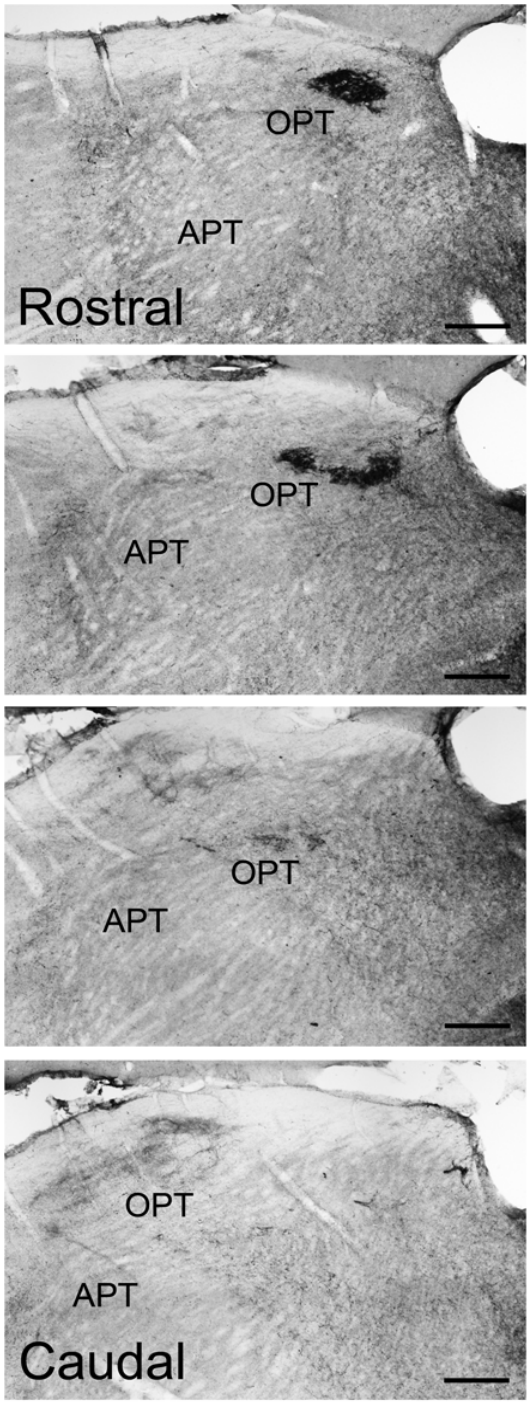

Figure 4.9. PACAP-immunoreactive (ir) fibers across the rostrocaudal extent of the olivary pretectal nucleus (OPT) of the Nile grass rat. Intense PACAP fiber labeling was seen in the most rostral regions of the OPT, while very little was observed in the more caudal regions of the OPT. APT = anterior pretectal nucleus. Scale bars: 20 μm.

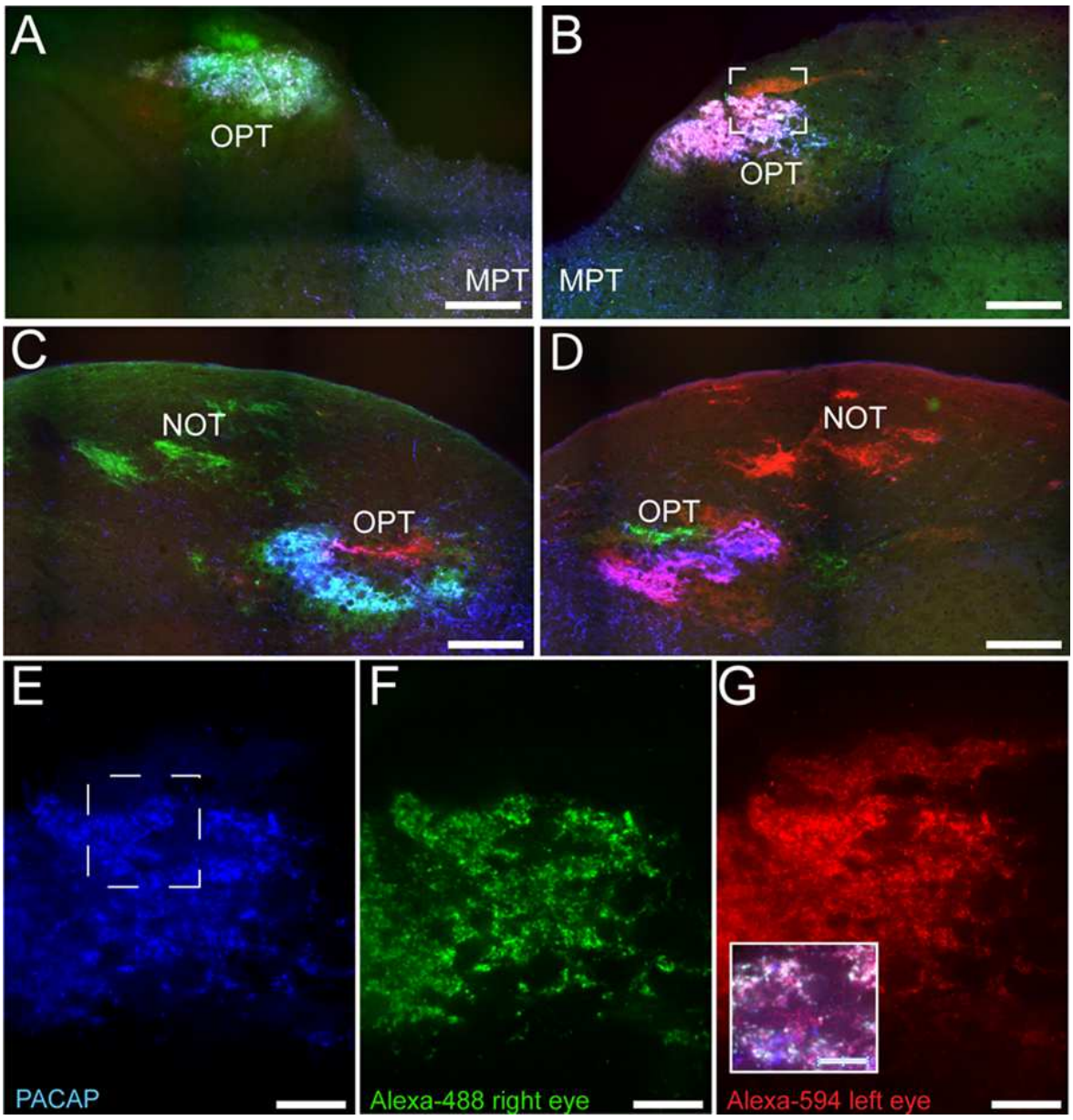

Figure 4.10. PACAP-immunoreactive (ir; blue) fibers and CT-β-labeled retinal fibers from the left (red) and right eye (green) eye in the olivary pretectal nucleus (OPT) of the Nile grass rat. PACAP-ir fibers were concentrated in regions with CT-β-labeled retinal fibers from the contralateral eye; this was the case both in the most rostral pole of the OPT (A & B) and immediately caudal to this region (C & D). High magnification images of PACAP-ir fibers (E) and retinal fibers from the right (F) and left (G) eye were taken from the boxed area shown in B.

Figure 4.10. (cont'd)

Within this most rostral portion of the OPT the area in which PACAP-ir fibers are most concentrated also receives the most input from each eye. The insert in G illustrates an overlay of all three labels present in the boxed area shown in E. MPT = medial pretectal nucleus; NOT = nucleus of the optic tract. Scale bars: A-D = 250 μm, E-G = 50 μm and insert in G = 25 μm.

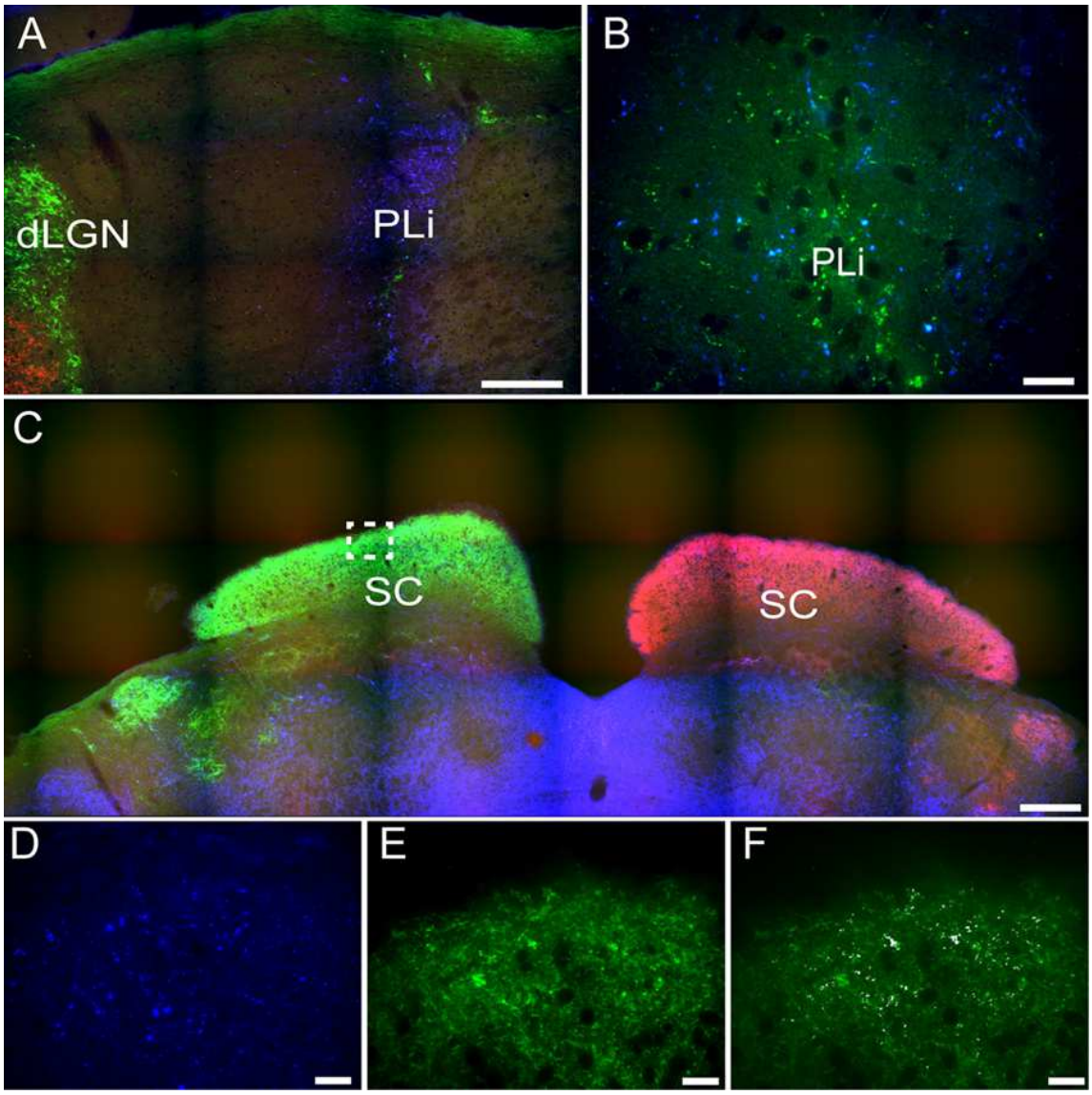

Figure 4.11. PACAP-immunoreactive (ir; blue) and CT-β-labeled retinal fibers from the left (red) and right eye (green) eye in the posterior limitans (PLi) and superior colliculus (SC). Many PACAP-ir fibers were present in the PLi (A), while a small number of these fibers also overlaid with retinal fibers from the contralateral eye (green; B). The SC is heavily innervated by retinal fibers from the contralateral eye (C) and some of these fibers also overlay with PACAP-ir labeled fibers (D-F higher magnification of boxed area in C; D = PACAP staining, E = retinal fibers, F = overlay with co-localization shown in white). Scale bars: A = 150 μm, B = 20 μm, C= 300 μm and D-F = 20 μm.

Superior colliculus (SC)

A few intensely labeled fibers were found in the SC of intact grass rats (Figure 4.8M) but they were absent in bilaterally enucleated ones (Figure 4.8N). In unilaterally enucleated animals PACAP-ir labeled fibers were denser on the side contralateral to the remaining eye and virtually eliminated on the ipsilateral side (Figure 4.8O-P). Similarly, there was a high degree of overlap between PACAP-ir fibers and CT-β-labeled retinal fibers from the contralateral eye (Figure 4.11C-F), again demonstrating the crossed nature of PACAP-containing retinal fibers in this region. As found in other rodents, PACAP-expressing neurons were found in the deep layers of the SC (not shown).

DISCUSSION

ipRGCs and PACAP in the retina of Nile grass rats

ipRGCs are required for the acute inhibition of activity by light in nocturnal rodents and are of special interest in Nile grass rats because light elicits the opposite response in these animals (Shuboni et al., 2012). Here, we found that the retina of the Nile grass rat expresses melanopsin-containing ganglion cells that represent ipRGCs. An increased number of melanopsin cells and enhanced melanopsin-immunoreactivity in dendritic processes were seen in grass rats kept in constant darkness compared to those maintained in a 12:12 light/dark cycle, though this difference did not reach statistical significance (p = 0.12). This trend, however, followed the same pattern as that seen with melanopsin-immunoreactivity in brown Norwegian rats (Hannibal et al., 2013) and albino Wistar rats (Hannibal et al., 2005). Interestingly, the total number of ipRGCs, even in constant darkness, was somewhat low in our grass rats compared to the closely related diurnal Sudanese grass rat (Karnas et al., 2013a). The reason for the difference

is unclear, but it may be related to the fact that our Nile grass rats were derived from a population living 3° South of the equator (Katona and Smale, 1997; McElhinny et al., 1997; Blanchong and Smale, 2000), whereas the Sudanese grass rats were derived from animals trapped 12° North of the equator (Challet et al., 2002; Cuesta et al., 2009).

Different subtypes of ipRGCs are defined mainly in mice (Baver et al., 2008; Schmidt and Kofuji, 2009; Berson et al., 2010; Ecker et al., 2010) and rats (Esquiva et al., 2013; Reifler et al., 2015) on the basis of a number of characteristics, including their sizes and the location of their dendrites within the retina. The three major subtypes seen in other species (M1-M3) were present in the Nile grass rat retina. Most M1-M3 cells were distributed evenly across the retina, but the density of displaced M1 cells (with cell bodies in the INL) was greater in the superior region (Figure 4.1); a larger number of ipRGCs are observed in the superior retina of nocturnal rats (Hannibal et al., 2002; Hattar et al., 2002; Esquiva et al., 2013; Galindo-Romero et al., 2013). In contrast, uniform distributions of all types of ipRGCs are seen in the mouse (Berson et al., 2010; Brown et al., 2010), hamster (Bergstrom et al., 2003; Morin et al., 2003) and human (Hannibal et al., 2004) retina, while macaques have higher numbers of ipRGCs in the central compared to the peripheral retina (Dacey et al., 2005; Hannibal et al., 2014). Many large clusters of ipRGCs were also observed near the retinal ciliary marginal zone of the superior, nasal, and temporal retina of Nile grass rats (Figure 4.1). Similar clusters are reported in the peripheral region of either the superior (Vugler et al., 2008; Valiente-Soriano et al., 2014) or nasal region of the retina (Semo et al., 2014) of nocturnal rodents. These cells have been shown to project to the ciliary body where they control the intrinsic pupillary light reflex in mice (Semo et al., 2014). Interestingly, in the Nile grass rat, all of the melanopsin cells clustered in the peripheral retina also contained PACAP. Thus, not only does it seem likely that these cells play a similar role in

the intrinsic pupillary light reflex in Nile grass rats, but it also suggests that PACAP may serve as a neurotransmitter regulating this reflex in the retina.

The relative numbers of different subtypes of ipRGCs vary somewhat from species to species. In Nile grass rats, 94% were M1 and M3 cells and only 6% were of the M2 subtype, whereas in Sudanese grass rats 25% are of the M2 subtype (Karnas et al., 2013a). In that species M1 cells represent 74% of the total (Karnas et al., 2013a), which is higher than what has been reported in nocturnal rodents (Berson et al., 2010; Schmidt and Kofuji, 2011; Karnas et al., 2013b). Another difference between Nile and Sudanese grass rats is that the number of displaced M1 cells was proportionally higher in the former (20% of ipRGCs) than in the latter (< 1% of ipRGCs) (Karnas et al., 2013a). Interestingly, in humans, as in Nile grass rats, the number of ipRGCs that are displaced is disproportionally high (50% of the total) (Hannibal et al., 2004).

PACAP has been identified in melanopsin-containing cells in a number of species and is present in axons projecting into the brain, where it plays a neuromodulatory role (Hannibal et al., 2002; Bergstrom et al., 2003; Hannibal and Fahrenkrug, 2004; Hannibal et al., 2004; Hannibal, 2006; Hannibal et al., 2014). Here, we found that 84-94 % (average 87.7 %) of the ipRGCs of Nile grass rats also expressed PACAP (Figure 4.2 and 4.3). The number of RGCs co-storing PACAP and melanopsin was slightly lower compared to that previously reported in the rat, hamster, monkey and human (Hannibal et al., 2002; Bergstrom et al., 2003; Hannibal et al., 2004; Hannibal et al., 2014). Since PACAP was found in all subtypes of melanopsin cells it seems unlikely that the PACAP-negative/melanopsin-positive cells or PACAP-positive/melanopsin-negative cells represent distinct populations of cells. More likely, this reflects a difference in expression of either melanopsin or PACAP since both genes are regulated

by light and by a circadian clock (Hannibal et al., 2005; Hannibal et al., 2013) and/or a technical limitation on our ability to detect very low levels of melanopsin/PACAP.

ipRGC projections

It is not possible to use transgenic procedures to aid in identification of axons within the grass rat brain that emanate from ipRGCs, as it is in mice, but our data suggest that PACAP may be used to do this instead. Specifically, by comparing distributions of PACAP-ir fibers in intact and enucleated animals, and by examining direct overlays of retinal and PACAP-ir fibers, we can make reasonable inferences about where the ipRGCs project in Nile grass rats. Using these approaches we found evidence of ipRGC projections in many regions of the Nile grass rat brain that likely play a role in masking, including the suprachiasmatic nucleus (SCN), lateral geniculate nucleus (LGN), pretectum, and superior colliculus (SC) (Figure 4.12). These areas are all known to receive such input in other species (Morin et al., 2003; Hannibal and Fahrenkrug, 2004; Dacey et al., 2005; Hattar et al., 2006; Brown et al., 2010; Ecker et al., 2010; Hannibal et al., 2014), though there is some variation in its patterns and densities. Many other hypothalamic areas receive input from ipRGCs in nocturnal rodents (Hannibal and Fahrenkrug, 2004; Hattar et al., 2006), and are of interest as they show patterns of activity that are not the same in those animals and grass rats (reviewed in Smale et al., 2008). However, retinal input to these areas is limited and PACAP fibers emanating from other sources are dense, making it impossible for us to determine if ipRGCs project to these regions.

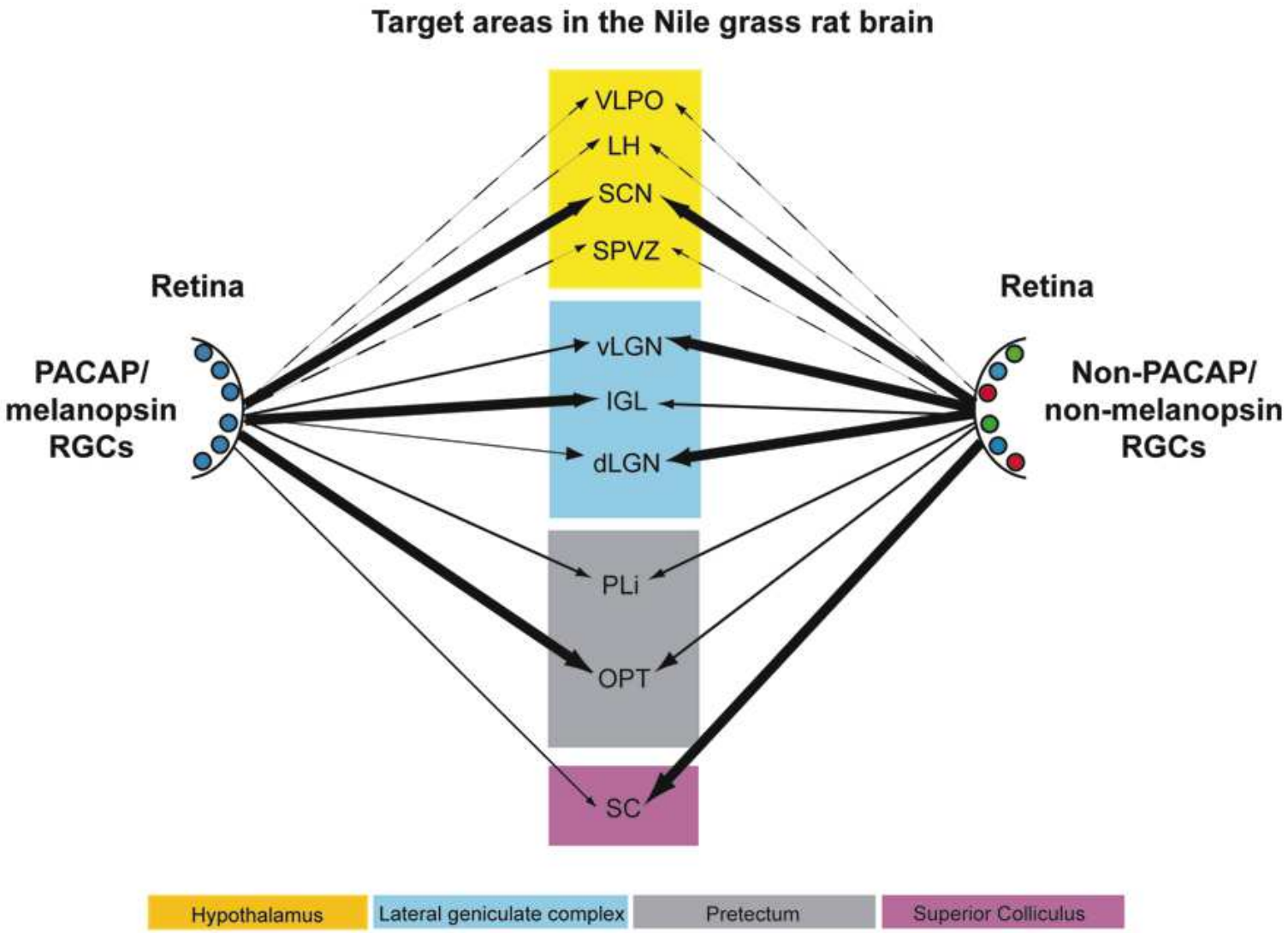

Figure 4.12. Schematic diagram of the retinal projections from PACAP/melanopsin-containing retinal ganglion cells (RGCs) (left) and RGCs not containing PACAP/melanopsin (right) in the Nile grass rat brain. The thickness of the arrows roughly

Figure 4.12. (cont'd)

indicates the density of the innervation to the various brain regions listed. Some projections of each type that are presumed to exist in other hypothalamic regions are presented with dashed lines. VLPO = ventrolateral preoptic area, LH = lateral hypothalamus, SCN = suprachiasmatic nucleus, SPVZ = subparaventricular zone, vLGN = ventral lateral geniculate nucleus, IGL = intergeniculate leaflet, dLGN = dorsal lateral geniculate nucleus, PLi = posterior limitans, OPT = olivary pretectal nucleus, SC = superior colliculus.

Suprachiasmatic nucleus (SCN)

We obtained evidence of bilateral projections from ipRGCs to the SCN in the Nile grass rat. Specifically, PACAP-immunoreactivity was reduced but still present bilaterally in the SCN following unilateral enucleation, and was almost completely eliminated when both eyes were removed. Bilateral tracing experiments also indicated that the major source of PACAP fibers within the SCN is the retina, and that PACAP cells within each eye project to both to the left and right SCN (Figure 4.4 and 4.5). The few non-retinal PACAP-ir fibers within the SCN may come from the IGL or vLGN, as there are weakly stained PACAP-ir neurons in both areas in grass rats (Figure 4.8). Such cells have not been reported in Wistar rats (Hannibal, 2002), raising the intriguing possibility that they may play a role in mediation of differences in the behavioral responses to light of these two species. It is not possible to tell which subtypes of ipRGCs project to the SCN of Nile grass rats. In mice, however, both M1 and non-M1 cells innervate this nucleus (Ecker et al., 2010) and most of the input comes from M1 cells (Baver et al., 2008).

ipRGC projections to the SCN of nocturnal mice carry information about light that comes both from its effect on the melanopsin protein and from cone/rod-driven pathways that converge

on the ipRGCs and this pathway mediates the entraining effects of light on circadian rhythms (Goz et al., 2008; Guler et al., 2008; Hatori et al., 2008). The ipRGCs are likely to convey photic information via similar mechanisms to the SCN of Nile grass rats, as photic responses of the circadian system are very similar in diurnal and nocturnal species (reviewed in Smale et al 2003). However, some differences in this system may exist in relation to the role that it plays in mediation of the more acute ("masking") responses to light, which are not the same in diurnal and nocturnal species. The extent to which masking depends on the SCN has been debated, but in the most recent and thorough study, SCN lesions in hamsters abolished light-induced suppression of activity (Li et al., 2005). However, preliminary data suggest that the SCN may not be necessary for a masking response to light in Nile grass rats, at least under some conditions (*Gall et al., unpublished observations*). Data derived from lesion studies of nocturnal rodents led Redlin (2001) to suggest that the neural pathways controlling masking may be redundant and that multiple retinorecipient brain regions are involved. More recently, Morin (2013) proposed that ipRGC projections to the SCN may play a key role in regulation of masking as well as photoentrainment. It will be important to determine whether and how this pathway contributes to one or both of these functions in diurnal species.

Lateral geniculate nucleus (LGN)

The LGN is another region that plays an important role in image and non-image forming visual functions and receives input from ipRGCs in nocturnal (hamsters: Bergstrom et al. 2003; mice: Brown et al. 2010, Ecker et al. 2010, Hattar et al. 2006; rats: Hannibal and Fahrenkrug 2004) and diurnal (macaque monkeys: Hannibal et al., 2014; Nile grass rats: present study) species. In the Nile grass rat we saw relatively little input from ipRGCs (as indicated by PACAP-

immunoreactivity) in either the dorsal LGN (dLGN) or the ventral LGN (vLGN; Figure 4.6, 4.7 and 4.8). In this respect, Nile grass rats are very different from nocturnal rodents, in which both the dLGN and vLGN are heavily innervated by ipRGCs (mice: Brown et al. 2010, Ecker et al. 2010; rats: Hannibal and Fahrenkrug 2004). This may reflect a reduced number of non-M1 ipRGCs in the Nile grass rat retina, as they are the primary ones that project to these regions of the LGN in nocturnal mice (Brown et al., 2010; Ecker et al., 2010). In the most rostral portion of the Nile grass rat dLGN, we did see some PACAP fibers of retinal origin and their distribution resembled that of axons emanating from the M1 cells in mouse retina (Hattar et al., 2006). The presence of these PACAP-ir fibers raises the possibility that ipRGCs play an important role in processing visual information in Nile grass rats, as they appear to do in nocturnal rodents (Brown et al., 2010; Ecker et al., 2010) and in primates and humans (Dacey et al., 2005; Hannibal et al., 2014). These fibers may also modulate masking, as lesions of the dLGN in mice actually enhance masking responses to low intensity light (Edelstein and Mrosovsky, 2001).

In contrast to the dorsal and ventral LGN, the intergeniculate leaflet (IGL) appears to receive dense input from ipRGCs in the Nile grass rat, as it does in other species (mice: Hattar et al. 2006; rats: Hannibal and Fahrenkrug 2004; hamsters: Bergstrom et al. 2003; macaques (pregeniculate complex): Hannibal et al. 2014). However, some PACAP-containing fibers within the IGL did not originate from the retina. The source of these fibers might be the contralateral IGL or vLGN, as these structures are known to project to the IGL in nocturnal rodents (Morin, 2013b) and have weakly stained PACAP-ir cell bodies (present results). In mice, fibers emanating from M1 and non-M1 ipRGCs are intermixed in the IGL (Ecker et al., 2010). The role of the ipRGC projection to the IGL has not been clearly established, but it is likely to be related to the temporal structuring of daily activity patterns. In nocturnal rodents the IGL is known to be

important for communication of both photic and non-photic information to the SCN and it appears to play an important role in modulation of masking through pathways that have not yet been clearly established (Morin, 2013b). In hamsters, IGL lesions enhance negative masking (i.e. the inhibitory effects of light on activity are increased) (Redlin et al., 1999), whereas in diurnal Nile grass rats, the positive masking response to light are reversed by IGL lesions (Gall et al., 2013); that is, light reduces locomotor activity in IGL lesioned animals. This indicates that the IGL may contribute to the differences in the masking response of intact diurnal and nocturnal rodents, something likely to be related to ipRGC input to this region.

Pretectum

PACAP fibers of retinal origin were also evident in two areas of the pretectum, the posterior limitans nucleus (PLi) and olivary pretectal area (OPT) (Figure 4.8, 4.9, 4.10 and 4.11), regions that receive input from ipRGCs in other species as well (Hannibal and Fahrenkrug, 2004; Hattar et al., 2006; Hannibal et al., 2014). The PLi is known in hamsters to both receive input from and send projections to the vLGN, IGL, other areas of the pretectum (including the OPT) and the superior colliculus (SC) in hamsters (Morin and Blanchard, 1998). The OPT region of the pretectum had a high amount of PACAP-ir fibers coming from the retina in our Nile grass rats (Figure 4.8, 4.9 and 4.10). Interestingly, we only saw these ipRGC fibers in the most rostral portion of the OPT, whereas in nocturnal mice they are present across its full rostrocaudal extent (Hattar et al., 2006). This is particularly interesting because lesions of the pretecum, including the OPT, attenuate the masking response of sleep patterns to light in Norway rats (Miller et al., 1998), and actually reverse masking of activity in diurnal Nile grass rats; that is, light triggers a decrease, rather than an increase, in their general activity (*Gall et al., unpublished observations*).

Further, effects of light on the OPT are quite different in Nile grass rats and nocturnal mice; specifically, light induces an increase in FOS in the OPT of the former species and a decrease the latter (Shuboni et al., 2015). Thus, it is tempting to speculate that differential responsiveness of the OPT to photic information reaching it through the ipRGCs contribute to differences in masking associated with chronotype.

In nocturnal mice, distinct subtypes of melanopsin cells differentially innervate the OPT. While the shell receives input from M1 cells, the core receives input from non-M1 cells (Hattar et al., 2006; Baver et al., 2008; Ecker et al., 2010). The M1 population can be further divided by which ones express the transcription factor, Brn3b. Specifically, whereas most M1 cells and all non-M1 cells express Brn3b in the adult mouse retina, there are some M1 cells, about 200 (which represents approximately 10% of all ipRGCs) that do not (Chen et al., 2011). These cells project extensively to the SCN and moderately to the IGL and are sufficient for both photoentrainment and masking. However, these cells do not project to the OPT and are not sufficient for the pupillary light reflex (PLR), which requires M1 and non-M1 cells expressing Brn3b that project to the OPT (Chen et al., 2011). Whether this is similar in Nile grass rats, needs to be determined.

Superior colliculus (SC)

In Nile grass rats, as in other species (hamsters: Morin et al. 2003; mice: Hattar et al. 2006; rats: Hannibal and Fahrenkrug 2004), the SC appears to receive some input from ipRGCs. It is clear that the projection to the SC is crossed, since removal of one eye led to a substantial decrease in PACAP-ir in the contralateral, but not the ipsilateral, SC (Figure 4.8). In mice, both M1 and non-M1 ipRGCs project to the SC (Ecker et al., 2010). The SC plays an important role in directing eye movements in response to visual cues, which suggests that ipRGC projections to

this structure may play a role in this aspect of visual processing. It may also contribute to masking, as lesions of the SC increase direct effects of low intensity light on wheel running activity in hamsters (Redlin et al. 2003). Although the SC may not be necessary for masking, it could play an important modulatory role (Redlin et al., 2003). Nothing is currently known about this issue in diurnal species.

Conclusion

In conclusion, ipRGCs, as defined by the presence of melanopsin, contain PACAP in the diurnal Nile grass rat, as they do in nocturnal rodents (hamsters: Bergstrom et al. 2003; rats: Hannibal and Fahrenkrug 2004) and diurnal primates (macaque monkeys: Hannibal et al. 2014; humans: Hannibal et al. 2004). Although there were some differences in their distribution across the retina, and in the relative numbers of the different sub-types of ipRGCs, the fundamental features of these cells were the same as those described in other species. The central projections of PACAP-containing cells in the retina to brain regions involved in image and non-image forming visual functions, such as masking, are also very similar across species, including Nile grass rats (Figure 4.12). However some interesting differences were apparent. For example, the ventral and dorsal LGN appear to receive less input from ipRGCs in Nile grass rats than in nocturnal murid rodents. Furthermore, whereas ipRGCs project to full rostrocaudal extent of the OPT in other species, the caudal OPT does not seem to receive such input in grass rats. Finally, it should be noted that there might be differences within target structures identified here with respect to which cell populations receive direct input from the ipRGCs. Thus, future studies are needed to test the hypothesis that differences in patterns of connectivity between ipRGCs and

their targets contribute to differences between diurnal and nocturnal species with respect to their masking responses to light.

CHAPTER 5: Similarities and differences in direct retinal input and in inhibitory and excitatory cell populations in ipRGC target areas

INTRODUCTION

In mammals, light not only synchronizes endogenous daily rhythms (i.e. circadian rhythms) to the environmental light/dark cycle, but it also acutely affects arousal states, a process known as masking. Masking responses to light are dependent upon the chronotype of the animal with light stimulating arousal in diurnal species and suppressing it in nocturnal ones (Redlin, 2001). The neural substrates underlying these chronotype differences are not well understood. However, in nocturnal species these direct effects of light are believed to be mediated through a subset of retinal ganglion cells that are intrinsically photosensitive (termed ipRGCs) due to their expression of the melanopsin protein; these ipRGCs are necessary for transmitting photic cues important for masking to the brain (Goz et al., 2008; Guler et al., 2008; Hatori et al., 2008). Though the brain regions to which ipRGCs project are similar in diurnal and nocturnal rodents (Hannibal and Fahrenkrug, 2004; Hattar et al., 2006; Langel et al., 2015), differences in circuitry within those brain regions (or downstream of them) could lead to differences in how diurnal and nocturnal species respond to the same light stimulus. For instance, ipRGCs could project to different populations of cells within a common target area. For example, in a diurnal species, but not a nocturnal one, inhibitory interneurons could receive the ipRGC signal, alter its valence, and send outputs to a population of target neurons. One alternative possibility is that ipRGC target cells are the same, and respond the same way to ipRGC signals, but the regions to which they project are different. Here we will focus on the first hypothesis by examining whether some

features of the internal circuitry within areas receiving input from ipRGCs differ in a diurnal and nocturnal brain.

Two brain areas that receive input from ipRGCs that are of special interest are the intergeniculate leaflet (IGL) of the thalamus and the olivary pretectal area (OPT) of the pretectum. In both nocturnal and diurnal species these regions receive input from ipRGCs (Hannibal and Fahrenkrug, 2004; Hattar et al., 2006; Langel et al., 2015) and contain neurons that are responsive to light as measured by the induction of the immediate early gene cFOS (Prichard et al., 2002; Juhl et al., 2007; Langel et al., 2014; Shuboni et al., 2015). Additionally, lesions that include the IGL or the OPT alter species typical responses to light (Miller et al., 1998; Redlin et al., 1999; Gall et al., 2013; *Gall et al., unpublished observations*). Thus, both the IGL and OPT may play an important role in modulating species specific masking responses to light. The question of whether differences within these structures promote species differences in masking responses to light has not yet been examined.

The two most important excitatory and inhibitory neurotransmitters in the brain are glutamate and gamma-aminobutyric acid (GABA), respectively. Glutamatergic neurons can be identified by the presence of vesicular glutamate transports (VGLUTs), which incorporate glutamate into synaptic vesicles (El Mestikawy et al., 2011; Brumovsky, 2013). VGLUTs exist in three isoforms (VGLUT1-3) that vary in their distribution across the brain. *Vglut1* mRNA is primarily found in the cerebral cortex and hippocampus, *Vglut2* mRNA is located throughout many subcortical structures including the thalamus, hypothalamus and brainstem and *Vglut3* mRNA is restricted to areas of the midbrain, striatum, cortex and hippocampus (El Mestikawy et al., 2011). The main inhibitory neurotransmitter in the brain, GABA, is synthesized from glutamate via the rate-limiting enzyme, glutamic acid decarboxylase (GAD), which can be used

as a marker of GABAergic neurons (Soghomonian and Martin, 1998). GAD exists in two isoforms, GAD65 and GAD67 (molecular weights of 65 and 67 kDa, respectively), which are produced from two separate genes (Soghomonian and Martin, 1998). Both GAD65 and GAD67 appear to be co-expressed in many of same brain regions, but their spatial distribution within neurons differs, such that GAD65 is confined to the axon terminal, while GAD67 is found throughout the cytoplasm (Esclapez et al., 1994; Soghomonian and Martin, 1998). In the present study, we selected *Vglut2* to label glutamatergic neurons and *Gad65* to label GABAergic neurons due to their distribution in many ipRGC target areas (Feldblum et al., 1993; Esclapez et al., 1994; El Mestikawy et al., 2011).

Here we examine the possibility that species differences in masking responses to light are due to chronotype differences in the internal circuitry, the "wiring diagram", of brain regions that receive input from ipRGCs. First, to determine whether differences exist in the input to light responsive neurons in the IGL and/or OPT, we examined cFOS-expressing neurons with close contacts from retinal fibers in these regions in diurnal Nile grass rats and nocturnal Norway rats (*Rattus norvegicus*) that were exposed to a 1-hour light pulse at night. Next, we determined whether differences exist in the distribution of excitatory (e.g. glutamate) and inhibitory (e.g. GABA) neuronal populations in multiple ipRGC target areas (IGL, OPT, ventrolateral preoptic area, suprachiasmatic nucleus, ventral subparaventricular zone, habenular nuclei and superior colliculus) in grass rats and Norway rats by labeling the mRNA for *Vglut2* and *Gad65*, respectively.

METHODS

Animals

Adult male Nile grass rats (65-97 g) from a breeding colony maintained at Michigan State University and male Norway rats (Long Evans strain, LE; initial weight: 175-199 g) purchased from Harlan laboratories (Indianapolis, IN, USA) were used in this study. Animals were individually housed in plexiglass cages (Nile grass rat: 48.3 x 25.7 x 15.2 cm^3; LE rat: 47.6 x 25.9 x 20.9 cm^2) and maintained in a 12:12 light/dark (LD) cycle (lights on at 06:00 h). Cool white fluorescent bulbs provided illumination during the daytime (~300 lux), while a dim red light (< 2 lux) was kept on constantly. Food (Nile grass rats: PMI Nutrition, Prolab RMH 2000, Brentwood, MO, USA; LE rats: Teklad Rodent diet 8640; Harlan, Madison, WI, USA) and water were provided *ad libitum*. General activity was detected with infrared sensors located on the lid of each cage and then recorded and analyzed with the VitalView system (MiniMitter, Bend, OR, USA). All light pulses used the same white fluorescent bulbs (~300 lux) as the daytime room lighting. All experiments were performed in accordance with the guidelines established by the National Institutes of Health Guide for the Care and Use of Laboratory Animals and the Michigan State University Institutional Animal Care and Use Committee. All efforts were made to minimize the number of animals used in these experiments.

Experiment 1: Retinal projections to cFOS expressing neurons in the IGL and OPT

Retinal injections and tissue collection

Grass rats (n = 17) and LE rats (n = 17) were anesthetized with isoflurane and then received 5 µL intravitreal injections of cholera toxin subunit β (CT-β) conjugated to Alexa Fluor 594 (Molecular Probes, Eugene, OR, USA; C-22842; LE rats: 5 µg/µL; grass rats: 4 µg/µL; dissolved

in 2% dimethyl sulfoxide (DMSO) in 0.9% saline vehicle) through a Hamilton syringe (Reno, NV, USA). Seven days later animals received injections of sodium pentobarbital (Nembutal; Ovation Pharmaceutical, Deerfield, IL, USA; LE rats: 1.5 cc; grass rats: 0.5 cc) immediately after being exposed to a 1-hour light pulse at Zetigeber time 16 (ZT16; where ZT0 = lights-on and ZT12 = lights-off) or at the same time on control night. Animals were then transcardially perfused with warm 0.01 M phosphate buffered saline (PBS; pH 7.4) followed by Stefanini's fixative (2% paraformaldehyde (PFA) and 0.2% picric acid in 0.1 M PBS; Sigma-Aldrich, St. Louis, MO, USA; pH 7.2). Brains were removed, post-fixed overnight, and cryoprotected in 20% (24 hours) and then in 30% (for at least 24) sucrose in 0.1 M phosphate buffer (PB) at 4 °C. Coronal brain sections (40 μm) were cut on a freezing microtome in 3 alternating series. Tissue was stored in cryoprotectant (Watson et al., 1986) at -20 °C until further processing.

Tissue processing

One series of sections from each animal was processed for immunofluorescent detection of cFOS and neuronal nuclear antigen (NeuN), a marker of mature neurons. Tissue was rinsed with 0.01 M PBS (10 minutes/rinse) between all steps and incubations included 0.25% Triton-X-100 (TX) and 0.25% normal donkey serum (NDS; Jackson ImmunoResearch laboratories, West Grove, PA, USA; 017-000-121). All rinses and incubations occurred at room temperature (RT) with gentle agitation, unless otherwise indicated. Sections were first treated with antigen retrieval buffer (citrate buffer, pH 6.0; Sigma-Aldrich) at 90 °C for 20 minutes. Next, tissue was incubated with hydrogen peroxide (H_2O_2) in 0.01 M PBS for 10 minutes, blocked with 10% NDS for 1 hour and then incubated with rabbit ant-cFOS (1:10,000; Santa Cruz Biotechnology, Dallas, TX; sc-52) at 4 °C for 48 hours. Sections were then incubated in the secondary biotinylated donkey anti-rabbit

(1:800; Jackson; 711-065-152) at 4 °C for 24 hours and streptavidin-conjugated Alexa 647 (1:500; Jackson; 016-600-084) for 1 hour at RT. The tissue was blocked again in 10% NDS for 1 h, incubated in mouse anti-NeuN (1:1,000; EMD Millipore, Billerica, MA, USA; MAB377) at 4 °C for 48 hours and then in Alexa Fluor 488 donkey anti-mouse (1:500; Jackson; 715-545-151) at RT for 24 hours. Following the IF procedure, sections were mounted on gelatin-coated slides, dehydrated and coverslipped using Harleco Krystalon (EMD Millipore).

Photomicrographs and analysis

Confocal images (512 x 512 pixels) of the IGL and OPT were taken of light pulsed and control animals (n = 4/group) on an Olympus FluoView FV1000 laser-scanning microscope using FV1000 ASW software. The tissue was excited with argon (488 nm; for NeuN), green helium neon (543 nm; for CT-β labeled fibers) and red helium neon (633 nm; for cFOS) lasers. For cell counts of cFOS and NeuN, Z-stack images (Z-thickness = 18 μm; step size: 1.5 μm) of one section through each area (bilaterally) were visualized using an UPLFLN 40x oil objective (1.30 NA). The confirmation of retinal contacts was performed with Z-stack images (step size: 1 μm) taken with an UPLSAPO 100X oil objective (1.40 NA) from randomly selected portions of the IGL with cFOS labeled neurons. In animals exposed to a light pulse at night, a total of 28 cFOS labeled neurons from 4 LE rats were selected to determine whether such neurons have close contact with retinal fibers; 30 cFOS labeled neurons from 4 grass rats were also selected. ImageJ software (version 1.48v, NIH, USA) was used to visualize the Z-stack images, to count cFOS labeled neurons and to determine whether these cFOS labeled neurons were in close contact with retinal fibers. Independent sample t-tests (2-tailed) were used to determine whether the numbers of cFOS labeled neurons in the IGL and OPT differed between control (n=4) and light pulsed

(n=4) animals; counts for each species were analyzed separately. SPSS version 21 (SPSS, Inc., an IBM Company, Chicago, IL, USA) was used for all statistical tests and tests were considered significant if $p < 0.05$. Data are presented as the mean ± standard error of the mean (SEM). All images were adjusted for brightness, contrast and size using Adobe Photoshop CS4 (Adobe, San Jose, CA, USA).

Experiment 2: Distribution of glutamatergic and GABAergic neurons in retinorecipient brain areas in a diurnal and a nocturnal species

Tissue collection

LE rats and grass rats received intraperitoneal injections of sodium pentobarbital (Nembutal; Ovation Pharmaceutical; LE rats: 1.5 cc; grass rats: 0.5 cc) during the day (ZT5-6; n = 4/species) and night (ZT17-18; n = 3/species). Animals were then perfused transcardially with warm saline followed by ice cold 4% PFA in 0.1 M PB. Brains were removed, post-fixed for 24 hours, cryoprotected in 20% (24 hours) and 30% (24-48 hours) sucrose in 0.1 M PB at 4 °C and rapidly frozen in powdered dry ice. Whole brains were then stored at -80 °C until further processing. An additional subset of animals was perfused immediately following a 1-hour light pulse at ZT16 (n=4/species) or the same time on a control night (n=4/species). The tissue collection was similar for these animals, except that they were perfused with 0.01 M PBS followed by Stefanini fixative and the brains were cut at 30 μm on a microtome after the sucrose immersion.

Preparation of riboprobes

Rat cDNA fragments for *Gad65* and *Vglut2* were previously subcloned into a pCRII-TOPO cloning vector (Invitrogen, Carlsbad, CA, USA; generously provided by Dr. Erich Ottem, Northern Michigan University, Marquette, MI, USA). Plasmids were purified using the Wizard *Plus* SV Minipreps DNA Purification System (Promega, Madison, WI, USA; A1330) and were sequenced by the Michigan State University Genomics Core for verification. cDNAs were cut and amplified from the plasmids via polymerase chain reaction (PCR) using M13 (-20) forward and M13 reverse primers with the Platinum PCR SuperMix (Invitrogen, 11306-016). Sp6 (antisense; Roche Diagnostics, Indianapolis, IN, USA; 10810274001) and T7 (sense; Roche; 10881767001) polymerases were used to transcribe RNA probes using a digoxigenin (DIG) labeling mix (Roche; 11277073910).

In situ hybridization (ISH) for Gad65 and Vglut2 mRNA

Coronal brain sections (40 μm) were cut on a cryostat and collected in 3 alternating series. One series of sections from each animal was processed for *Gad65* mRNA, while a second series was processed for *Vglut2* mRNA. Free-floating brain sections were washed in 2X saline sodium citrate (SSC, pH 7.0) for 5 minutes and then treated with proteinase K (1μg/mL; in 50 mM EDTA, 0.1 M Tris Buffer pH 8.0) for 10 minutes at 37˚C followed by fixation in 4% paraformaldehyde/0.1M PB for 5 minutes. Sections were rinsed for 5 minutes in 2X SSC, incubated with 0.25% acetic acid in 0.1M triethanolamine for 10 min and rinsed for 5 minutes in 2X SSC. Sections were then transferred to hybridization solution (60% formamide, 10 mM Tris-hyrdochloride (HCl) (pH 7.5), 200 μg/mL tRNA, 1X Denhardt's solution, 0.6 M sodium chloride (NaCl), 0.25% sodium dodecyl sulfate, 1 mM ethylenediaminetetraacetic acid (EDTA; pH 8.0),

10% dextran sulfate sodium) containing the DIG-labeled riboprobes (approximately 250 ng/mL) for 16-18 h at 58 °C. After hybridization, sections were rinsed twice in 2X SSC/50% formamide for 10 minutes at 58 °C, treated with RNase A for 30 min at 37 °C, rinsed twice in 2X SSC for 10 minutes at 58 °C and rinsed once in .4X SSC for 30 minutes at 58 °C. Sections were then transferred to blocking reagent (DIG nucleic acid detection kit, Roche; diluted 1:100; 11175041910) for 1 hour followed by an incubation in alkaline phosphatase-conjugated anti-DIG (Roche; diluted 1:5,000) in DIG buffer 1 (0.1 M Tris-HCl, 0.15 M NaCl, pH 7.5) with 0.1% TX for 3 hours at RT. To remove excess antibody, sections were rinsed twice in DIG buffer 1 (15 minutes each) and then once for 5 minutes in DIG buffer 3 (0.1 M Tris-HCl, 0.1 M NaCl, 0.05 M magnesium chloride, pH 9.5). Color development was performed with 5-bromo-4-chloro-3-indolyl phosphate (375 μg/mL) and 4-Nitro blue tetrazolium chloride (188 μg/mL) in DIG buffer 3 overnight. The enzymatic reaction was ended by rinsing the sections in 10 mM Tris-HCl (pH 8.0) with 1 mM EDTA for 30 minutes. Sections were then mounted on gelatin-coated slides, dehydrated and coverslipped using permount (Fisher Scientific, Pittsburgh, PA, USA).

Immunohistochemistry (IHC) for cFOS

The IHC protocol for cFOS was similar to that used in Experiment 1 with the following exceptions: rinses were 5 minutes, sections were blocked with 5% NDS, the cFOS primary antibody (diluted 1:25,000) incubation was overnight at RT, the secondary antibody incubation was for 2 hours at RT, and after a 1 hour incubation in avidin-biotin complex (ABC) solution (0.9% each of avidin and biotin solutions) sections were rinsed three times in 0.125 M acetate buffer (pH 7.2) for 10 min, pre-incubated in 0.025% diaminobenzidine (DAB, Sigma-Aldrich) enhanced with 2.5% nickel sulfate (Sigma-Aldrich) in acetate buffer for 30 seconds and reacted

with 0.01% H_2O_2. Sections were then mounted on gelatin-coated slides, dehydrated and coverslipped using permount (Fisher Scientific).

Photomicrographs and analysis

All images of *Gad65* mRNA, *Vglut2* mRNA and cFOS staining were captured with a digital camera (MBF Bioscience Inc., 2007) attached to a Nikon light microscope (Eclipse 80i, Nikon Instruments Inc., NY, USA). Images were adjusted for brightness, contrast and size using Adobe Photoshop CS4 (Adobe, San Jose, CA, USA). To determine whether the patterns of excitatory (e.g. glutamate) and inhibitory (e.g. GABA) neuronal populations within various brain areas differ in a diurnal and nocturnal brain, the distribution of glutamate (*Vglut2* mRNA) and GABA (*Gad65* mRNA) was noted in various brain areas of both LE rats and grass rats. Two brain regions of particular interest are the IGL of the lateral geniculate nucleus (LGN) and OPT, so the distribution of *Vglut2* and *Gad65* cell bodies in these areas are described first. Information on the patterns of cFOS labeling after light stimulation in both of these areas are also noted. We then focus on the patterns of *Vglut2* and *Gad65* mRNA labeling in brain areas that receive input from ipRGCs, such as the ventrolateral preoptic area, suprachiasmatic nucleus, ventral subparaventricular zone, habenular nuclei and superior colliculus. The relative densities of *Vglut2* and *Gad65* labeled cells was recorded based on the following six categories: very dense (++++), dense (+++), moderate (++), sparse (+), very sparse (+/-) and absent (-). Very sparse was indicated if only a few labeled cells were found across that entire brain region.

RESULTS

Experiment 1: Retinal projections to cFOS expressing neurons in the IGL and OPT

Exposure to a 1-hour light pulse at ZT16 significantly increased cFOS expression in the IGL of both LE rats ($t(6) = 3.04$, $p = 0.02$) and grass rats ($t(6) = 3.75$, $p < 0.01$). Specifically, cFOS levels in the IGL were low on the control night in both species (LE rats: 4.88 ± 1.68; grass rats: 5.88 ± 1.63) and were markedly increased after the light pulse (LE rats: 16.13 ± 3.30; grass rats: 17.13 ± 2.52). To determine whether these cFOS-expressing neurons are in close contact with retinal fibers, confocal Z-stack images were used to locate close contacts between retinal fibers and cFOS-immunoreactive (ir) neurons (Figure 5.1A and B). A surprisingly large percentage of neurons expressing cFOS in response to light receive input directly from the retina in both species, but this percentage was somewhat higher in LE rats (> 96%) than in grass rats (> 76%; Figure 5.1C). cFOS-labelled neurons were extremely sparse and variable in the OPT of light pulsed LE rats (2.9 ± 1.30) and grass rats (10.25 ± 6.22), so retinal contacts on them were not quantified.

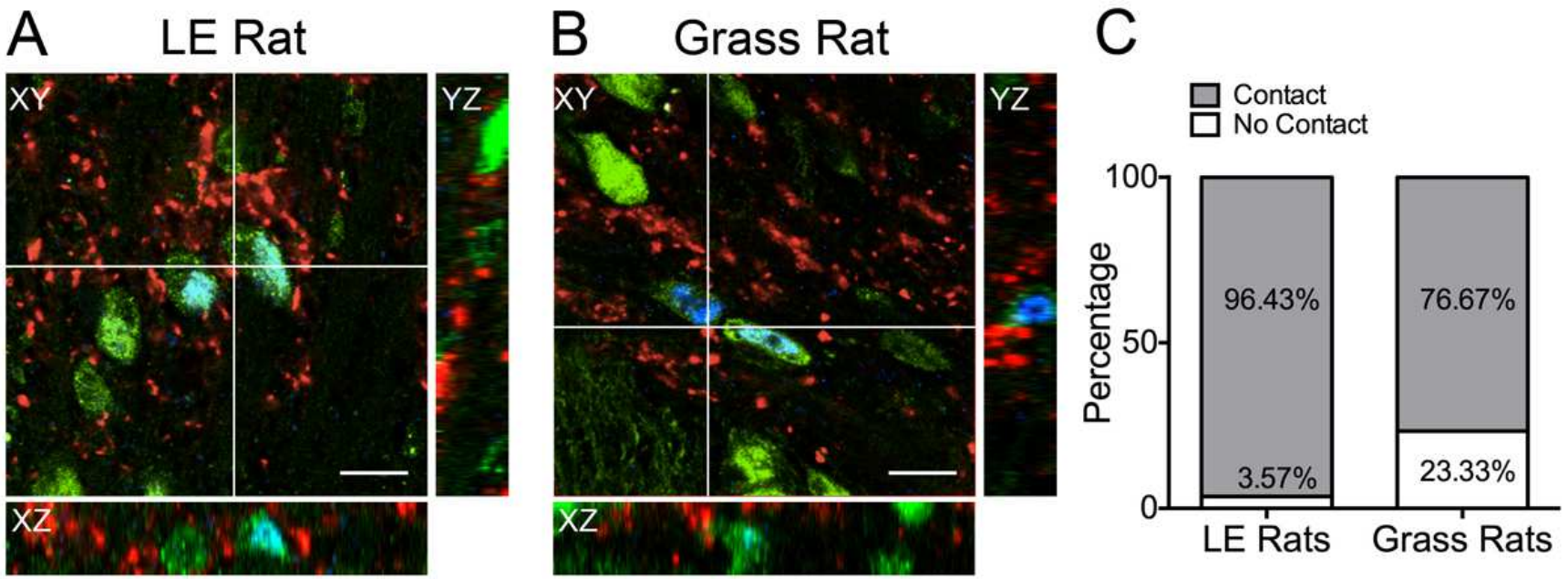

Figure 5.1. Most neurons expressing cFOS in response to light in the intergeniculate leaflet (IGL) receive direct input from the retina. Orthogonal views of representative neurons (NeuN; green) expressing cFOS (blue) that have close contacts with retinal fibers (red) in a Long Evans (LE) rat (A) and grass rat (B). The bar graph (C) indicates the overall percentage of neurons that have with close contact with retinal fibers (shaded bars) and those that do not (white bars) in both LE rats and grass rats. Scale bars: 10 μm.

Experiment 2: Distribution of glutamatergic and GABAergic neurons in retinorecipient brain areas in a diurnal and a nocturnal species

Densities of cell bodies containing *Vglut2* and *Gad65* in the brain regions described below are summarized in Table 5.1 with areas in which we saw species differences highlighted in bold.

Glutamaterigic, GABAergic and cFOS expressing neurons in the lateral geniculate nucleus and olivary pretectal area

The general distribution of *Vglut2* and *Gad65* mRNA in the LGN was very similar in LE rats and grass rats (Figure 5.2). *Vglut2* cells were very dense within the dorsal LGN (dLGN) in both species (Figure 5.2A and B). In LE rats, the ventral portion of the LGN (vLGN) contained a moderate density of *Vglut2* and these cells were distributed evenly across the mediolateral extent of this nucleus (Figure 5.2A); this pattern was evident from the middle to caudal vLGN (Figure 5.3). In grass rats, however, *Vglut2* cells were sparsely labeled in the vLGN and were primarily localized at its lateral and medial boundaries (Figure 5.3).

The IGL, a region of special interest because of its role in circadian rhythm regulation and masking, is typically outlined as the region positioned between the dLGN and vLGN, but it also extends into to an area ventral and medial to the vLGN; these boundaries have been described in great detail in rats and hamsters on the basis of the distributions of neuropeptide Y-containing neurons, cells that project to the suprachiasmatic nucleus (SCN), retinal inputs and morphological characteristics of neurons in this region (Morin et al., 1992; Moore and Card, 1994; Morin and Blanchard, 1995). Interestingly, while the region of the IGL that is positioned between the dLGN and vLGN contained almost no *Vglut2* cells, the region that extends ventrally

and medial to the vLGN had a moderate density of *Vglut2* neurons in both LE rats and grass rats (Figure 5.2A and B; 5.4A and B); this pattern was apparent across the rostrocaudal extent of the nucleus. Thus, in Table 5.1 we have separated the IGL into these two divisions, which we refer to as the "lateral-to-medial strip" (which contains virtually no *Vglut2* cells) and the "ventromedial" IGL (which contains a moderate number of *Vglut2* cells).

While the dorsal portion of the LGN was primarily glutamatergic, both the vLGN and IGL contained a high density of cells expressing *Gad65* and this pattern was very similar in the two species (Figure 5.2C and D; 5.4C and D). The dLGN of both LE rats and grass rats also contained a moderate density of *Gad65* cells scattered throughout (Figure 5.2C and D). Finally, the distribution of cFOS was similar in the IGL of light pulsed LE rats and grass rats; specifically, cFOS-immunoreactive (ir) cells were present in both the lateral-to-medial strip and the ventromedial region of the IGL (Figure 5.4E and F).

The distribution of *Vglut2* and *Gad65* cells in the OPT was similar in LE rats and grass rats (Figure 5.5). In both species *Vglut2* cells were heavily concentrated in the central ("core") division of the OPT and were quite sparse in the region surrounding it (the "shell" of the OPT) (Figure 5.5A and B). *Gad65* cells, however, were dense in the shell and moderate in the core of the OPT in both species (Figure 5.5C and D). Interestingly, the pattern of cFOS labeling in light pulsed animals was slightly different in LE rats and grass rats. In LE rats far more cFOS- ir neurons were in the shell area of the OPT than in its core (Figure 5.5E), while in grass rats cFos-ir neurons were more evenly distributed across the core and shell regions (Figure 5.5F).

Table 5.1. Distribution of *Vglut2* and *Gad65* mRNA in Long Evans (LE) rats and grass rats.

Brain Region	*Vglut2*		*Gad65*	
	LE Rat	Grass Rat	LE Rat	Grass Rat
Hypothalamus				
Ventrolateral preopic area	++	++	++++	++++
Suprachiasmatic nucleus	+	+	++++	++++
Ventral subparaventricular zone	++	++	++++	++++
Thalamus				
Dorsal lateral geniculate nucleus	++++	++++	++	++
Ventral lateral geniculate nucleus	**++***	**+**	++++	++++
Intergeniculate leaflet				
Lateral-to-medial strip	+/-	+/-	++++	++++
Ventromedial	++	++	++++	++++
Epithalamus				
Medial habenular nucleus	++++	++++	-	-
Lateral habenular nucleus	++++	++++	**+/-**	**++/+++***
Dorsolateral sector	++++	++++	++	++
Midbrain				
Olivary pretectal nucleus				
Core	+++	+++	++	++
Shell	+	+	+++	+++
Superior colliculus	++	++	++++	++++

The relative densities of *Vglut2* and *Gad65* cells are indicated as very dense (++++), dense (+++), moderate (++), sparse (+), very sparse (+/-) and absent (-). Asterisks indicate that density depends on level (rostral to caudal) and bold font indicates differences in density between LE rats and grass rats.

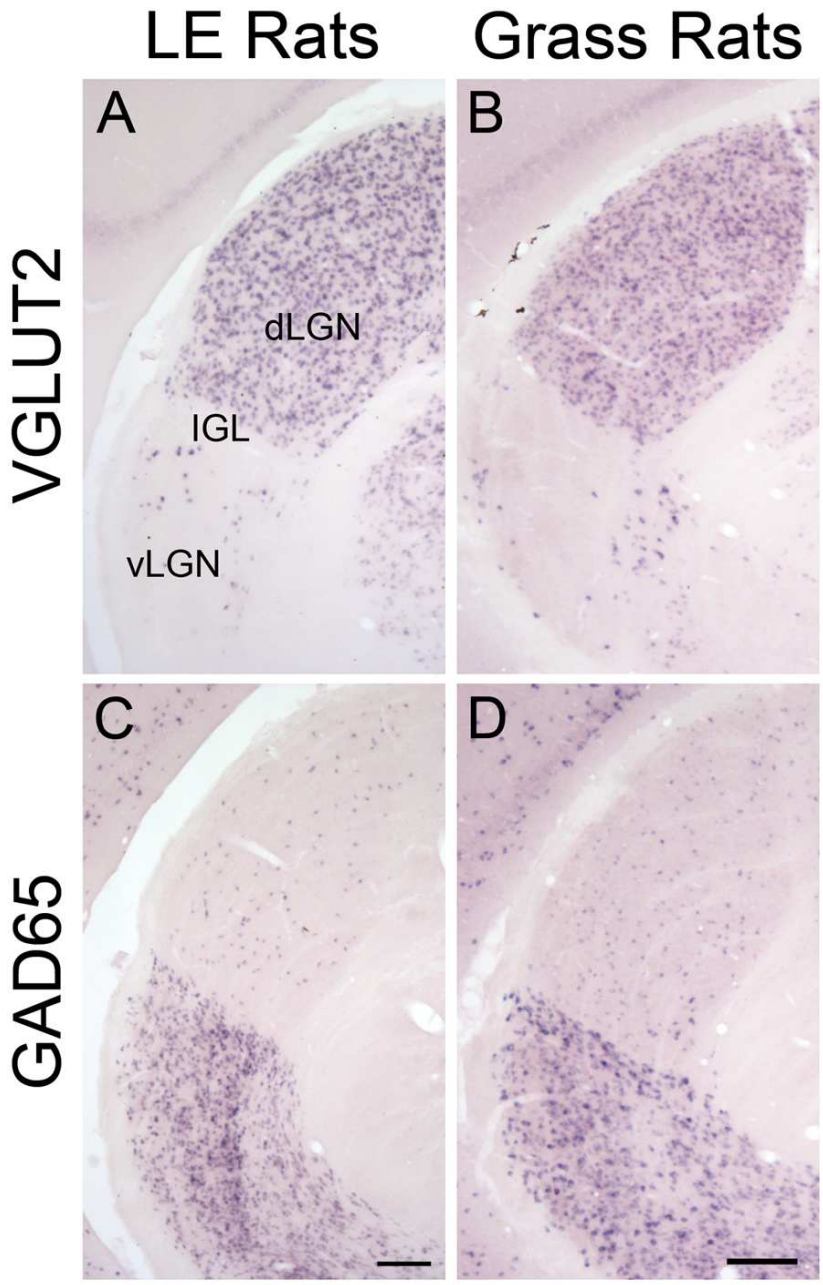

Figure 5.2. *Vglut2* and *Gad65* mRNA in the lateral geniculate nucleus (LGN) of Long Evans (LE) rats and grass rats. *Vglut2* cells were heavily concentrated in the dorsal LGN (dLGN); they were present but relatively sparse in the intergeniculate leaflet (IGL) and ventral LGN (vLGN) of both LE rats (A) and grass rats (B). *Gad65* cells, by contrast, were dense in the IGL and vLGN and moderate in the dLGN of both species (C and D). Scale bars: 200 μm.

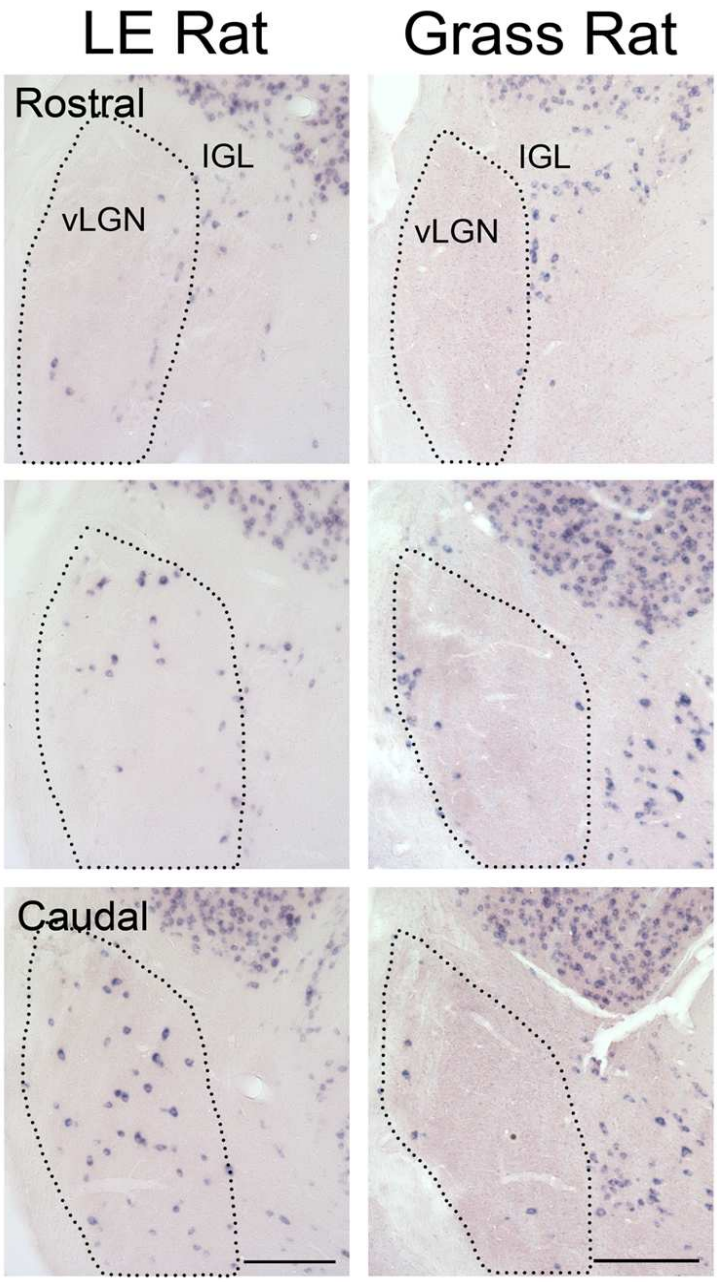

Figure 5.3. *Vglut2* mRNA through the rostrocaudal extent of the ventral lateral geniculate nucleus (LGN) of Long Evans (LE) rats and grass rats. In LE rats, the middle to caudal regions of vLGN contained a moderate density of *Vglut2* cells. In grass rats, *Vglut2* cells were sparse and seen primarily in the lateral and medial regions of the vLGN. In both species, *Vglut2* cells were found in the ventromedial intergeniculate leaflet (IGL) that is medial to the vLGN. Scale bars: 200 μm.

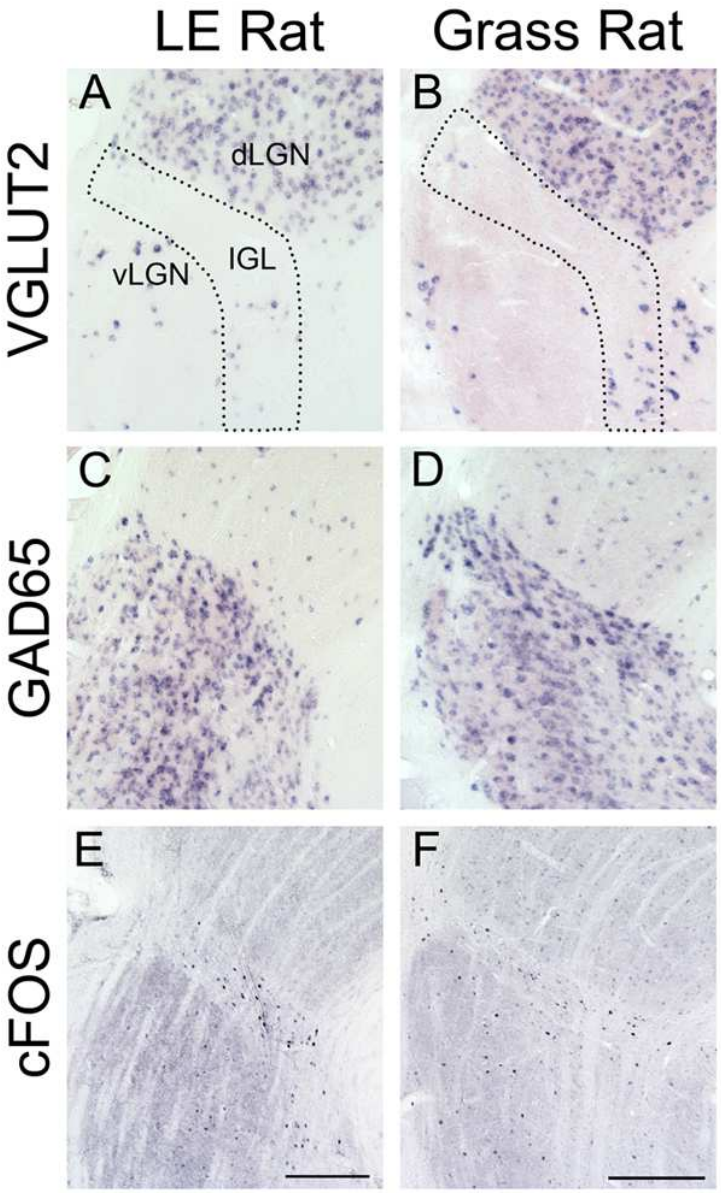

Figure 5.4. *Vglut2*, *Gad65* and cFOS labeled cells in the intergeniculate leaflet (IGL) of Long Evans (LE) rats and grass rats. *Vglut2* cells were dense in the dorsal LGN (dLGN), though some were present in the ventromedial intergeniculate leaflet (IGL) and ventral LGN (vLGN) of both LE rats (A) and grass rats (B). *Gad65* cells, however, were dense in the IGL and vLGN, though some were present in the dLGN of both species (C and D). cFOS labeling after a light pulse was similar in LE rats and grass rats, such that cFOS labeled neurons were in both the medial-to-lateral strip and ventromedial IGL. Scale bars: 200 μm.

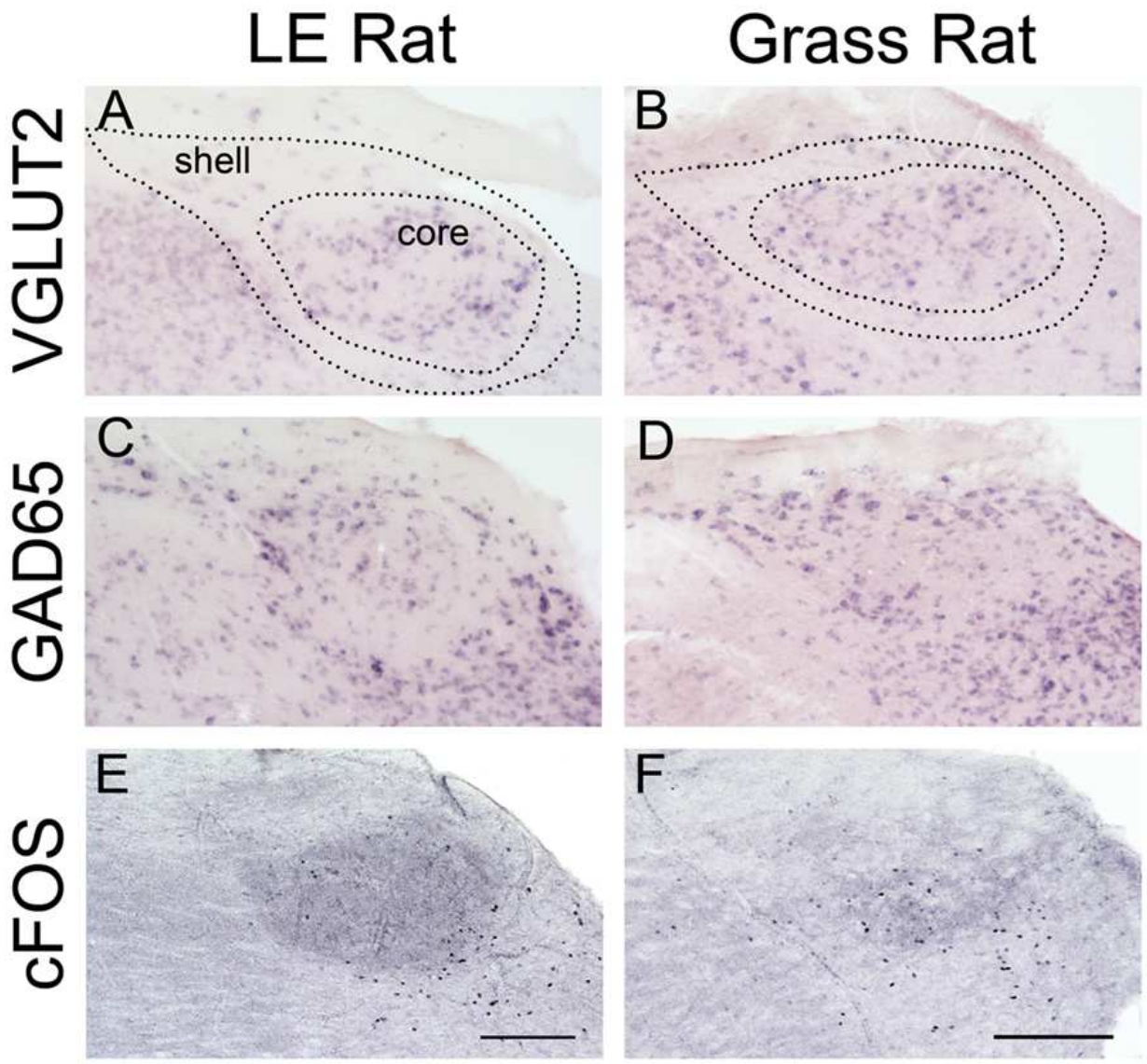

Figure 5.5. *Vglut2*, *Gad65* and cFOS labeled cells in the olivary pretectal nucleus (OPT) of Long Evans (LE) rats and grass rats. *Vglut2* cells were localized mainly in the core region of the OPT (A and B), while *Gad65* cells were found both in its core and shell (C, D) in both LE rats and grass rats. Interestingly, in the OPT of light pulsed LE rats, cFOS was concentrated in the shell and very sparse in the core (E), whereas in light pulsed grass rats it was more evenly distributed across the core and shell of the OPT (F). Scale bars: 200 μm.

Glutamatergic and GABAergic neuronal populations in other regions receiving input from ipRGCs

Vglut2 and *Gad65* staining was noted in various hypothalamic areas that are known to receive input from ipRGCs and that modulate arousal states. In the ventrolateral preoptic area (VLPO), a sleep promoting brain region that is distinguishable by a dense cluster of galanin producing cells (Novak et al., 2000; Gaus et al., 2002), a moderate density of *Vglut2* neurons was present in both LE rats and grass rats (Figure 5.6A and B); this region also contained a dense cluster of *Gad65* positive cells both species (Figure 5.6C and D). The suprachiasmatic nucleus (SCN) had very few *Vglut2* cells in LE rats and grass rats (Figure 5.7A and B), while the area directly dorsal to (the ventral subparaventricular area, vSPZ) had a moderate density of *Vglut2* cells in both of the species (Figure 5.7A and B). Dense *Gad65* cell labeling was observed in the SCN and vSPZ of both LE rats and grass rats (Figure 5.7C and D).

A striking species difference was observed in the distribution of GABAergic neurons in the habenular complex. While both the lateral and medial habenula contain a dense population of *Vglut2* cells in both species (Figure 5.8A and B), a clear cluster of *Gad65* cells was present in the lateral habenula (LHb) of grass rats but these cells were virtually absent in this region in LE rats (Figure 5.8C and D). In grass rats, these *Gad65* neurons are present throughout the rostrocaudal extent of the LHb, though the density is greater in its middle to caudal regions (Figure 5.9); in LE rats, *Gad65* is almost completely absent throughout the rostrocaudal distance of this area (Figure 5.9). This striking species difference was apparent in animals perfused during the night as well as during the day. A cluster of *Gad65* neurons was also visible in an area near the dorsolateral sector of the habenular complex, where *Vglut2* cells were also seen in both LE rats

and grass rats (Figure 5.8 and 5.9); this area at the border of the LHb is known to receive retinal input from ipRGCs in mice (Hattar et al., 2006).

The superior colliculus (SC) receives considerable input from the retina and some of that comes from ipRGCs (Hannibal and Fahrenkrug, 2004; Hattar et al., 2006; Langel et al., 2015). A moderate density of *Vglut2* cells and an intense density of *Gad65* cells were seen in this area in both LE rats and grass rats (Figure 5.10).

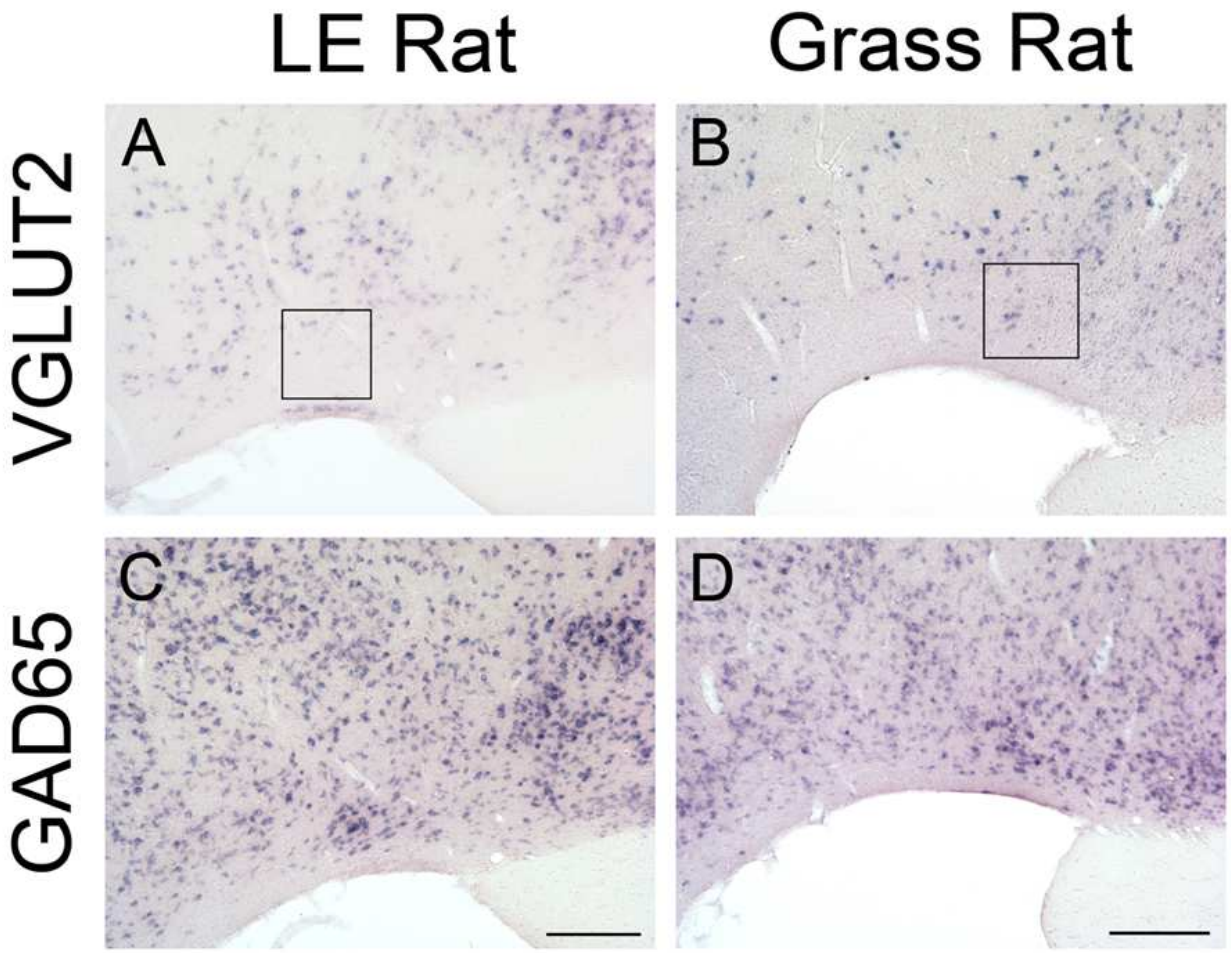

Figure 5.6. *Vglut2* and *Gad65* mRNA in the ventrolateral preoptic area (VLPO) of Long Evans (LE) rats and grass rats. The box (190 x 190 μm) represents the location of the VLPO in LE rats (A) and grass rats (B) based on previous reports of galanin stained neurons (Novak et al., 2000; Gaus et al., 2002). Few *Vglut2* cells were observed in the VLPO (A and B), but a cluster of *Gad65* cells (C and D) were seen in this region in both species. Scale bars: 200 μm.

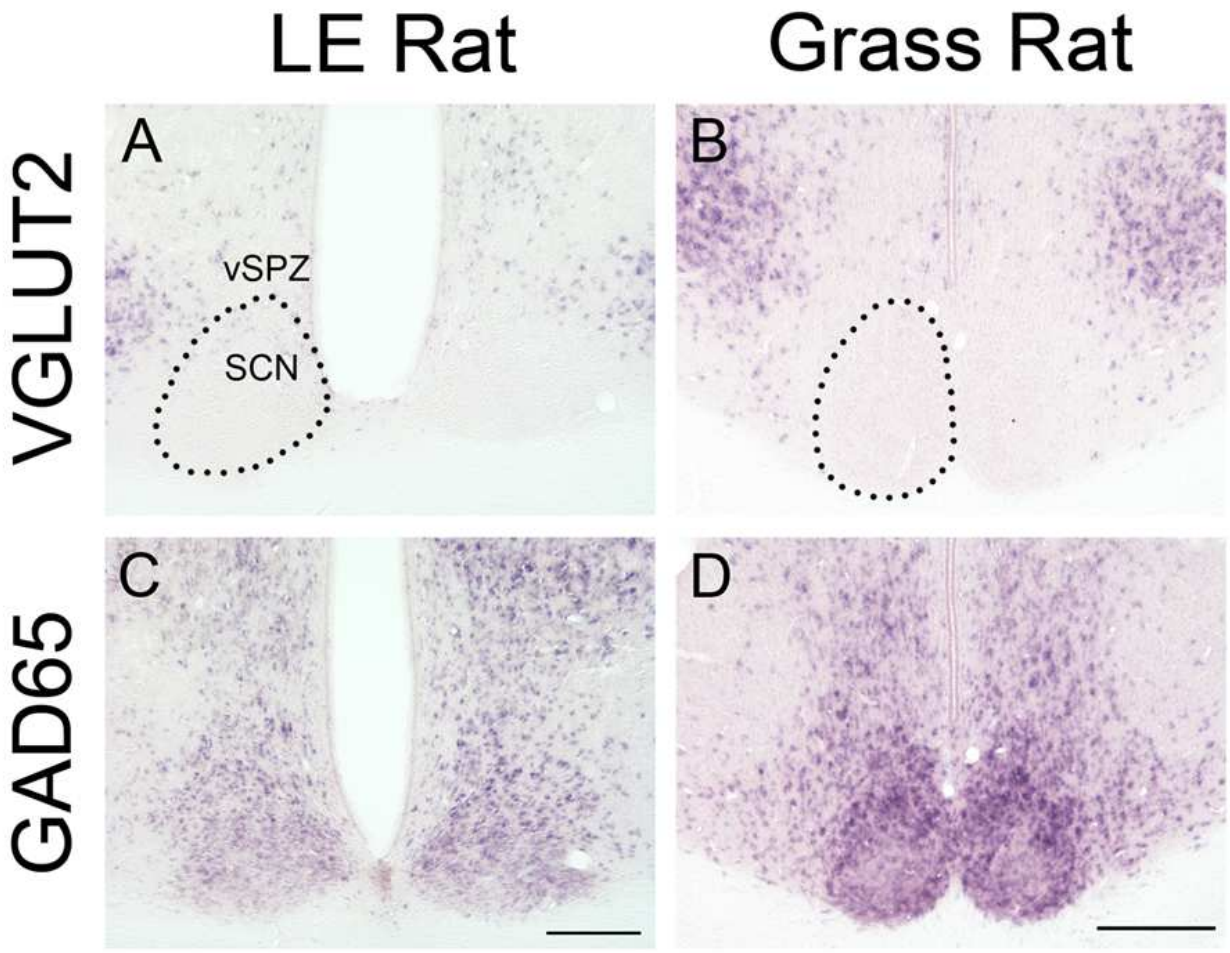

Figure 5.7. *Vglut2* and *Gad65* mRNA in the suprachiasmatic nucleus (SCN) and ventral subparaventricular zone (vSPZ) of Long Evans (LE) rats and grass rats. Very few cells were *Vglut2* in the SCN, while a moderate number of these cells were presnt in the vSPZ in both species (A and B). *Gad65* cells were dense in both of these areas in both species (C and D). Scale bars: 200 μm.

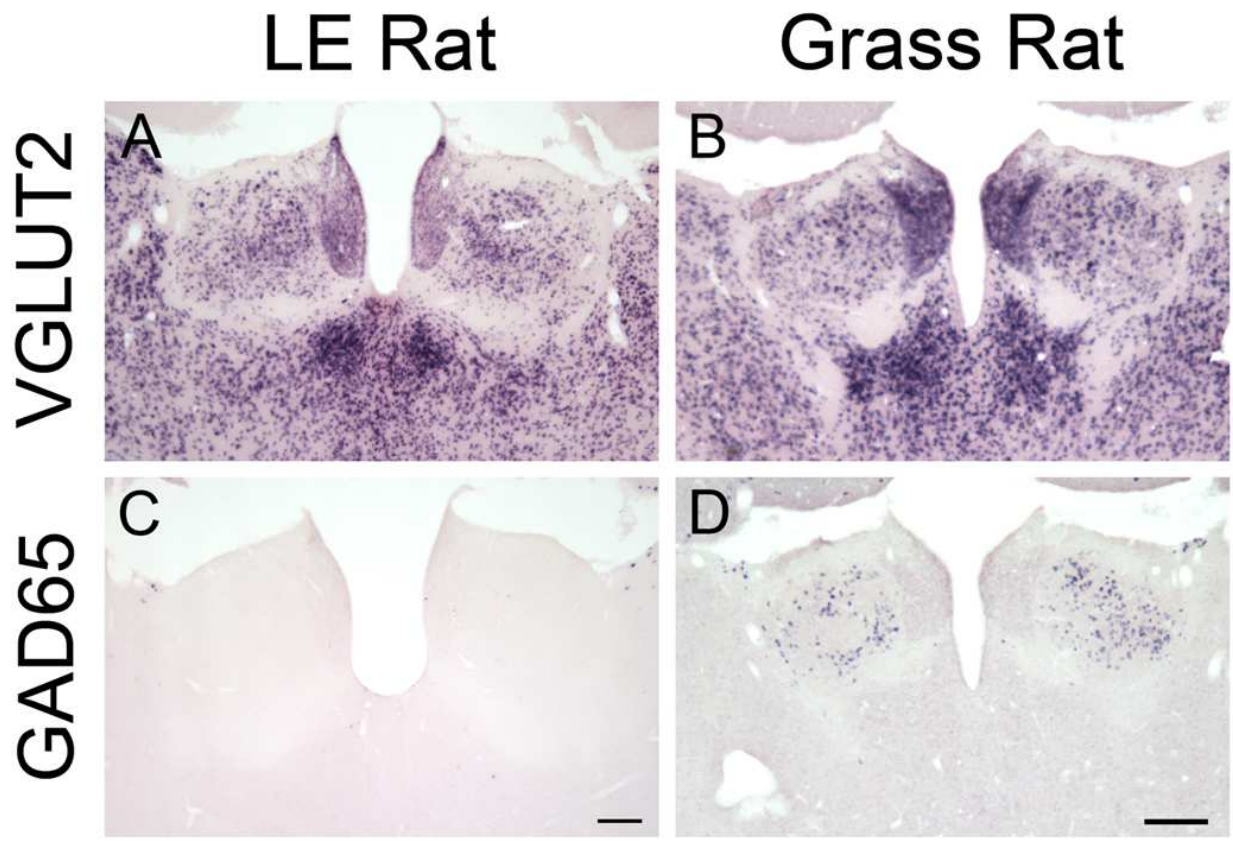

Figure 5.8. *Vglut2* and *Gad65* mRNA in the habenular nucleus of Long Evans (LE) rats and grass rats. *Vglut2* cells were dense in both the medial and lateral parts of the habenula in both LE rats (A) and grass rats (B). In LE rats, very few, if any, *Gad65* cells were found in the habenula (C), while in grass rats a substantial and distinct cluster *Gad65* cells was present in the lateral habenula (D). Scale bars: 200 μm.

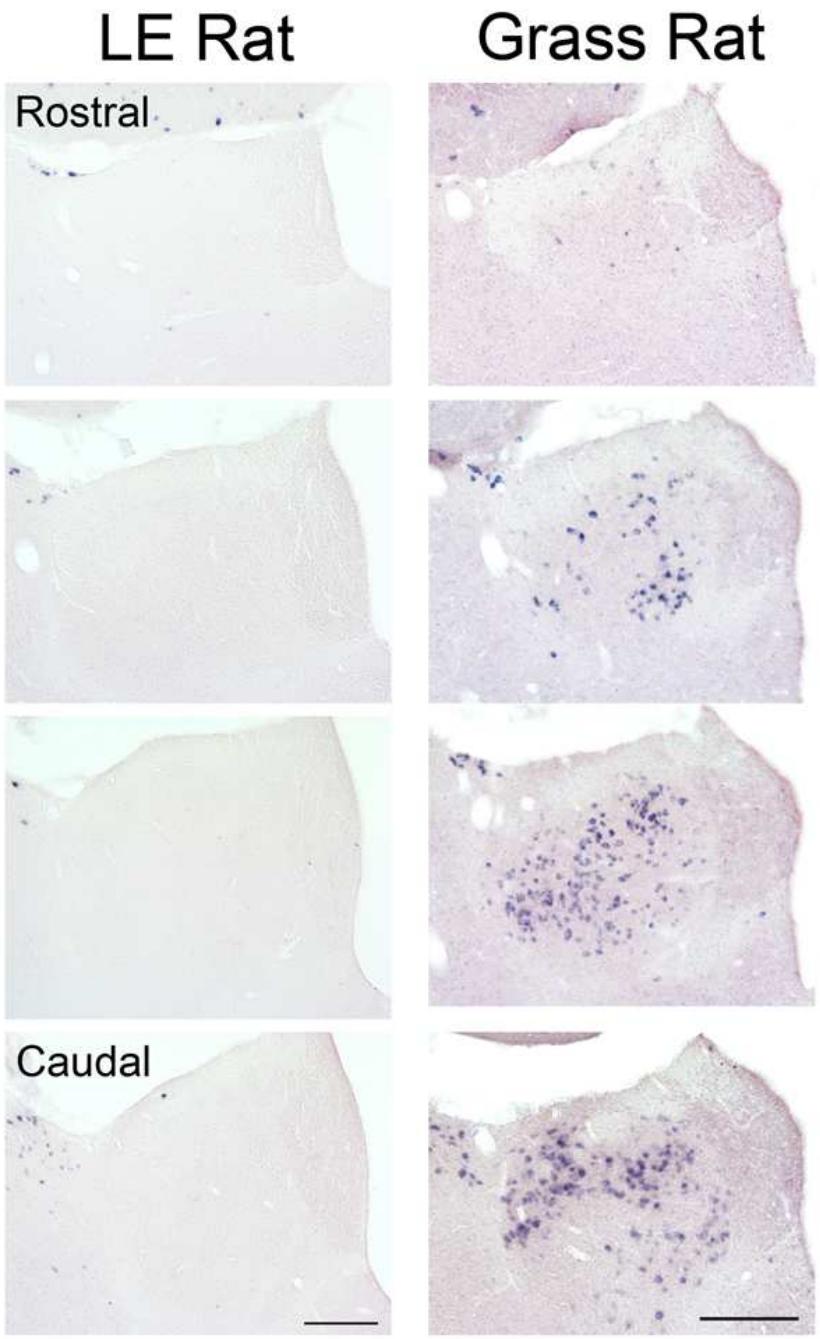

Figure 5.9. *Gad65* mRNA across the rostrocaudal extent of the habenular nucleus of Long Evans (LE; left) rats and grass rats (right). Very few, if any, *Gad65* cells were observed in the lateral habenula of LE rats, while many were seen in this area of the grass rats. In grass rats, the density of *Gad65* cells was greater in the middle to caudal levels of lateral habenula. Scale bars: 200 μm.

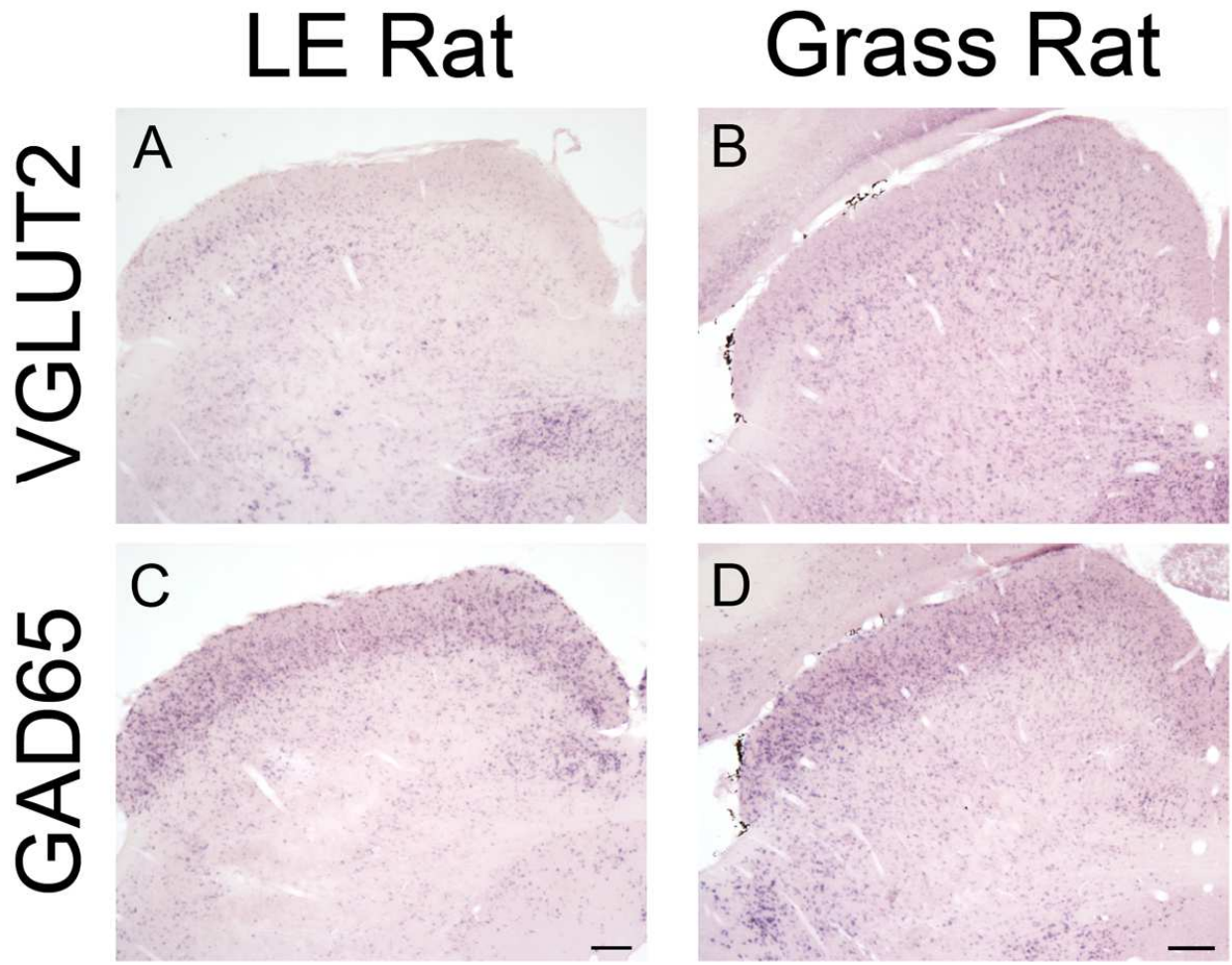

Figure 5.10. *Vglut2* and *Gad65* mRNA in the superior colliculus (SC) of Long Evans (LE) rats and grass rats. Moderate levels of *Vglut2* were found in the SC of both LE rats (A) and grass rats (B), while dense labeling for Gad65 was present in this region in both species (C and D). Scale bars 200 μm.

DISCUSSION

One potential explanation for the differences in how diurnal and nocturnal species respond to light is that circuitry within brain areas that receive input from ipRGCs is not the same. Here we first sought to determine whether differences exist in the input to light responsive neurons within the intergeniculate leaflet (IGL), an area that receives input from ipRGCs and that has been implicated in masking in both nocturnal and diurnal species (Redlin et al., 1999;

Gall et al., 2013; Langel et al., 2015; Shuboni et al., 2015). We used confocal microscopy, which cannot confirm synaptic connections but can provide strong evidence that they exist, to address this question. Surprisingly, we found that within the IGL the majority of light responsive neurons (as indicated by the expression of cFOS) had contacts with retinal fibers in both nocturnal LE rats and diurnal grass rats (Figure 5.1). There was a hint of a species difference with a higher percentage of cFOS-expressing neurons that were in close contact with retinal fibers in LE rats (96%) than in grass rats (76%). It may be that some IGL neurons are responsive to changes in arousal state that are induced by light via indirect pathways. For example, some neurons in the IGL receive input from orexin fibers (Nixon and Smale, 2004, 2005; Thankachan and Rusak, 2005; Pekala et al., 2011), application of orexin depolarizes the membrane and increases firing rates in some IGL neurons (Pekala et al., 2011; Palus et al., 2015) and orexin has a major influence on arousal and locomotor activity, in general (Tsujino and Sakurai, 2013). Though we only quantified axosomatic contacts, many synaptic connections from retinal fibers are on distal dendrites of IGL neurons (Moore and Card, 1994). Thus, some of the IGL neurons that did not appear be contacted by retinal fibers here may in fact have axodendric contacts. Overall, the important conclusion that we can draw from the current data is that a very high percentage of neurons within the IGL that express cFOS after a light pulse appear to receive direct input from the retina in both a nocturnal and a diurnal species.

In our second study, we examined the question of whether differences exist in the distribution of excitatory and inhibitory cells in brain regions that receive ipRGC input in diurnal grass rats and nocturnal LE rats, as a test of the hypothesis that these differences could contribute to differences in their masking responses to light. We were particularly interested in the IGL and the olivary pretectal nucleus (OPT) because lesions to these areas alter species typical responses

to light (Miller et al., 1998; Redlin et al., 1999; Gall et al., 2013). Overall, the distribution of cells containing *Vglut2* and *Gad65* was very similar within the IGL and OPT of grass rats and LE rats, but we did see some differences. In both species, the IGL is highly GABAergic, as reported previously in hamsters and rats (Moore and Card, 1994; Morin and Blanchard, 2001). We also found that glutamate cells are present in the ventromedial portion of the IGL, but not the lateral-to-medial strip (Figure 5.2 and 5.4), both of which are regions in which cFOS is expressed in response to a light pulse. In early studies, the IGL was considered to be part of the ventral lateral geniculate nucleus (vLGN), specifically the internal dorsal division of the vLGN (what we refer to as the lateral-to-medial strip of the IGL here) (Niimi et al., 1963; Hickey and Spear, 1976; Harrington, 1997). Later work in hamsters and rats suggested that the boundaries of what we now consider to be the IGL should be extended into the region ventral to its medial aspect; this was based on the distributions of neuropeptide Y-containing neurons, cells that project to the suprachiasmatic nucleus (SCN), retinal inputs and morphological characteristics of neurons in this area (Morin et al., 1992; Moore and Card, 1994; Morin and Blanchard, 1995). The IGL of mice is also defined by distinct labeling of ipRGC projections, specifically of the M1 subtype (Hattar et al., 2006). The distinct labeling of *Vglut2* in the ventromedial IGL across its rostrocaudal extent in both LE rats and grass rats, as described here, may also serve as a defining feature of this area. Overall, these results suggest that the IGL is very similar with respect to the distribution of excitatory and inhibitory neurons in diurnal grass rats and nocturnal LE rats. However, it is possible that differences exist in neuronal populations that are responsive to light in the rostromedial IGL, where both GABA and glutamate are present.

The distribution of *Vglut2* and *Gad65* within the OPT was also similar in the species. Specifically, *Vglut2* was dense in the core of the OPT and quite sparse in the shell, while *Gad65*

was dense in the shell and moderate in the core (Figure 5.5). In mice, different ipRGC subtypes innervate the shell and core of the OPT; whereas M1 ipRGCs target the shell, non-M1 subtypes target the core (Hattar et al., 2006; Baver et al., 2008; Ecker et al., 2010). Additionally, neurons in the shell of the OPT, and not the core, project to the Edinger-Westphal nucleus, a pathway responsible for the pupillary light reflex (Baver et al., 2008). Interestingly, we saw cFOS primarily in the shell of the OPT in LE rats and both in the core and shell of the OPT in grass rats (Figure 5.5). Thus, in LE rats, it is likely that these cFOS expressing neurons are in GABAergic neurons of the OPT, since primarily *Gad65* cells are located in the shell. Whether these differences in the OPT of grass rats and LE rats reflect differences in the types of cells responding to photic stimulation important for masking still needs to be determined.

We did find a difference in the density of *Vglut2* cells in the vLGN of LE rats and grass rats. In LE rats, the density of *Vglut2* cells was moderate through the medial to caudal extent of the nucleus, while in grass rats *Vglut2* cells were sparse in the medial and lateral boundaries (Figure 5.3). The vLGN is similar to the IGL in that they both project to and receive projections from many subcortical visual nuclei in hamsters and rats (e.g. pretectal nuclei (including the OPT), superior colliculus, IGL, contralateral vLGN) (Morin and Blanchard, 1998; Moore et al., 2000; Comoli et al., 2012). The vLGN also receives input from arousal-promoting nuclei of the brainstem (dorsal raphe and locus coeruleus) (Harrington, 1997). Additionally, neurons within the vLGN respond to light with an increase in cFOS (Marchant and Morin, 2001; Prichard et al., 2002). Thus, the vLGN may serve to integrate non-image-forming visual information from ipRGCs (Hattar et al., 2006; Ecker et al., 2010) and arousal information from brainstem nuclei. Taken together, it is tempting to speculate that the difference in levels of glutamate within the

vLGN of LE rats and grass rats might contribute to differences in their masking responses to light.

Vglut2 and *Gad65* cells were noted in ipRGC target areas beyond the LGN and OPT, including the ventrolateral preoptic area (VLPO), suprachiasmatic nucleus (SCN), ventral subparaventricular zone (vSPZ) and superior colliculus. We found that the overall distributions of both *Vglut2* and *Gad65* were very similar in LE rats and grass rats. In the VLPO of both species a dense cluster of *Gad65* cells was present, while *Vglut2* cells were moderate in this region (Figure 5.6). This pattern agrees with previous reports of clustered cells containing GABA and galanin in the VLPO of a number of species (Sherin et al., 1998; Novak et al., 2000; Gaus et al., 2002) and these neurons are believed to be important for the sleep-promoting function of the VLPO (Sherin et al., 1996; Sherin et al., 1998; Brown et al., 2012). We also found that the SCN and vSPZ were highly GABAergic in both LE rats and grass rats, and that these regions had relatively little glutamate in both species (Figure 5.7). This is consistent with previous reports indicating that nearly all SCN neurons are GABAergic (rats: Moore and Speh, 1993; mice: Abrahamson and Moore, 2001; hamsters: Morin and Blanchard, 2001), while only a few are glutamatergic (rats: Kiss et al., 2007); the vSPZ shows a similar pattern in these studies (Abrahamson and Moore, 2001; Kiss et al., 2007). We found that the superior colliculus contained both glutamatergic and GABAergic cells in both species, as has been reported to be the case in Norway rats previously (Mize, 1992; Ziegler et al., 2002); *Gad65* was more dense than *Vglut2* in this region (Figure 5.10). Overall, though we did not find a species difference in the overall distribution of *Vglut2* and *Gad65* in the areas outlined above, it still needs to be determined whether differences exist in which cells in these areas are responsive to light.

A striking species difference was observed in the density of GABAergic cells in the lateral habenula (LHb; Figure 5.8 and 5.9). While *Gad65* cells were completely absent in this structure in LE rats, a dense cluster of them was present in the middle to caudal regions of this nucleus in grass rats (Figure 5.8C and D, 5.9); this difference was apparent whether the animals were perfused during the day or night. Previous reports have also indicated almost no GABAergic cells in the LHb of different strains of nocturnal mice and rats (Lein et al., 2007; Brinschwitz et al., 2010; Li et al., 2011; Allen Institute for Brain Science, 2015) and a few in diurnal squirrel monkeys (*Saimiri sciureus*) (Smith et al., 1987). The present data raise fascinating questions about the role of these GABAergic neurons in grass rats, and whether and how they might contribute to differences in the temporal patterning of their behavior compared to that of nocturnal LE rats. This possibility is based off the inputs to and the projections from cells in the LHb. Little is known about this in grass rats, but in nocturnal rodents the LHb is interconnected with many brain areas involved in functions that are rhythmic (e.g. arousal states). It receives input directly from the SCN, whose rhythms are very similar in grass rats and Norway rats, and the vSPZ, which has rhythms that are quite different in these species (Morin et al., 1994; Smale et al., 2003; Schwartz et al., 2004; Schwartz et al., 2011); the lateral hypothalamus, locus coeruleus and raphe nuclei also project to the LHb (Vertes et al., 1999; Kowski et al., 2008; Bianco and Wilson, 2009; Li et al., 2011). Thus, it may be that these structures that project to the LHb differentially influence cells and circuits within this area of grass rats and LE rats due to the species difference in GABAergic cells within the LHb, as we found here. Furthermore, differences within the LHb could have important effects on behaviors that are phase reversed (e.g. sleep/wake cycles) in diurnal and nocturnal species, as the LHb projects to the lateral hypothalamus, locus coeruleus and raphe nuclei, all areas involved in regulation of sleep and

arousal (Herkenham and Nauta, 1979; Araki et al., 1988; Bianco and Wilson, 2009; Quina et al., 2015).

A role for the LHb in the regulation of circadian rhythms of nocturnal species is suggested by several experimental findings as well. First, cells within the LHb are rhythmic, both with respect to the clock gene/protein expression (Guilding et al., 2010; Zhao et al., 2015b) and electrical activity (Zhao and Rusak, 2005; Guilding et al., 2010). Furthermore, lesions of the fasciculus retroflexus (the major efferent fiber bundle of the LHb) alter the temporal organization of activity (Paul et al., 2011) and reduce the quantity of REM sleep (Haun et al., 1992; Valjakka et al., 1998). Nothing is currently known about how the LHb might influence circadian rhythms in any diurnal species.

There is also some evidence that the LHb may be involved in masking. Although it does not receive direct retinal input, neurons within it are responsive to light, as measured by increases in neural firing rates (Zhao and Rusak, 2005) and cFOS expression (mice: LeGates et al., 2012; grass rats: Shuboni et al., 2015). Furthermore, there are retinal inputs to the region dorsolateral to it in both in mice and grass rats (Gaillard et al., 2013; Morin and Studholme, 2014); these fibers appear to originate exclusively from M1 ipRGCs in mice (Hattar et al., 2006; Ecker et al., 2010). Thus, future studies are needed to determine whether the LHb plays a role in masking in diurnal and nocturnal species, as well as whether the GABAergic neurons that we see in this region of grass rat might contribute to the direct effect light on activity in these diurnal animals.

In addition, the LHb is involved in the regulation of various aspects of cognition, mood, pain and reward, and recently has received a great deal of attention for its role in anxiety and mood disorders, Parkinson's disease and drug addiction (for review see: Aizawa et al., 2013; Lee

and Goto, 2013; Yadid et al., 2013; Benarroch, 2015; Zhao et al., 2015a). This is largely due the LHb's role in relaying information from the limbic forebrain to many mid-brain structures, such as periaqueductal gray, raphe nuclei, rostromedial tegmental nucleus, substantia nigra pars compacta and ventral tegmental area (Herkenham and Nauta, 1979; Araki et al., 1988; Quina et al., 2015). Most studies examining the functional role of the LHb on these circuits do not take time of day into account, but it is likely that such regulation is rhythmic (as is the case for most brain regions and behaviors). It is therefore important to determine whether GABAergic neurons are present in LHb of other diurnal species, and absent in other nocturnal ones, as well as determining the function of these cells. This could provide new insights into the role that the LHb plays in various aspects of clinical and neurodegenerative disorders.

Conclusion

In summary, the present data reveal similarities and differences between nocturnal LE rats and diurnal grass rats in (1) retinal input to light responsive cells in the IGL, an area important for masking, and (2) the distribution of glutamatergic and GABAergic cell populations in various ipRGC target areas. We found that a high percentage of cells in the IGL appear to receive direct input from the retina in both LE rats and grass rats and that the distribution of *Vglut2* and *Gad65* is very similar in many ipRGC target areas. However, two areas that were different were the vLGN (more *Vglut2* cells in LE rats than grass rats) and the LHb (*Gad65* cell present in grass rats, but not LE rats). It is tempting to speculate that this could contribute to chronotype specific patterns of behavior by altering the valence of signals coming in to these regions from ipRGCs and/or from the SCN. Future studies are needed to further test this

hypothesis, as well as to determine whether GABAergic neurons are present in the LHb of other diurnal mammals.

CONCLUSION

Light has profound effects on our behavior and physiology. In fact, inappropriate temporal patterns of light exposure of varying intensity can have detrimental effects on our health and wellbeing by increasing the likelihood of sleep disorders, reproductive failure, problems with metabolism, mood disorders, and some forms of cancer (Schroeder and Colwell, 2013; Fonken and Nelson, 2014; Bedrosian et al., 2015; Kripke et al., 2015; Stevens and Zhu, 2015). These effects are due to (1) a mismatch between the internal circadian timekeeping system and environmental lighting and (2) more direct effects of light on behavior and physiology via masking. Although masking influences of light on behavior and sleep patterns have received more recent attention, especially in nocturnal rodents (Altimus et al., 2008; Lupi et al., 2008; Tsai et al., 2009; Morin and Studholme, 2011; Muindi et al., 2013), the neural pathways promoting this process and how they may differ between diurnal and nocturnal mammals are not well understood. The goal of the work in this dissertation was to first evaluate chronotype differences in masking and then to examine aspects of the neural circuitry that may mediate this process in systems of day- and night-active mammals.

Masking within and between species

In Chapter 1, I discussed the importance of masking in temporal niche selection and how masking responses to light seem to be dependent upon the chronotype of the animal. This raises the question of whether mechanisms controlling masking and the circadian drive for activity are associated. The results presented in Chapter 2 provide evidence that this is the case in day- and night-active individuals of the same species (the Nile grass rat), at least with respect to some behaviors such as wheel running. In that chapter, I also found that not all masking responses

were reversed in day- and night-active individuals; in fact, light had no effect on general activity in the night-active animals suggesting that light does not completely inhibit arousal and general activity as it does in nocturnal species (Shuboni et al., 2012). This finding also suggests that these grass rats retain some diurnal characteristics even when the presence of a running wheel induces night-active wheel running. These data also have important implications for conclusions based off wheel running behavior, especially in the context of masking, since the mechanisms driving wheel running versus general activity within the cage or in the field may be quite different. For example, wheel running appears to be driven by reward pathways associated with addiction and may itself be an addictive behavior, which is not likely to be the case with general activity, or at least not to the same extent (Novak et al., 2012).

In addition to examining patterns of masking across individuals within a species, I also determined which specific behaviors are induced or suppressed in response to light *between* two murid species, the diurnal Nile grass rat and nocturnal Norway rat; these two species respond in opposite ways to light in general activity (Chapter 3). I found that light suppressed sleep/rest in most, but not all, diurnal grass rats, while light induced sleep/rest in all nocturnal Norway rats. Interestingly, even brief light exposure (5 minutes pulses or millisecond flashes) can induce sleep in nocturnal mice (Morin and Studholme, 2009, 2011; Studholme et al., 2013), and increase subjective alertness in humans (Zeitzer et al., 2011). These light effects on sleep seem to be mediated through the melanopsin protein, since, in nocturnal mice, melanopsin is necessary to induce sustained increases in both SWS and REM sleep (Altimus et al., 2008; Lupi et al., 2008; Tsai et al., 2009; Morin and Studholme, 2011; Muindi et al., 2013). The direct role that melanopsin plays in mediating the masking effects of light in diurnal species, such as humans, still needs to be determined. There is, however, some evidence that this is the case, as short

wavelength light (within the range of melanopsin sensitivity) does suppress subjective sleepiness in humans (reviewed in: Cajochen, 2007). Additionally, other aspects of sleep (such as quality) during and following the light pulse need to be assessed in diurnal species, like humans, to see how masking influences of light at night may contribute to sleep disorders.

Neural pathways of masking

As discussed in Chapter 1, extensive research on mouse models lacking ipRGCs indicates the importance of these cells in relaying photic information necessary for masking to the brain (Goz et al., 2008; Guler et al., 2008; Hatori et al., 2008). While the projections of ipRGCs have been extensively mapped in mice using various transgenic strategies (Hattar et al., 2006; Brown et al., 2010; Ecker et al., 2010), the central projections of these cells in other species, such as the rat, hamster and macaque, have been examined via the use of PACAP, a neuropeptide found exclusively within ipRGCs in the retina (Hannibal et al., 2000; Hannibal et al., 2002; Bergstrom et al., 2003; Hannibal and Fahrenkrug, 2004; Hannibal et al., 2004; Hannibal et al., 2014). To determine whether differences in the input pathway from ipRGCs to the brain may account for species differences in masking responses to light, I characterized the melanopsin system in the diurnal Nile grass rat and compared it to that reported in other nocturnal rodents (Chapter 4). I found that the same basic subtypes of ipRGCs exist in the grass rat retina as in other diurnal and nocturnal mammals, and that, as in other species, a vast majority of these cells also contain PACAP (87.7% melanopsin cells contained PACAP, while 97.4% of PACAP cells contained melanopsin) (rats: Hannibal et al., 2002; hamsters: Bergstrom et al., 2003; humans: Hannibal et al., 2004; macaques: Hannibal et al., 2014).

The distribution of PACAP-labeled fibers projecting from the retina to the grass rat brain suggests that the targets of ipRGCs in the grass rat are very similar to those of nocturnal species (Chapter 4). However, I did find an indication that ipRGC projections to the OPT are somewhat different. In grass rats these cells primarily target the rostral OPT, but not its more caudal levels, while in mice extensive innervation from ipRGCs is observed across the full rostrocaudal extent of this nucleus (Hattar et al., 2006). Little is known about functional differences that exist across the rostrocaudal axis of the OPT and nothing at all is known about whether or how such differences might be associated with masking. However, brain lesions of the OPT suggest that this area may play a role more generally in promoting species characteristic masking responses (*Gall, unpublished observations*; Miller et al., 1998). In addition, I found very few ipRGC fibers in the dorsal and ventral LGN, while a dense projection from ipRGCs to these areas has been described in mice, particularly from non-M1 cells (Brown et al., 2010; Ecker et al., 2010). Interestingly, in mice, the projections of M1 versus non-M1 subtypes of ipRGCs are distributed differently in the brain (Hattar et al., 2006; Baver et al., 2008; Brown et al., 2010; Ecker et al., 2010; McNeill et al., 2011); we were unable to address this issue, as we could not differentiate the projections from various ipRGC subtypes with the methods that we used. Thus, future research is needed to evaluate differences in M1-M5 ipRGC projections and the specific functions of each subtype in various visual functions (image-forming and non-image-forming) in diurnal and nocturnal species. Overall, however, the similarities in ipRGCs and their projections to the brain seen here suggest that differences in masking responses to light in diurnal and nocturnal species emerge from processes downstream of these cells and perhaps in the areas that receive direct input from them.

One hypothesis to explain how differences in masking responses to light of diurnal and nocturnal species emerge is that ipRGCs project to different populations of cells. For example, in one species, ipRGCs may project to excitatory neurons, while in the other species they may project to inhibitory interneurons that alter the valence of ipRGC signals going to their targets. To test aspects of this hypothesis, I first examined whether neurons that express cFOS in response to light receive direct input from the retina in one ipRGC target area that has been implicated in masking, the IGL, and whether this differs in a diurnal and nocturnal species (Chapter 5). While I found that most neurons expressing cFOS in response to light have close contacts with retinal fibers in both diurnal grass rats (76%) and nocturnal Norway rats (96%), there was a higher percentage of these cells that do not have close contacts form retinal fibers in the grass rat compared to the Norway rat. It may be that such cFOS-expressing neurons are responsive to light via indirect pathways or via axodendritic input (that wasn't measured here). Overall, these data suggest a similarity in the species that a very high percentage of cFOS-expressing neurons in the IGL following light simulation receive direct input from the retina.

A second question about the circuitry within ipRGC target regions of diurnal grass rats and nocturnal Norway rats that was examined here was whether differences exist in the distribution of excitatory (e.g. glutamate) and inhibitory (e.g. GABA) neuronal populations (Chapter 5). While many ipRGC targets were very similar in the distributions of glutamate and GABA cells, there were striking differences in the vLGN (higher density of glutamate cells in Norway rats than grass rats) and LHb (GABAergic cells present in grass rats, but not Norway rats). These patterns suggest that the vLGN and/or LHb are sites that may promote chronotype-specific masking responses by altering the valence of signals coming to these regions from ipRGCs. The difference in the LHb is particularly interesting, since previous reports using

different strains of nocturnal mice and rats have indicated very little GABA (if any) in this region (Lein et al., 2007; Brinschwitz et al., 2010; Li et al., 2011; Allen Institute for Brain Science, 2015). The LHb is also highly integrated with various brain regions that modulate circadian rhythms and a variety of features of other behavioral processes (seep, reward, pain, cognition) (for review see: Aizawa et al., 2013; Lee and Goto, 2013; Yadid et al., 2013; Benarroch, 2015; Zhao et al., 2015a). Whether the inhibitory neurons that are present in the LHb of grass rats, but not other nocturnal rodents, inhibit local circuits or directly inhibit targets involved in the behaviors mentioned above needs to be determined. A particularly interesting aspect of this difference is whether these GABAergic cells may also modulate reward circuits that influence the motivation to run in a wheel at specific times of day in day- and night-active grass rats (Chapter 2). Thus, future research is needed to address such issues.

Future directions and questions

In summary, the studies in this dissertation clearly demonstrate behavioral differences in light responses in day- and night-active individuals, as well as similarities and differences in the neural pathways that may promote such effects. There are, however, many questions that still need to be addressed. For example, how might the neural mechanisms promoting masking responses within a species be similar or different from those promoting this process between species? What is the nature of the interactions between rods/cones and melanopsin in a diurnal cone-rich retina and might these contribute to differences in masking responses of Nile grass rats and nocturnal rodents? Are differences in the rostrocaudal extent of the OPT important for species differences in masking? Are ipRGC projections to sleep-promoting cells in the ventrolateral preoptic area necessary for light to affect sleep and arousal in diurnal and nocturnal

species? Does the LHb of other diurnal rodents (e.g. chipmunks) contain a population of GABAergic neurons, as it does in diurnal grass rats? Is this region devoid of GABAergic cells in nocturnal rodents beyond Norway rats and mice (e.g. in flying squirrels)? Do differences in GABAergic content in the LHb contribute to differences in behavioral masking, either within (Chapter 2) or between (Chapter 3) species? Do they contribute to differences in circadian regulation of activity patterns in nocturnal and diurnal species? Do these GABAergic neurons in the LHb play a role in the modulation of mood, reward and cognition by light and/or by the circadian timekeeping system in grass rats? Thus, the current data raise a suite of questions that should be addressed in future research aimed at elucidating fundamental mechanisms responsible for individual and species differences in behavioral masking as well as in circadian timekeeping systems.

REFERENCES

REFERENCES

Abrahamson EE, Moore RY (2001) Suprachiasmatic nucleus in the mouse: retinal innervation, intrinsic organization and efferent projections. Brain Res 916:172-191.

Aizawa H, Cui W, Tanaka K, Okamoto H (2013) Hyperactivation of the habenula as a link between depression and sleep disturbance. Frontiers in Human Neuroscience 7.

Allen Institute for Brain Science (2015) Allen Mouse Brain Atlas. In. http://mouse.brain-map.org.

Altimus CM, Guler AD, Villa KL, McNeill DS, LeGates TA, Hattar S (2008) Rods-cones and melanopsin detect light and dark to modulate sleep independent of image formation. Proc Natl Acad Sci U S A 105:19998-20003.

Araki M, McGeer PL, Kimura H (1988) The efferent projections of the rat lateral habenular nucleus revealed by the pha-l anterograde tracing method. Brain Res 441:319-330.

Aschoff J (1960) Exogenous and endogenous components in circadian rhythms. Cold Spring Harb Symp Quant Biol 25:11-28.

Aschoff J (1963) Comparative physiology - Diurnal rhythms. Annu Rev Physiol 25:581-&.

Aschoff J, von Goetz C (1986) Effects of feeding cycles on circadian rhythms in squirrel monkeys. J Biol Rhythms 1:267-276.

Aschoff J, Vongoetz C (1988) Masking of circadian activity rhythms in hamsters by darkness. Journal of Comparative Physiology a-Sensory Neural and Behavioral Physiology 162:559-562.

Aschoff J, Vongoetz C (1989) Masking of circadian activity rhythms in canaries by light and dark. J Biol Rhythms 4:29-38.

Aschoff J, Vongoetz C, Vongoetz C (1988) Masking of circadian activity rhythms in male golden hamsters by the presence of females. Behavioral Ecology and Sociobiology 22:409-412.

Barak O, Kronfeld-Schor N (2013) Activity rhythms and masking response in the diurnal fat sand rat under laboratory conditions. Chronobiol Int 30:1123-1134.

Baver SB, Pickard GE, Sollars PJ, Pickard GE (2008) Two types of melanopsin retinal ganglion cell differentially innervate the hypothalamic suprachiasmatic nucleus and the olivary pretectal nucleus. Eur J Neurosci 27:1763-1770.

Bedrosian TA, Fonken LK, Nelson RJ (2015) Endocrine effects of circadian disruption. Annu Rev Physiol.

Belenky MA, Smeraski CA, Provencio I, Sollars PJ, Pickard GE (2003) Melanopsin retinal ganglion cells receive bipolar and amacrine cell synapses. J Comp Neurol 460:380-393.

Benarroch EE (2015) Habenula Recently recognized functions and potential clinical relevance. Neurology 85:992-1000.

Bergstrom AL, Hannibal J, Hindersson P, Fahrenkrug J (2003) Light-induced phase shift in the Syrian hamster (Mesocricetus auratus) is attenuated by the PACAP receptor antagonist PACAP6-38 or PACAP immunoneutralization. Eur J Neurosci 18:2552-2562.

Berson DM, Dunn FA, Takao M (2002) Phototransduction by retinal ganglion cells that set the circadian clock. Science 295:1070-1073.

Berson DM, Castrucci AM, Provencio I (2010) Morphology and mosaics of melanopsin-expressing retinal ganglion cell types in mice. J Comp Neurol 518:2405-2422.

Bianco IH, Wilson SW (2009) The habenular nuclei: a conserved asymmetric relay station in the vertebrate brain. Philosophical Transactions of the Royal Society B-Biological Sciences 364:1005-1020.

Blanchong JA, Smale L (2000) Temporal patterns of activity of the unstriped Nile rat, *Arvicanthis niloticus*. J Mammal 81:595-599.

Blanchong JA, McElhinny TL, Mahoney MM, Smale L (1999) Nocturnal and diurnal rhythms in the unstriped Nile rat, *Arvicanthis niloticus*. J Biol Rhythms 14:364-377.

Brinschwitz K, Dittgen A, Madai VI, Lommel R, Geisler S, Veh RW (2010) Glutamatergic axons from the lateral habenula mainly terminate on GABAergic neurons of the ventral midbrain. Neuroscience 168:463-476.

Brown RE, Basheer R, McKenna JT, Strecker RE, McCarley RW (2012) Control of sleep and wakefulness. Physiol Rev 92:1087-1187.

Brown TM, Gias C, Hatori M, Keding SR, Semo Ma, Coffey PJ, Gigg J, Piggins HD, Panda S, Lucas RJ (2010) Melanopsin contributions to irradiance coding in the thalamo-cortical visual system. Plos Biology 8.

Brumovsky PR (2013) VGLUTs in peripheral neurons and the spinal cord: Time for a review. ISRN neurology 2013:829753.

Butler MP, Silver R (2011) Divergent photic thresholds in the non-image-forming visual system: entrainment, masking and pupillary light reflex. Proceedings of the Royal Society B-Biological Sciences 278:745-750.

Cajochen C (2007) Alerting effects of light. Sleep Medicine Reviews 11:453-464.

Castillo-Ruiz A, Nixon JP, Smale L, Nunez AA (2010) Neural activation in arousal and reward areas of the brain in day-active and night-active grass rats. Neuroscience 165:337-349.

Challet E, Pitrosky B, Sicard B, Malan A, Pevet P (2002) Circadian organization in a diurnal rodent, Arvicanthis ansorgei Thomas 1910: Chronotypes, responses to constant lighting conditions, and photoperiodic changes. J Biol Rhythms 17:52-64.

Chen SK, Badea TC, Hattar S (2011) Photoentrainment and pupillary light reflex are mediated by distinct populations of ipRGCs. Nature 476:92-95.

Cohen R, Smale L, Kronfeld-Schor N (2010) Masking and temporal niche switches in spiny mice. J Biol Rhythms 25:47-52.

Comoli E, Favaro PD, Vautrelle N, Leriche M, Overton PG, Redgrave P (2012) Segregated anatomical input to sub-regions of the rodent superior colliculus associated with approach and defense. Frontiers in Neuroanatomy 6.

Cuesta M, Clesse D, Pevet P, Challet E (2009) From daily behavior to hormonal and neurotransmitters rhythms: Comparison between diurnal and nocturnal rat species. Horm Behav 55:338-347.

Cui Q, Ren C, Sollars PJ, Pickard GE, So KF (2015) The injury resistant ability of melanopsin-expressing intrinsically photosensitive retinal ganglion cells. Neuroscience 284C:845-853.

Dacey DM, Liao HW, Peterson BB, Robinson FR, Smith VC, Pokorny J, Yau KW, Gamlin PD (2005) Melanopsin-expressing ganglion cells in primate retina signal colour and irradiance and project to the LGN. Nature 433:749-754.

Doyle SE, Yoshikawa T, Hillson H, Menaker M (2008) Retinal pathways influence temporal niche. Proc Natl Acad Sci U S A 105:13133-13138.

Ebihara S, Tsuji K (1980) Entrainment of the circadian activity rhythm to the light cycle: Effective light intensity for a zeitgeber in the retinal degenerate C3H mouse and the normal C57BL mouse. Physiol Behav 24:523-527.

Ecker JL, Dumitrescu ON, Wong KY, Alam NM, Chen SK, LeGates T, Renna JM, Prusky GT, Berson DM, Hattar S (2010) Melanopsin-expressing retinal ganglion-cell photoreceptors: cellular diversity and role in pattern vision. Neuron 67:49-60.

Edelstein K, Mrosovsky N (2001) Behavioral responses to light in mice with dorsal lateral geniculate lesions. Brain Res 918:107-112.

El Mestikawy S, Wallen-Mackenzie A, Fortin GM, Descarries L, Trudeau LE (2011) From glutamate co-release to vesicular synergy: vesicular glutamate transporters. Nature Reviews Neuroscience 12:204-216.

Engelund A, Fahrenkrug J, Harrison A, Hannibal J (2010) Vesicular glutamate transporter 2 (VGLUT2) is co-stored with PACAP in projections from the rat melanopsin-containing retinal ganglion cells. Cell Tissue Res 340:243-255.

Engelund A, Fahrenkrug J, Harrison A, Luuk H, Hannibal J (2012) Altered pupillary light reflex in PACAP receptor 1-deficient mice. Brain Res 1453:17-25.

Erkert HG, Gburek V, Scheideler A (2006) Photic entrainment and masking of prosimian circadian rhythms (Otolemur garnettii, Primates). Physiol Behav 88:39-46.

Esclapez M, Tillakaratne NJK, Kaufman DL, Tobin AJ, Houser CR (1994) Comparative localization of two forms of glutamic acid decarboxylase and thier mRNAs in rat brain supports the concept of functional differences between the forms. J Neurosci 14:1834-1855.

Esquiva G, Lax P, Cuenca N (2013) Impairment of intrinsically photosensitive retinal ganglion cells associated with late stages of retinal degeneration. Invest Ophthalmol Vis Sci 54:4605-4618.

Estevez ME, Fogerson PM, Ilardi MC, Borghuis BG, Chan E, Weng SJ, Auferkorte ON, Demb JB, Berson DM (2012) Form and function of the M4 cell, an intrinsically photosensitive retinal ganglion cell type contributing to geniculocortical vision. J Neurosci 32:13608-13620.

Feldblum S, Erlander MG, Tobin AJ (1993) Different distributions of GAD65 and GAD67 mRNAs suggest that the two glutamate decarboxylases play distinctive functional roles. J Neurosci Res 34:689-706.

Fernandez-Duque E, de la Iglesia H, Erkert HG (2010) Moonstruck primates: Owl monkeys (*Aotus*) need moonlight for nocturnal activity in their natural environment. PloS one 5.

Fonken LK, Nelson RJ (2014) The effects of light at night on circadian clocks and metabolism. Endocr Rev 35:648-670.

Foster RG, Provencio I, Hudson D, Fiske S, Degrip W, Menaker M (1991) Circadian photoreception in the retinally degenerate mouse (*rd/rd*). Journal of Comparative Physiology a-Sensory Neural and Behavioral Physiology 169:39-50.

Fox MA, Guido W (2011) Shedding light on class-specific wiring: Development of intrinsically photosensitive retinal ganglion cell circuitry. Mol Neurobiol 44:321-329.

Freedman MS, Lucas RJ, Soni B, von Schantz M, Munoz M, David-Gray Z, Foster R (1999) Regulation of mammalian circadian behavior by non-rod, non-cone, ocular photoreceptors. Science 284:502-504.

Gaillard F, Karten HJ, Sauve Y (2013) Retinorecipient areas in the diurnal murine rodent *Arvicanthis niloticus*: A disproportionally large superior colliculus. J Comp Neurol 521:1699-1726.

Gaillard F, Bonfield S, Gilmour GS, Kuny S, Mema SC, Martin BT, Smale L, Crowder N, Stell WK, Sauve Y (2008) Retinal anatomy and visual performance in a diurnal cone-rich laboratory rodent, the Nile grass rat (*Arvicanthis niloticus*). J Comp Neurol 510:525-538.

Galindo-Romero C, Jimenez-Lopez M, Garcia-Ayuso D, Salinas-Navarro M, Nadal-Nicolas PM, Agudo-Barriuso M, Villegas-Perez MP, Aviles-Trigueros M, Vidal-Sanz M (2013) Number and spatial distribution of intrinsically photosensitive retinal ganglion cells in the adult albino rat. Exp Eye Res 108:84-93.

Gall AJ, Smale L, Yan L, Nunez AA (2013) Lesions of the intergeniculate leaflet lead to a reorganization in circadian regulation and a reversal in masking responses to photic stimuli in the Nile grass rat. PloS one 8:e67387.

Gander PH, Moore-ede MC (1983) Light-dark masking of circadian temperature and activity rhythms in squirrel monkeys. Am J Physiol 245:R927-R934.

Gaus SE, Strecker RE, Tate BA, Parker RA, Saper CB (2002) Ventrolateral preoptic nucleus contains sleep-active, galaninergic neurons in multiple mammalian species. Neuroscience 115:285-294.

Gooley JJ, Lu J, Chou TC, Scammell TE, Saper CB (2001) Melanopsin in cells of origin of the retinohypothalamic tract. Nat Neurosci 4:1165-1165.

Goz D, Studholme K, Lappi DA, Rollag MD, Provencio I, Morin LP (2008) Targeted destruction of photosensitive retinal ganglion cells with a saporin conjugate alters the effects of light on mouse circadian rhythms. PloS one 3.

Guilding C, Hughes ATL, Piggins HD (2010) Circadian oscillators in the epithalamus. Neuroscience 169:1630-1639.

Guler AD, Ecker JL, Lall GS, Haq S, Altimus CM, Liao H-W, Barnard AR, Cahill H, Badea TC, Zhao H, Hankins MW, Berson DM, Lucas RJ, Yau K-W, Hattar S (2008) Melanopsin cells are the principal conduits for rod-cone input to non-image-forming vision. Nature 453:102-105.

Gutman R, Dayan T (2005) Temporal partitioning: An experiment with two species of spiny mice. Ecology 86:164-173.

Hagenauer MH, Lee TM (2008) Circadian organization of the diurnal Caviomorph rodent, Octodon degus. Biological Rhythm Research 39:269-289.

Hannibal J (2002) Pituitary adenylate cyclase-activating peptide in the rat central nervous system: An immunohistochemical and in situ hybridization study. J Comp Neurol 453:389-417.

Hannibal J (2006) Roles of PACAP-containing retinal ganglion cells in circadian timing. International Review of Cytology - a Survey of Cell Biology, Vol 251 251:1-39.

Hannibal J, Fahrenkrug J (2004) Target areas innervated by PACAP-immunoreactive retinal ganglion cells. Cell Tissue Res 316:99-113.

Hannibal J, Brabet P, Fahrenkrug J (2008) Mice lacking the PACAP type I receptor have impaired photic entrainment and negative masking. American Journal of Physiology-Regulatory Integrative and Comparative Physiology 295:R2050-R2058.

Hannibal J, Georg B, Fahrenkrug J (2013) Differential expression of melanopsin mRNA and protein in Brown Norwegian rats. Exp Eye Res 106:55-63.

Hannibal J, Moller M, Ottersen OP, Fahrenkrug J (2000) PACAP and glutamate are co-stored in the retinohypothalamic tract. J Comp Neurol 418:147-155.

Hannibal J, Hindersson P, Knudsen SM, Georg B, Fahrenkrug J (2002) The photopigment melanopsin is exclusively present in pituitary adenylate cyclase-activating polypeptide-containing retinal ganglion cells of the retinohypothalamic tract. J Neurosci 22.

Hannibal J, Mikkelsen JD, Clausen H, Holst JJ, Wulff BS, Fahrenkrug J (1995) Gene-expression of pituitary adenylate-cyclase activating polypeptide (PACAP) in the rat hypothalamus. Regul Pept 55:133-148.

Hannibal J, Kankipati L, Strang CE, Peterson BB, Dacey D, Gamlin PD (2014) Central projections of intrinsically photosensitive retinal ganglion cells in the macaque monkey. J Comp Neurol 522:2231-2248.

Hannibal J, Hindersson P, Ostergaard J, Georg B, Heegaard S, Larsen PJ, Fahrenkrug J (2004) Melanopsin is expressed in PACAP-containing retinal ganglion cells of the human retinohypothalamic tract. Invest Ophthalmol Vis Sci 45:4202-4209.

Hannibal L, Georg B, Hindersson P, Fahrenkrug J (2005) Light and darkness regulate melanopsin in the retinal ganglion cells of the albino Wistar rat. J Mol Neurosci 27:147-155.

Harmar AJ, Fahrenkrug J, Gozes I, Laburthe M, May V, Pisegna JR, Vaudry D, Vaudry H, Waschek JA, Said SI (2012) Pharmacology and functions of receptors for vasoactive intestinal peptide and pituitary adenylate cyclase-activating polypeptide: IUPHAR Review 1. Br J Pharmacol 166:4-17.

Harrington ME (1997) The ventral lateral geniculate nucleus and the intergeniculate leaflet: Interrelated structures in the visual and circadian systems. Neurosci Biobehav Rev 21:705-727.

Harrington ME, Hoque S, Hall A, Golombek D, Biello S (1999) Pituitary adenylate cyclase activating peptide phase shifts circadian rhythms in a manner similar to light. J Neurosci 19:6637-6642.

Hatori M, Le H, Vollmers C, Keding SR, Tanaka N, Schmedt C, Jegla T, Panda S (2008) Inducible ablation of melanopsin-expressing retinal ganglion cells reveals their central role in non-image forming visual responses. PloS one 3:e2451.

Hattar S, Liao HW, Takao M, Berson DM, Yau KW (2002) Melanopsin-containing retinal. ganglion cells: Architecture, projections, and intrinsic photosensitivity. Science 295:1065-1070.

Hattar S, Kumar M, Park A, Tong P, Tung J, Yau KW, Berson DM (2006) Central projections of melanopsin-expressing retinal ganglion cells in the mouse. J Comp Neurol 497:326-349.

Hattar S, Lucas RJ, Mrosovsky N, Thompson S, Douglas RH, Hankins MW, Lem J, Biel M, Hofmann F, Foster RG, Yau KW (2003) Melanopsin and rod-cone photoreceptive systems account for all major accessory visual functions in mice. Nature 424:76-81.

Haun F, Eckenrode TC, Murray M (1992) Habenula and thalamus cell transplants restore normal sleep behaviors disrupted by denervation of the interpeduncular nucleus. J Neurosci 12:3282-3290.

Herkenham M, Nauta WJH (1979) Efferent connections of the habenular nuclei in the rat. J Comp Neurol 187:19-47.

Hickey TL, Spear PD (1976) Retinogeniculate projections in hooded and albino rats: An autoradiographic study. Exp Brain Res 24:523-529.

Hut RA, Kronfeld-Schor N, van der Vinne V, De la Iglesia H (2012) In search of a temporal niche: environmental factors. Prog Brain Res 199:281-304.

Illnerova H, Vanecek J, Krecek J, Wetterberg L, Saaf J (1979) Effect of one minute exposure to light at night on rat pineal serotonin N-acetyltransferase and melatonin. J Neurochem 32:673-675.

Jagannath A, Hughes S, Abdelgany A, Pothecary CA, Di Pretoro S, Pires SS, Vachtsevanos A, Pilorz V, Brown LA, Hossbach M, MacLaren RE, Halford S, Gatti S, Hankins MW, Wood MJA, Foster RG, Peirson SN (2015) Isoforms of melanopsin mediate different behavioral responses to light. Curr Biol 25:2430-2434.

Janik D, Mikkelsen JD, Mrosovsky N (1995) Cellular colocalization of fos and neuropeptide-y in the intergeniculate leaflet after nonphotic phase-shifting events. Brain Res 698:137-145.

Johnson RF, Morin LP, Moore RY (1988) Retinohypothalamic projections in the hamster and rat demonstrated using cholera toxin. Brain Res 462:301-312.

Juhl F, Hannibal J, Fahrenkrug J (2007) Photic induction of c-Fos in enkephalin neurons of the rat intergeniculate leaflet innervated by retinal PACAP fibres. Cell Tissue Res 329:491-502.

Jusuf PR, Lee SCS, Hannibal J, Grunert U (2007) Characterization and synaptic connectivity of melanopsin-containing ganglion cells in the primate retina. Eur J Neurosci 26:2906-2921.

Kalsbeek A, Cutrera RA, Van Heerikhuize JJ, Van der Vliet J, Buijs RM (1999) GABA release from suprachiasmatic nucleus terminals is necessary for the light-induced inhibition of nocturnal melatonin release in the rat. Neuroscience 91:453-461.

Kanematsu N, Honma S, Katsuno Y, Honma K-I (1994) Immediate response to light of rat pineal melatonin rhythm: Analysis by in vivo microdialysis. Am J Physiol 266:R1849-R1855.

Karnas D, Hicks D, Mordel J, Pevet P, Meissl H (2013a) Intrinsic photosensitive retinal ganglion cells in the diurnal rodent, *Arvicanthis ansorgei*. PloS one 8:e73343-e73343.

Karnas D, Mordel J, Bonnet D, Pevet P, Hicks D, Meissl H (2013b) Heterogeneity of intrinsically photosensitive retinal ganglion cells in the mouse revealed by molecular phenotyping. J Comp Neurol 521:912-932.

Kas MJH, Edgar DM (1999) A nonphotic stimulus inverts the diurnal-nocturnal phase preference in *Octodon degus*. J Neurosci 19:328-333.

Katona C, Smale L (1997) Wheel-running rhythms in *Arvicanthis niloticus*. Physiol Behav 61:365-372.

Kawaguchi C, Isojima Y, Shintani N, Hatanaka M, Guo X, Okumura N, Nagai K, Hashimoto H, Baba A (2010) PACAP-Deficient Mice Exhibit Light Parameter-Dependent Abnormalities on Nonvisual Photoreception and Early Activity Onset. PloS one 5.

Keeler CE (1927a) Rodless retina, an ophthalmic mutation in the house mouse, mus musculus. J Exp Zool 46:355-407.

Keeler CE (1927b) Iris movements in blind mice. Am J Physiol 81:107-112.

Keeler CE (1928) Blind mice. J Exp Zool 51:495-508.

Keeler CE, Sutcliffe E, Chaffee EL (1928) Normal and "rodless" retinae of the house mouse with respect to the electromotive force generated through stimulation by light. Proc Natl Acad Sci U S A 14:477-484.

Kiss J, Halasz B, Csaki A, Liposits Z, Hrabovszky E (2007) Vesicular glutamate transporter 2 protein and mRNA containing neurons in the hypothalamic suprachiasmatic nucleus of the rat. Brain Res Bull 74:397-405.

Kowski AB, Geisler S, Krauss M, Veh RW (2008) Differential projections from subfields in the lateral preoptic area to the lateral habenular complex of the rat. J Comp Neurol 507:1465-1478.

Krajnak K, Dickenson L, Lee TM (1997) The induction of Fos-like proteins in the suprachiasmatic nuclei and intergeniculate leaflet by light pulses in degus (*Octodon degus*) and rats. J Biol Rhythms 12:401-412.

Kripke DF, Elliott JA, Welsh DK, Youngstedt SD (2015) Photoperiodic and circadian bifurcation theories of depression and mania. F1000Research 4:107.

Kronfeld-Schor N, Dominoni D, de la Iglesia H, Levy O, Herzog ED, Dayan T, Helfrich-Forster C (2013) Chronobiology by moonlight. Proceedings of the Royal Society B-Biological Sciences 280.

Labor USDo (2005) Work on flexible and shift schedules, 2004 summary. In: (Statistics BoL, ed). Washington, D.C.

Langel J, Yan L, Nunez AA, Smale L (2014) Behavioral masking and cFos responses to light in day- and night-active grass rats. J Biol Rhythms 29:192-202.

Langel JL, Smale L, Esquiva G, Hannibal J (2015) Central melanopsin projections in the diurnal rodent, Arvicanthis niloticus. Frontiers in Neuroanatomy 9.

Lee Y-A, Goto Y (2013) Habenula and ADHD: Convergence on time. Neurosci Biobehav Rev 37:1801-1809.

LeGates TA, Altimus CM, Wang H, Lee H-K, Yang S, Zhao H, Kirkwood A, Weber ET, Hattar S (2012) Aberrant light directly impairs mood and learning through melanopsin-expressing neurons. Nature 491:594-598.

Lein ES et al. (2007) Genome-wide atlas of gene expression in the adult mouse brain. Nature 445:168-176.

Levy O, Dayan T, Kronfeld-Schor N (2007) The relationship between the golden spiny mouse circadian system and its diurnal activity: An experimental field enclosures and laboratory study. Chronobiol Int 24:599-613.

Lewy AJ, Wehr TA, Goodwin FK, Newsome DA, Markey SP (1980) Light suppresses melatonin secretion in humans. Science 210:1267-1269.

Li B, Piriz J, Mirrione M, Chung C, Proulx CD, Schulz D, Henn F, Malinow R (2011) Synaptic potentiation onto habenula neurons in the learned helplessness model of depression. Nature 470:535-U125.

Li XD, Gilbert J, Davis FC (2005) Disruption of masking by hypothalamic lesions in Syrian hamsters. Journal of Comparative Physiology a-Neuroethology Sensory Neural and Behavioral Physiology 191:23-30.

Lucas RJ, Douglas RH, Foster RG (2001) Characterization of an ocular photopigment capable of driving pupillary constriction in mice. Nat Neurosci 4:621-626.

Lucas RJ, Hattar S, Takao M, Berson DM, Foster RG, Yau KW (2003) Diminished pupillary light reflex at high irradiances in melanopsin-knockout mice. Science 299:245-247.

Lupi D, Semo Ma, Foster RG (2012) Impact of age and retinal degeneration on the light input to circadian brain structures. Neurobiol Aging 33:383-392.

Lupi D, Oster H, Thompson S, Foster RG (2008) The acute light-induction of sleep is mediated by OPN4-based photoreception. Nat Neurosci 11:1068-1073.

Lupi D, Cooper HM, Froehlich A, Standford L, McCall MA, Foster RG (1999) Transgenic ablation of rod photoreceptors alters the circadian phenotype of mice. Neuroscience 89:363-374.

Mahoney M, Bult A, Smale L (2001) Phase response curve and light-induced Fos expression in the suprachiasmatic nucleus and adjacent hypothalamus of Arvicanthis niloticus. J Biol Rhythms 16:149-162.

Marchant EG, Morin LP (2001) Light augments FOS protein induction in brain of short-term enucleated hamsters. Brain Res 902:51-65.

McElhinny TL, Smale L, Holekamp KE (1997) Patterns of body temperature, activity, and reproductive behavior in a tropical murid rodent, *Arvicanthis niloticus*. Physiol Behav 62:91-96.

McNeill DS, Sheely CJ, Ecker JL, Badea TC, Morhardt D, Guido W, Hattar S (2011) Development of melanopsin-based irradiance detecting circuitry. Neural Development 6.

Meijer JH, Robbers Y (2014) Wheel running in the wild. Proceedings of the Royal Society B-Biological Sciences 281.

Miller AM, Obermeyer WH, Behan M, Benca RM (1998) The superior colliculus-pretectum mediates the direct effects of light on sleep. Proc Natl Acad Sci U S A 95:8957-8962.

Mize RR (1992) The organization of GABAergic neurons in the mammalian superior colliculus. Prog Brain Res 90:219-248.

Moore RY, Eichler VB (1972) Loss of a circadian adrenal corticosterone rhythm following suprachiasmatic lesions in rat. Brain Res 42:201-206.

Moore RY, Lenn NJ (1972) Retinohypothalamic projection in rat. J Comp Neurol 146:1-14.

Moore RY, Speh JC (1993) GABA is the principal neurotransmitter of the circadian system. Neurosci Lett 150:112-116.

Moore RY, Card JP (1994) Intergeniculate leaflet: An anatomically and functionally distinct subdivision of the lateral geniculate complex. J Comp Neurol 344:403-430.

Moore RY, Weis R, Moga MM (2000) Efferent projections of the intergeniculate leaflet and the ventral lateral geniculate nucleus in the rat. J Comp Neurol 420:398-418.

Morin LP (2013a) Nocturnal light and nocturnal rodents: Similar regulation of disparate functions? J Biol Rhythms 28:95-106.

Morin LP (2013b) Neuroanatomy of the extended circadian rhythm system. Exp Neurol 243:4-20.

Morin LP (2015) A path to sleep is through the eye. eneuro 2.

Morin LP, Blanchard J (1995) Organization of the hamster intergeniculate leaflet: NPY and ENK projections to the suprachiasmatic nucleus, intergeniculate leaflet and posterior limitans nucleus. Vis Neurosci 12:57-67.

Morin LP, Blanchard JH (1998) Interconnections among nuclei of the subcortical visual shell: The intergeniculate leaflet is a major constituent of the hamster subcortical visual system. J Comp Neurol 396:288-309.

Morin LP, Blanchard JH (2001) Neuromodulator content of hamster intergeniculate leaflet neurons and their projection to the suprachiasmatic nucleus or visual midbrain. J Comp Neurol 437:79-90.

Morin LP, Studholme KM (2009) Millisecond light pulses make mice stop running, then display prolonged sleep-like behavior in the absence of light. J Biol Rhythms 24:497-508.

Morin LP, Studholme KM (2011) Separation of function for classical and ganglion cell photoreceptors with respect to circadian rhythm entrainment and induction of photosomnolence. Neuroscience 199:213-224.

Morin LP, Studholme KM (2014) Retinofugal projections in the mouse. J Comp Neurol 522:3733-3753.

Morin LP, Blanchard J, Moore RY (1992) Intergeniculate leaflet and suprachiasmatic nucleus organization and connections in the golden hamster. Vis Neurosci 8:219-230.

Morin LP, Blanchard JH, Provencio I (2003) Retinal ganglion cell projections to the hamster suprachiasmatic nucleus, intergeniculate leaflet, and visual midbrain: Bifurcation and melanopsin immunoreactivity. J Comp Neurol 465:401-416.

Morin LP, Goodlesssanchez N, Smale L, Moore RY (1994) Projections of the suprachiasmatic nuclei, subparaventricular zone and retrochiasmatic area in the golden hamster. Neuroscience 61:391-410.

Mrosovsky N (1994) In praise of masking: Behavioral responses of retinally degenerate mice to dim light. Chronobiol Int 11:343-348.

Mrosovsky N (1999) Masking: History, definitions, and measurement. Chronobiol Int 16:415-429.

Mrosovsky N, Hattar S (2003) Impaired masking responses to light in melanopsin-knockout mice. Chronobiol Int 20:989-999.

Mrosovsky N, Thompson S (2008) Negative and positive masking responses to light in retinal degenerate slow (rds/rds) mice during aging. Vision Res 48:1270-1273.

Mrosovsky N, Foster RG, Salmon PA (1999) Thresholds for masking responses to light in three strains of retinally degenerate mice. Journal of Comparative Physiology a-Sensory Neural and Behavioral Physiology 184:423-428.

Mrosovsky N, Lucas RJ, Foster RG (2001) Persistence of masking responses to light in mice lacking rods and cones. J Biol Rhythms 16:585-587.

Mrosovsky N, Salmon PA, Foster RG, McCall MA (2000) Responses to light after retinal degeneration. Vision Res 40:575-578.

Muindi F, Zeitzer JM, Colas D, Heller HC (2013) The acute effects of light on murine sleep during the dark phase: importance of melanopsin for maintenance of light-induced sleep. Eur J Neurosci 37:1727-1736.

Niimi K, Kanaseki T, Takimoto T (1963) The comparative anatomy of the ventral nucleus of the lateral geniculate body in mammals. J Comp Neurol 121:313-323.

Nixon JP, Smale L (2004) Individual differences in wheel-running rhythms are related to temporal and spatial patterns of activation of orexin A and B cells in a diurnal rodent (*Arvicanthis niloticus*). Neuroscience 127:25-34.

Nixon JP, Smale L (2005) Orexin fibers form appositions with Fos expressing neuropeptide-Y cells in the grass rat intergeniculate leaflet. Brain Res 1053:33-37.

Novak CM, Smale L, Nunez AA (2000) Rhythms in Fos expression in brain areas related to the sleep-wake cycle in the diurnal Arvicanthis niloticus. American Journal of Physiology-Regulatory Integrative and Comparative Physiology 278:R1267-R1274.

Novak CM, Burghardt PR, Levine JA (2012) The use of a running wheel to measure activity in rodents: Relationship to energy balance, general activity, and reward. Neurosci Biobehav Rev 36:1001-1014.

Ostergaard J, Hannibal J, Fahrenkrug J (2007) Synaptic contact between melanopsin-containing retinal ganglion cells and rod bipolar cells. Invest Ophthalmol Vis Sci 48:3812-3820.

Otalora BB, Hagenauer MH, Rol MA, Madrid JA, Lee TM (2013) Period gene expression in the brain of a dual-phasing rodent, the *Octodon degus*. J Biol Rhythms 28:249-261.

Ottoni EB (2000) EthoLog 2.2: A tool for the transcription and timing of behavior observation sessions. Behavior Research Methods Instruments & Computers 32:446-449.

Palus K, Chrobok L, Lewandowski MH (2015) Orexins/hypocretins modulate the activity of NPY-positive and -negative neurons in the rat intergeniculate leaflet via OX1 and OX2 receptors. Neuroscience 300:370-380.

Panda S, Sato TK, Castrucci AM, Rollag MD, DeGrip WJ, Hogenesch JB, Provencio I, Kay SA (2002) Melanopsin (Opn4) requirement for normal light-induced circadian phase shifting. Science 298:2213-2216.

Panda S, Provencio I, Tu DC, Pires SS, Rollag MD, Castrucci AM, Pletcher MT, Sato TK, Wiltshire T, Andahazy M, Kay SA, Van Gelder RN, Hogenesch JB (2003) Melanopsin is required for non-image-forming photic responses in blind mice. Science 301:525-527.

Park HT, Baek SY, Kim BS, Kim JB, Kim JJ (1993) Profile of fos-like immunoreactivity induction by light stimuli in the intergeniculate leaflet is different from that of the suprachiasmatic nucleus. Brain Res 610:334-339.

Paul MJ, Indic P, Schwartz WJ (2011) A role for the habenula in the regulation of locomotor activity cycles. Eur J Neurosci 34:478-488.

Paxinos G, Watson C (2005) The Rat Brain in Stereotaxic Coordinates, 5th Edition. Burlington, MA, USA: Elsevier Academic Press.

Pekala D, Blasiak T, Raastad M, Lewandowski MH (2011) The influence of orexins on the firing rate and pattern of rat intergeniculate leaflet neurons - electrophysiological and immunohistological studies. Eur J Neurosci 34:1406-1418.

Pendergast JS, Yamazaki S (2011) Masking Responses to Light in Period Mutant Mice. Chronobiol Int 28:657-663.

Pires SS, Hughes S, Turton M, Melyan Z, Peirson SN, Zheng L, Kosmaoglou M, Bellingham J, Cheetham ME, Lucas RJ, Foster RG, Hankins MW, Halford S (2009) Differential expression of two distinct functional isoforms of melanopsin (Opn4) in the mammalian retina. J Neurosci 29:12332-12342.

Prichard JR, Stoffel RT, Quimby DL, Obermeyer WH, Benca RM, Behan M (2002) Fos immunoreactivity in rat subcortical visual shell in response to illuminance changes. Neuroscience 114:781-793.

Provencio I, Foster RG (1995) Circadian rhythms in mice can be regulated by photoreceptors with cone-like characteristics. Brain Res 694:183-190.

Provencio I, Wong SY, Lederman AB, Argamaso SM, Foster RG (1994) Visual and circadian responses to light in aged retinally degenerate mice. Vision Res 34:1799-1806.

Provencio I, Jiang GS, De Grip WJ, Hayes WP, Rollag MD (1998) Melanopsin: An opsin in melanophores, brain, and eye. Proc Natl Acad Sci U S A 95:340-345.

Provencio I, Rodriguez IR, Jiang GS, Hayes WP, Moreira EF, Rollag MD (2000) A novel human opsin in the inner retina. J Neurosci 20:600-605.

Quina LA, Tempest L, Ng L, Harris JA, Ferguson S, Jhou TC, Turner EE (2015) Efferent pathways of the mouse lateral habenula. J Comp Neurol 523:32-60.

Ramanathan C, Stowie A, Smale L, Nunez AA (2010) Phase Preference for the Display of Activity is Associated with the Phase of Extra-Suprachiasmatic Nucleus Oscillators Within and Between Species. Neuroscience 170:758-772.

Redlin U (2001) Neural basis and biological function of masking by light in mammals: Suppression of melatonin and locomotor activity. Chronobiol Int 18:737-758.

Redlin U, Mrosovsky N (1999a) Masking by light in hamsters with SCN lesions. Journal of Comparative Physiology a-Sensory Neural and Behavioral Physiology 184:439-448.

Redlin U, Mrosovsky N (1999b) Masking of locomotor activity in hamsters. Journal of Comparative Physiology a-Sensory Neural and Behavioral Physiology 184:429-437.

Redlin U, Mrosovsky N (2004) Nocturnal activity in a diurnal rodent (*Arvicanthis niloticus*): The importance of masking. J Biol Rhythms 19:58-67.

Redlin U, Vrang N, Mrosovsky N (1999) Enhanced masking response to light in hamsters with IGL lesions. Journal of Comparative Physiology a-Sensory Neural and Behavioral Physiology 184:449-456.

Redlin U, Cooper HM, Mrosovsky N (2003) Increased masking response to light after ablation of the visual cortex in mice. Brain Res 965:1-8.

Refinetti R (2006) Variability of diurnality in laboratory rodents. Journal of Comparative Physiology a-Neuroethology Sensory Neural and Behavioral Physiology 192:701-714.

Refinetti R (2008) The diversity of temporal niches in mammals. Biological Rhythm Research 39:173-192.

Reifler AN, Chervenak AP, Dolikian ME, Benenati BA, Meyers BS, Demertzis ZD, Lynch AM, Li BY, Wachter RD, Abufarha FS, Dulka EA, Pack W, Zhao X, Wong KY (2015) The rat retina has five types of ganglion-cell photoreceptors. Exp Eye Res 130:17-28.

Rotics S, Dayan T, Levy O, Kronfeld-Schor N (2011) Light masking in the field: An experiment with nocturnal and diurnal spiny mice under semi-natural field conditions. Chronobiol Int 28:70-75.

Ruby NF, Brennan TJ, Xie XM, Cao V, Franken P, Heller HC, O'Hara BF (2002) Role of melanopsin in circadian responses to light. Science 298:2211-2213.

Scheer F, Ter Horst GJ, Van der Vliet J, Buijs RM (2001) Physiological and anatomic evidence for regulation of the heart by suprachiasmatic nucleus in rats. American Journal of Physiology-Heart and Circulatory Physiology 280:H1391-H1399.

Schmidt TM, Kofuji P (2009) Functional and morphological differences among intrinsically photosensitive retinal ganglion cells. J Neurosci 29:476-482.

Schmidt TM, Kofuji P (2011) Structure and function of bistratified intrinsically photosensitive retinal ganglion cells in the mouse. J Comp Neurol 519:1492-1504.

Schmidt TM, Chen S-K, Hattar S (2011) Intrinsically photosensitive retinal ganglion cells: many subtypes, diverse functions. Trends Neurosci 34:572-580.

Schmidt TM, Alam NM, Chen S, Kofuji P, Li W, Prusky GT, Hattar S (2014) A Role for Melanopsin in Alpha Retinal Ganglion Cells and Contrast Detection. Neuron 82:781-788.

Schroeder AM, Colwell CS (2013) How to fix a broken clock. Trends Pharmacol Sci 34:605-619.

Schwartz MD, Smale L (2005) Individual differences in rhythms of behavioral sleep and its neural substrates in Nile grass rats. J Biol Rhythms 20:526-537.

Schwartz MD, Nunez AA, Smale L (2004) Differences in the suprachiasmatic nucleus and lower subparaventricular zone of diurnal and nocturnal rodents. Neuroscience 127:13-23.

Schwartz MD, Urbanski HF, Nunez AA, Smale L (2011) Projections of the suprachiasmatic nucleus and ventral subparaventricular zone in the Nile grass rat (Arvicanthis niloticus). Brain Res 1367:146-161.

Semo M, Gias C, Ahmado A, Vugler A (2014) A role for the ciliary marginal zone in the melanopsin-dependent intrinsic pupillary light reflex. Exp Eye Res 119:8-18.

Sherin JE, Shiromani PJ, McCarley RW, Saper CB (1996) Activation of ventrolateral preoptic neurons during sleep. Science 271:216-219.

Sherin JE, Elmquist JK, Torrealba F, Saper CB (1998) Innervation of histaminergic tuberomammillary neurons by GABAergic and galaninergic neurons in the ventrolateral preoptic nucleus of the rat. J Neurosci 18:4705-4721.

Sherwin CM (1998) Voluntary wheel running: A review and novel interpretation. Anim Behav 56:11-27.

Shuboni DD (2013) Masking: the acute effects of light on the brain and behavior. (Doctoral dissertation) http://catalog.lib.msu.edu/record=b10279955~S39a.

Shuboni DD, Cramm S, Yan L, Nunez AA, Smale L (2012) Acute behavioral responses to light and darkness in nocturnal *Mus musculus* and diurnal *Arvicanthis niloticus*. J Biol Rhythms 27:299-307.

Shuboni DD, Cramm SL, Yan L, Ramanathan C, Cavanaugh BL, Nunez AA, Smale L (2015) Acute effects of light on the brain and behavior of diurnal Arvicanthis niloticus and nocturnal Mus musculus. Physiol Behav 138:75-86.

Sisk CL, Stephan FK (1982) Central visual pathways and the distribution of sleep in 24-hr and 1-hr light-dark cycles. Physiol Behav 29:231-239.

Smale L, Lee T, Nunez AA (2003) Mammalian diurnality: Some facts and gaps. J Biol Rhythms 18:356-366.

Smale L, Nunez AA, Schwartz MD (2008) Rhythms in a diurnal brain. Biological Rhythm Research 39:305-318.

Smale L, McElhinny T, Nixon J, Gubik B, Rose S (2001) Patterns of wheel running are related to Fos expression in neuropeptide-Y-containing neurons in the intergeniculate leaflet of *Arvicanthis niloticus*. J Biol Rhythms 16:163-172.

Smith Y, Seguela P, Parent A (1987) Distribution of GABA-immunoreactive neurons in the thalamus of the squirrel monkey (Saimiri sciureus). Neuroscience 22:579-591.

Soghomonian JJ, Martin DL (1998) Two isoforms of glutamate decarboxylase: why? Trends Pharmacol Sci 19:500-505.

Stephan FK, Zucker I (1972) Circadian-rhythms in drinking behavior and locomotor activity of rats are eliminated by hypothalamic-lesions. Proc Natl Acad Sci U S A 69:1583-1586.

Stevens RG, Zhu Y (2015) Electric light, particularly at night, disrupts human circadian rhythmicity: is that a problem? Philosophical Transactions of the Royal Society B-Biological Sciences 370.

Studholme KM, Gompf HS, Morin LP (2013) Brief light stimulation during the mouse nocturnal activity phase simultaneously induces a decline in core temperature and locomotor activity followed by EEG-determined sleep. American Journal of Physiology-Regulatory Integrative and Comparative Physiology 304:R459-R471.

Thankachan S, Rusak B (2005) Juxtacellular recording/labeling analysis of physiological and anatomical characteristics of rat intergeniculate leaflet neurons. J Neurosci 25:9195-9204.

Todd WD, Gall AJ, Weiner JA, Blumberg MS (2012) Distinct Retinohypothalamic Innervation Patterns Predict the Developmental Emergence of Species-Typical Circadian Phase Preference in Nocturnal Norway Rats and Diurnal Nile Grass Rats. J Comp Neurol 520:3277-3292.

Tomotani BM, Flores DEFL, Tachinardi P, Paliza JD, Oda GA, Valentinuzzi VS (2012) Field and Laboratory Studies Provide Insights into the Meaning of Day-Time Activity in a Subterranean Rodent (*Ctenomys aff. knighti*), the Tuco-Tuco. PloS one 7:e37918.

Tsai JW, Hannibal J, Hagiwara G, Colas D, Ruppert E, Ruby NF, Heller HC, Franken P, Bourgin P (2009) Melanopsin as a Sleep Modulator: Circadian Gating of the Direct Effects of Light on Sleep and Altered Sleep Homeostasis in Opn4(-/-) Mice. PLoS biology 7.

Tsujino N, Sakurai T (2013) Role of orexin in modulating arousal, feeding, and motivation. Frontiers in Behavioral Neuroscience 7.

Valiente-Soriano FJ, Garcia-Ayuso D, Ortin-Martinez A, Jimenez-Lopez M, Galindo-Romero C, Villegas-Perez MP, Agudo-Barriuso M, Vugler AA, Vidal-Sanz M (2014) Distribution of melanopsin positive neurons in pigmented and albino mice: evidence for melanopsin interneurons in the mouse retina. Frontiers in Neuroanatomy 8.

Valjakka A, Vartiainen J, Tuomisto L, Tuomisto JT, Olkkonen H, Airaksinen MM (1998) The fasciculus retroflexus controls the integrity of REM sleep by supporting the generation of hippocampal theta rhythm and rapid eye movements in rats. Brain Res Bull 47:171-184.

Van Gelder RN (2008) Non-visual photoreception: Sensing light without sight. Curr Biol 18:R38-R39.

Vandewalle G, Balteau E, Phillips C, Degueldre C, Moreau V, Sterpenich V, Albouy G, Darsaud A, Desseilles M, Dang-Vu TT, Peigneux P, Luxen A, Dijk DJ, Maquet P (2006) Daytime light exposure dynamically enhances brain responses. Curr Biol 16:1616-1621.

Vaudry D, Falluel-Morel A, Bourgault S, Basille M, Burel D, Wurtz O, Fournier A, Chow BKC, Hashimoto H, Galas L, Vaudry H (2009) Pituitary adenylate cyclase-activating polypeptide and its receptors: 20 years after the discovery. Pharmacol Rev 61:283-357.

Vertes RP, Fortin WJ, Crane AM (1999) Projections of the median raphe nucleus in the rat. J Comp Neurol 407:555-582.

Vivanco P, Angeles Rol M, Antonio Madrid J (2009) Two steady-entrainment phases and graded masking effects by light generate different circadian chronotypes in *Octodon degus*. Chronobiol Int 26:219-241.

Vivanco P, Angeles Rol M, Antonio Madrid J (2010a) Pacemaker phase control versus masking by light: Setting the circadian chronotype in dual *Octodon degus*. Chronobiol Int 27:1365-1379.

Vivanco P, Bano Otalora B, Angeles Rol M, Antonio Madrid J (2010b) Dissociation of the circadian system of *Octodon degus* by T28 and T21 light-dark cycles. Chronobiol Int 27:1580-1595.

Vugler AA, Semo M, Joseph A, Jeffery G (2008) Survival and remodeling of melanopsin cells during retinal dystrophy. Vis Neurosci 25:125-138.

Watson RE, Wiegand SJ, Clough RW, Hoffman GE (1986) Use of cryoprotectant to maintain long-term peptide immunoreactivity and tissue morphology. Peptides 7:155-159.

Weinert D, Weinandy R, Gattermann R (2007) Photic and non-photic effects on the daily activity pattern of Mongolian gerbils. Physiol Behav 90:325-333.

Yadid G, Gispan I, Lax E (2013) Lateral habenula deep brain stimulation for personalized treatment of drug addiction. Frontiers in Human Neuroscience 7:806-806.

Zeitzer JM, Ruby NF, Fisicaro RA, Heller HC (2011) Response of the human circadian system to millisecond flashes of light. PloS one 6.

Zhao H, Rusak B (2005) Circadian firing-rate rhythms and light responses of rat habenular nucleus neurons in vivo and in vitro. Neuroscience 132:519-528.

Zhao H, Zhang B-L, Yang S-J, Rusak B (2015a) The role of lateral habenula-dorsal raphe nucleus circuits in higher brain functions and psychiatric illness. Behav Brain Res 277:89-98.

Zhao XW, Stafford BK, Godin AL, King WM, Wong KY (2014) Photoresponse diversity among the five types of intrinsically photosensitive retinal ganglion cells. Journal of Physiology-London 592:1619-1636.

Zhao Z, Xu H, Liu Y, Mu L, Xiao J, Zhao H (2015b) Diurnal expression of the per2 gene and protein in the lateral habenular nucleus. International journal of molecular sciences 16:16740-16749.

Ziegler DR, Cullinan WE, Herman JP (2002) Distribution of vesicular glutamate transporter mRNA in rat hypothalamus. J Comp Neurol 448:217-229.